Frequency Support of Micro-grid using Fleet of Electric Vehicles

A revised thesis submitted in fulfillment of the requirement for the award of the degree of

DOCTOR OF PHILOSOPHY

IN

ELECTRICAL AND INSTRUMENTATION ENGINEERING

Submitted By

Karanveer Dhingra

(Registration No: 901404010)

Under the guidance of

Dr. Mukesh Singh

Associate Professor

Electrical and Instrumentation Engineering Department

ELECTRICAL AND INSTRUMENTATION ENGINEERING DEPARTMENT

THAPAR INSTITUTE OF ENGINEERING AND TECHNOLOGY, PATIALA – 147004

November 2020

CERTIFICATE

I, Karanveer Dhingra, Regn. No. 901404010, hereby declare that the thesis entitled **"Frequency Support of Micro-grid using Fleet of Electric Vehicles"** submitted to the Electrical and Instrumentation Engineering Department at Thapar Institute of Engineering and Technology, Patiala, Punjab, India is an authenticated record of my own work for the award of the degree of "Doctor of Philosophy" under the supervision of Dr. Mukesh Singh. This report has not been submitted to any other institution for award of any other degree.

Karanveer Dhingra 08/01/2021

Karanveer Dhingra

Regn. No. 901404010

Place: Patiala

Date: 08/01/2021

This is to certify that the above statement made by the candidate is correct to the best of my knowledge.

Verified by:

Mukesh

Dr. Mukesh Singh

Associate Professor

Electrical and Instrumentation Engineering Department,

Thapar Institute of Engineering and Technology, Patiala.

ABSTRACT

In the today's scenario, frequency deviation is a common issue in islanded microgrids (MG) due to the intermittent nature of renewable energy sources (RES). It generally occurs due to the mismatch between power generation and load demand of the MG. If the power generation by RES is more as compared to the load demand then frequency of the system increases on the contrary, if the load demand is more as compared to power generation then frequency of the system decreases. In order to overcome these deviations in frequency, it is very important to make the balance between load demand and power generation. This issue can be minimized by providing the inertia to the system. However, RES have low or no rotational mass and therefore, they are not able to provide the inertia to the system. On the other hand, it has been observed that virtual inertia to the system can be provided by using the energy storage system (ESS). Further, it has been found that electric vehicles (EVs) can behave as both storage and source of power for the MG. By considering these factors, concept of virtual synchronous generator (VSG) mechanism using a charging station (CS) is proposed to provide the inertia to the system where, a fleet of EVs parked in the CS acts as an ESS for MG. Case studies have been carried out to verify the frequency support of MG using VSG mechanism. In these case studies, irradiation level of the PV array and load of the MG system have been changed arbitrarily to induce the power mismatch in the system. Through simulation results, it has been verified that the frequency of the system can be supported by the bidirectional flow of power between the CS and MG using VSG control mechanism.

Apart from this, sudden ingress and egress of EVs at the CS has been considered

while providing the frequency support to the MG. However, the EVs which ingress and egress from the CS may have different battery voltage ratings with different charging needs. Moreover, the ingress and egress of EVs at the CS may be irregular. In such a case, support to MG's frequency through EVs will be tough. In this work, a smart CS has been designed which can support the MG's frequency, even during the sudden ingress and egress of different type of EVs. Simulations have been carried out in Matlab Simulink by taking into account the different cases like a sudden change of load on MG and sudden ingress/egress of EVs at the CS. The novelty of this work lies in catering to the sudden ingress and egress of EVs at the CS while providing the support to MG's frequency through VSG mechanism.

Moreover, novel handshaking process among multiple CS has been carried out by using VSG. These multiple CS co-ordinate with each other to accomplish the handshaking process by controlling the charging and discharging of EV batteries through VSG mechanism. Fleet of EVs placed at these CS act as an energy storage device for MG. Aggregator plays a role to collect the information from multiple CS about the charging requirements of the EVs. To accomplish the process of handshaking, simulations have been carried out in MATLAB simscape by considering the different case studies. In these case studies, diverse fleet of EVs are assumed to be deployed at the CS. From the simulation results, it has been observed that each individual EV deployed at the CS participate in the charging and discharging of their batteries to achieve the process of handshaking and hence to provide the support to MG's frequency through VSG mechanism.

ACKNOWLEDGMENTS

I deem its my duty to express a word of hearty gratitude to all those helping hands that in the process of writing this thesis have become part and parcel of this endeavor. First of all, I wish to acknowledge the benevolence of omnipotent Almighty who gave me strength, courage and patience to overcome all obstacles.

With profound sense of gratitude and heartiest regard, I express my sincere feelings of indebtedness to my supervisor Dr. Mukesh Singh, Associate Professor, Electrical and Instrumentation Engineering Department, Thapar Institute of Engineering and Technology for his valuable guidance, motivation, encouragement, moral support and invaluable co-operation. The generous and positive attitude with which he solved my queries will always have a shadow on my character. I deeply admire the delightful ambiance for learning provided by him that made this thesis possible. It has been a great pleasure and experience to work under his sanctuary.

I am grateful to Head of Department, Prof. R. S. Kaler who made my study a knowledgeable experience during my stay in the department. I am much beholden to the Director, Dean (RSP) and the Management of Thapar Institute of Engineering and Technology, who provided me all the necessary resources and encouraged to produce results. I am thankful to my doctoral committee members Dr. Presanit Basak, Dr. Parag Nijhawan, and Dr. Neeraj Kumar for their constructive suggestions and ensuring the correct pace of the progress of my research work. I sincerely thank the faculty and support staff of Electrical and Instrumentation engineering department for their constant motivation.

I would like to pay deep gratitude to my parents Sh. Avtar Singh Dhingra and Smt. Jagdeep Kiran for their unconditional love, affection, and encouragement

through all the good and bad times. I would like to shower hearty gratitude to my bother in law Mr. Manjeet Singh Virk and my sister Ms. Gurpreet Kaur for their moral support and sacrifices which helped me to achieve this target.

Words can not truly express my feelings and appreciation to all friends and colleagues in lab, Ms. Anyuti Tiwari and Mr. Anish Jindal who shard their knowledge and worked as a team to make my journey during this work memorable and pleasant. These words of gratitude may have missed the names of lots of well wishers, friends and beloved ones. I pay regard to one and everyone who knowingly or unknowingly supported me during this journey of knowledge.

Karanveer Dhingra

List of Publications

Journal Publications (SCI/SCIE)

1. Karanveer Dhingra and Mukesh Singh "Frequency support in a microgrid using virtual synchronous generator based charging station," IET Renewable Power Generation, vol. 12, no. 9, pp. 1034–1044, Jul. 2018, ISSN : 1752-1416. DOI : 10.1049/iet-rpg.2017.0713.

2. Karanveer Dhingra and Mukesh Singh "Smart Charging Station to Cater the Sudden Ingress and Egress of EVs while Supporting the Frequency of MG through VSG," Arabian Journal for Science and Engineering, Springer, vol 45, pp 6715- 6727, June 2020, DOI: org/10.1007/s13369-020-04627-y.

3. Karanveer Dhingra and Mukesh Singh "Handshaking of VSG with Charging Station to Support the Frequency in Microgrid," Electrical Engineering, Springer, vol. 102, pp 2349- 2362, June 2020, DOI: 10.1007/s00202-020-01029-z.

Conference Publications

- Karanveer Dhingra and Mukesh Singh, "Comparison of the Virtual Synchronous Generator and Droop Control Techniques to Cater the Unexpected Ingress and Egress of EVs at the CS," In International Conference on Automation, Computational and Technology Management (ICACTM), London, (pp. 539-543). IEEE, 2019.

Contents

Certificate i

Abstract iii

Acknowledgment v

List of Important Abbreviations xv

1 Introduction 1

1.1 Virtual synchronous generator 3

1.2 Electric vehicles and their role in frequency regulation of MG 5

1.3 EVs battery as an energy storage system 6

1.4 Phase locked loop for measurement of frequency 7

1.5 Thesis Organization 8

2 Literature Review 11

2.1 Participation of EVs in power system 11

2.2 Different techniques for frequency regulation of MG 12

2.3 Virtual synchronous generator control mechanism 13

2.4 Research Gaps 17

3 Frequency control techniques in a Microgrid 19

3.1 Introduction 19

3.1.1 Motivation 21

3.1.2 Contribution . . . 22
3.1.3 Organization . . . 22
3.2 Proposed Work . . . 22
3.3 Control Strategy . . . 24
3.4 Results and Discussion . . . 27
3.5 Summary . . . 29

4 VSG based frequency support in MG using EVs 30
4.1 Introduction . . . 30
4.1.1 Motivation . . . 35
4.1.2 Novelty . . . 35
4.1.3 Contribution . . . 35
4.1.4 Organization . . . 36
4.2 Proposed Methodology . . . 36
4.2.1 Charging station . . . 37
4.2.2 Design of Buck-Boost Converter . . . 38
4.2.3 Stability analysis of buck boost converter . . . 39
4.2.4 Power converter (DC-AC) . . . 45
4.2.5 Distributed energy sources . . . 45
4.3 Virtual Synchronous Generator . . . 49
4.4 Mathematical formulation of the Current Controller . . . 52
4.5 Results and Discussions . . . 54
4.5.1 Case study 1 . . . 54
4.5.2 Case study 2 . . . 59
4.5.3 Case study 3 . . . 60
4.6 Summary . . . 63

5 VSG mechanism for catering unexpected EVs 66
5.1 Introduction . . . 66
5.1.1 Motivation . . . 68

5.1.2 Contribution . . . 69
5.1.3 Organization . . . 69
5.2 Proposed Methodology . . . 69
5.3 Control Strategy . . . 73
5.4 Results and Discussion . . . 76
5.4.1 Case 1: Change of load on MG while catering the ingress/ egress of EVs at the CS . . . 77
5.4.2 Case 2: Change in load on MG while considering no movement of EVs at the CS . . . 79
5.4.3 Case 3: Sudden ingress of EVs at the CS . . . 81
5.5 Summary . . . 84

6 Handshaking of CSs through VSG **85**
6.1 Introduction . . . 86
6.1.1 Motivation . . . 87
6.1.2 Contribution . . . 88
6.1.3 Organization . . . 88
6.2 System Framework . . . 88
6.2.1 Coordination of Charging Station with Aggregator . . . 89
6.2.2 Control mechanism . . . 90
6.3 Mathematical formulation . . . 92
6.4 Results and Discussion . . . 96
6.4.1 Case 1 . . . 96
6.4.2 Case 2 . . . 100
6.4.3 Case 3 . . . 105
6.5 Summary . . . 107

7 Conclusion and Future Scope **109**
7.1 Conclusion . . . 109
7.2 Future Scope . . . 110

List of Figures

1.1 MG in islanded mode 2

1.2 Schematic diagram of VSG 4

1.3 Phase locked loop for frequency measurement 8

3.1 Generalized diagram of the proposed system 23

3.2 Frequency Droop Control for Diesel Generator 25

3.3 Frequency of MG (a) Droop (b) VSG technique 27

3.4 Frequency of MG (a) Droop (b) VSG technique 28

4.1 Schematic diagram of the proposed islanded microgrid 36

4.2 Buck Boost converter 38

4.3 Switch S_1 is in on condition 39

4.4 Switch S_2 is in on condition 41

4.5 Bode plot of the buck boost converter 43

4.6 Buck-boost converter control strategy 44

4.7 Diesel engine governor model 47

4.8 Speed Control Model of Diesel Engine 47

4.9 VSG control mechanism 50

4.10 Current control scheme 50

4.11 Reference signal generation for PWM 51

4.12 Block diagram for swing equation 51

4.13 (a) Load on the system (b) Frequency of the system (c) Power delivered and absorbed by the CS (d) Power delivered by diesel generator . . . 55

4.14 (a) Power delivered and absorbed by the CS (b) Charging and discharging current of the EV's battery (c) SoC of the EV's battery during charging and discharging operation 56

4.15 (a) Load on the MG system (b) Frequency of the system (c) Power delivered and absorbed by the CS (d) Power supplied by the diesel generator 57

4.16 (a) Power delivered and absorbed by the CS (b) Charging and discharging current of the EV's battery (c) SoC of the EV's battery during charging and discharging operation 58

4.17 (a) Power provided by the PV array (b) Frequency of the system (c) Power delivered and absorbed by the CS (d) Power delivered by the diesel generator 61

4.18 (a) Power delivered and absorbed by the CS (b) Charging and discharging current of the EV's battery (c) SoC of EV's battery during charging and discharging operation 62

5.1 Schematic layout of the proposed work 70

5.2 Design of charging station 72

5.3 Control coordination among buck boost converter and power conveter 72

5.4 Charging and discharging of EVs during their ingress and egress at the CS 78

5.5 (a) Frequency deviation in the MG. (b) Power released or consumed by the CS 79

5.6 Charging and discharging of EV batteries during change in load on MG 80

5.7 (a) Frequency deviation in the system due to load change on MG. (b) Power released or consumed by the CS 80

5.8 Sudden ingress of EVs at the CS 83

5.9 Frequency deviation in the system due to sudden ingress of EVs at the CS 83

6.1 Coordination of charging station with aggregator 89
6.2 Schematic diagram of the proposed system 90
6.3 Control strategy of power converter 92
6.4 EVs deployed at the CS_1 for participation in charging and discharging process 97
6.5 EVs deployed at the CS_2 for participation in charging and discharging process 97
6.6 EVs deployed at the CS_3 for participation in charging and discharging process 97
6.7 **Frequency of the system** 98
6.8 SoC of EVs at CS_1 during change in load of MG 98
6.9 SoC of EVs at CS_2 during change in load of MG 99
6.10 SoC of EVs at CS_3 during change in load of MG 99
6.11 Dynamic behavior of EVs at the CS_1 101
6.12 Dynamic behavior of EVs at the CS_2 101
6.13 Dynamic behavior of EVs at the CS_3 101
6.14 SoC of EVs considering their dynamic movement at CS_1 102
6.15 SoC of EVs considering their dynamic movement at CS_2 102
6.16 SoC of EVs considering their dynamic movement at CS_3 102
6.17 Change in the Irradiance of PV array 105
6.18 Effect of change in Irradiation level of PV array on the EVs parked at CS_1 105
6.19 Effect of change in Irradiation level of PV array on the EVs parked at CS_2 106
6.20 Effect of change in Irradiation level of PV array on the EVs parked at CS_3 106
6.21 SoC of EVs parked at CS_1 during change in irradiation level of PV array 106
6.22 SoC of EVs parked at CS_2 during change in irradiation level of PV array 107
6.23 SoC of EVs parked at CS_3 during change in irradiation level of PV array 107

List of Tables

4.1 Parameters of diesel generator 49

4.2 Simulation parameters 65

5.1 Design parameters of buck-boost converter 73

5.2 EV specifications at CS for Case 1 81

5.3 EV specifications at CS for Case 3 82

5.4 Parameters of the considered system 82

6.1 Parameters of the system 99

6.2 Specifications of EVs For Case 2 at CS_1 104

6.3 Specifications of EVs For Case 2 at CS_2 104

6.4 Specifications of EVs For Case 2 at CS_3 104

LIST OF IMPORTANT ABBREVIATIONS

Acronym	**Meaning**
BESS	Battery energy storage system
CS	Charging station
CSI	Current source inverter
DL	DC link
DES	Distributed energy sources
ESS	Energy storage system
EV	Electric vehicle
G2V	Grid to vehicle
Hz	Hertz
kW	Killo watt
MG	Microgrid
MATLAB	Matrix Laboratory
PV	Photovoltaic
PWM	Pulse Width Modulator
RES	Renewable energy sources
SoC	State of charge
VSG	Virtual synchronous generator
V2G	Vehicle to grid
VSI	Voltage source inverter

Chapter 1

Introduction

Microgrids (MG) plays very important role in the power sector. MG consists of various energy sources such as PV system, wind plant, bio-mass, combined heat and power, fuel cells etc. All these energy resources act as distributed energy sources (DES) for the MG. MGs are the smaller variants of conventional grid. However, MGs are different from conventional electrical grids, as they provide a close concurrence between power generation and power use. Conventional power grids are totally dependent on the fossil fuels but in the today's scenario, the rate at which fossil fuels are depleting is very large. MG is the possible solution to the scarcity of fossil fuels and can meet the future energy demands. Energy storage system (ESS) plays a very important role in the MG as they can provide the back-up power to the grid. As compared to the DES, ESS used in the MG have no start up or shut down cost. The response time of the ESS is also very small as compare to DES. ESS includes electro chemical battery, compressed air energy storage, flywheel energy storage, super capacitor, super conducting magnetic energy storage etc. MG can operate in two ways, islanded and grid connected mode [1] [2] [3]. In former, it supplies the power only to the loads attached with it. While in later, it is integrated with the grid. Most of the MG remain connected with the main grid, however, some of the MG work in islanded mode. Fig. 1.1 shown below, is representing the MG in islanded mode.

A MG could supply the power to the residential, commercial as well as to the

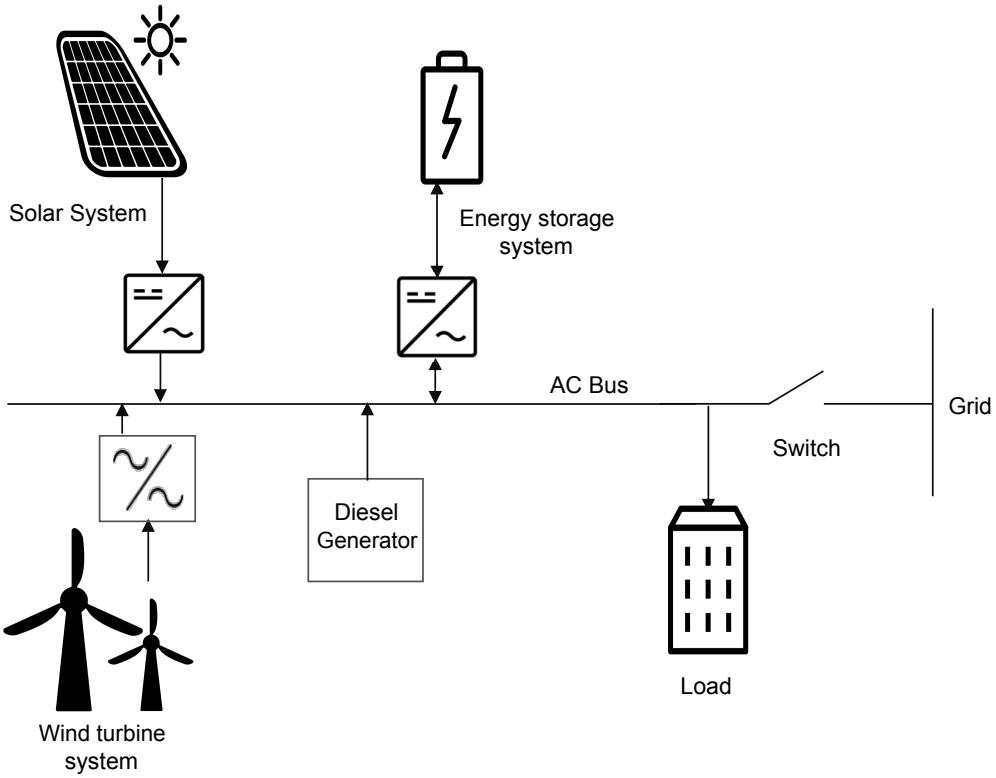

Figure 1.1: MG in islanded mode

industrial consumers. In general, commercial and industrial consumers are defined as critical/sensitive loads, that require high degree of power quality and reliability. With the increase in load demand, integration of the renewable energy sources (RES) with the MG is increasing day by day. RES plays a major role in the reduction of emission of harmful gases and lead to the generation of green electricity [4]. However, due to the intermittent nature of RES, stability of the MG is a major concern. Voltage and frequency deviation are the two main issues need to be taken care, while the MG operates in islanded mode. Few authors [5] [6] have discussed about the protection of MG using different techniques. Frequency deviation generally occurs due to mismatch of power generation and load demand. For instance, sudden fluctuation in load or power generation will lead to temporary increase or decrease of frequency. If the load demand of the system suddenly rises to a level which is more than the power supply then there will be temporary decrease in frequency of the system. On the other hand, if load demand suddenly reduced by large amount in comparison with

the power supply then temporary frequency fluctuation will appear. These deviations occur more frequently in Islanded MG, because they depend on the power generated by the RES, which are intermittent in nature. This intermittent nature of RES leads to the power unbalance in a system, which causes fluctuation in frequency [7]. These fluctuations in frequency can be minimized by providing the inertia to the system. But in the case of MG, DES have either low or no inertia. So due to the absence of inertia, it will be difficult to support the frequency by DES only, when the transients arise in system. This problem can be overcome by using the virtual synchronous generators (VSG) to regulate the frequency of the MG. However, virtual inertia will only provide temporary support for limiting the frequency transients in a power system.

Two types of control inverters can be used for the operation of MG, one is current source inverter (CSI) and second is voltage source inverter (VSI). Where, CSI are used to obtain the desired output current and voltage at the output of CSI depend on the load impedance. On the other hand, VSI are used to obtain the desired output voltage and frequency. In the case of VSI, a dc link capacitor having fixed voltage acts as an input for the inverter. While, in case of CSI, a large inductor having variable voltage acts an input for the inverter. In this work, VSI has been used to obtain the desired voltage and frequency at the output of the inverter.

1.1 Virtual synchronous generator

VSG consist of ESS, power converter and proper control mechanism, fig. 1.2 depicts the schematic diagram of VSG.The main role of VSG is to inherit the dynamic properties of a real synchronous generator so that stability of the system can be enhanced.

Inertia of real synchronous generator may affect the active and reactive power of the DGs which can be minimized with the help of VSG [8]. With the help of VSG mechanism virtual inertia is provided to the system, to regulate the frequency of the

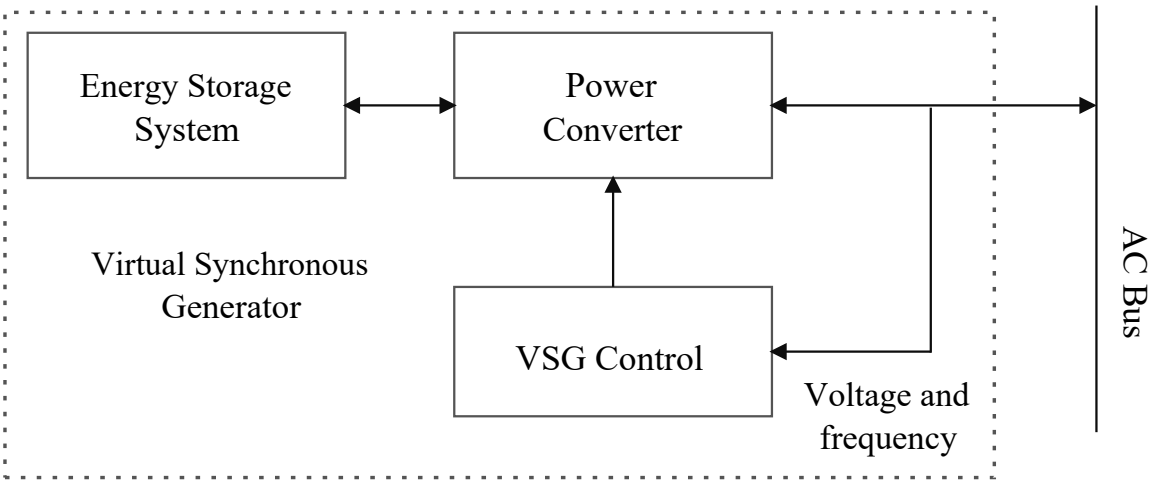

Figure 1.2: Schematic diagram of VSG

MG. This inertia can be emulated either from the wind turbines or by using ESS. The total amount of active power that VSG extract from ESS is,

$$\Delta P_{vsg} = \Delta P_{inertia} + \Delta P_{droop} \tag{1.1}$$

In Eq. 1.1, $\Delta P_{inertia}$ is the power required for emulating the virtual inertia and ΔP_{droop} is the droop power that is proportional to the frequency deviation.

$$\Delta P_{inertia} = 2H_{vsg}.w_g \frac{dw_g}{dt} \tag{1.2}$$

In Eq. 1.2, H_{vsg} represents the virtual inertia constant and w_g is the actual frequency of the grid.

$$\Delta P_{droop} = K_{droop}(w_g - w_{nom}) \tag{1.3}$$

In Eq.1.3, K_{droop} is the proportional constant and w_{nom} is the reference frequency of the grid.

Both droop control and VSG control techniques can be used for frequency regulation purpose in MG. However, lack of inertia have not been considered in droop control method, while the VSG control method overcomes this problem by providing virtual

inertia to the system [9]. If the virtual inertia is large, the rate of change of frequency can be reduced easily. The flow of power between ESS and MG is controlled by VSG control mechanism in case frequency change or rate of frequency change exceeds from the predefined limit [10].

1.2 Electric vehicles and their role in frequency regulation of MG

Electric vehicles (EVs) can play a significant role in the power system. EVs can reduce the consumption of fossil fuels that further leads to reduction in emission of harmful gases. With the use of EVs, emissions of gases such as CO_2, NO_2 can be reduced to large extent [11]. The progress of EVs will be highly reliant on whether charging stations (CS) can be designed for easy access. CS could be designed at homes, workplaces, or other major areas such as cinema halls, universities and Industries. EVs' battery can be charged through several ways but CS are recognized as the primary source to satisfy the energy demand of EVs. CS is a place where EVs can accomplish their charging demand through plug in mode. However, the locations of CS should be such that EVs can anywhere locate the CS within its driving circle. Most of the EV owners drive the vehicle from residence to work place in the morning and back to residence in the evening. The owners of EVs those are going to work place or in shopping complexes can park their EVs at the CS. The duration for which the EVs are in idle state while parked in parking lot of work places or shopping complexes can act as ESS for the MG. This duration can be utilized to provide the ancillary services to MG in terms of frequency regulation or voltage support. The aim of modeling the CS is to systematize the bi-directional flow of power between battery operated EVs and the MG.

In future, the penetration of EVs in the market will increase, which can be used for providing the support to the MG. Battery operated EVs can act both as source

of generation as well as load for the MG. EVs can provide power to the CS while parked in a parking lot. Frequency of MG can be regulated by the bi-directional flow of power between CS and MG. CS discharge the power to the MG when the power generated by DES is less than the load demand. On the other hand, power is delivered to the CS when the power generated by the DES is in excess as compared to the load demand. EV owner's can get reward by parking their EVs in the parking lot of CS for the frequency regulation purpose of MG. Two types of charging of EVs parked at the CS can take place, one is the centralized charging and other is the decentralized charging. In the centralized charging, uncertain arrival and departure of EVs at the CS can be considered. On the other hand, in the case of decentralized charging queuing model based methods can be adopted for the charging purpose of EVs.

1.3 EVs battery as an energy storage system

There are different types of batteries which can be used in the EVs. In the past, most commonly used battery in EVs was lead acid battery but nowadays with the advancement in technology lithium ion and Nickel Metal Hydride batteries plays more important role. EVs parked at the CS can deliver or fetch the energy to provide support to the MG. However, an individual EV can not provide the support to the MG, its the combined participation of a fleet of EVs to support the MG having RES. Fleet of EVs parked at the CS can behave as an ESS for the MG. Different type of ESS can be used in the VSG control mechanism. Depending on the main source of power in MG [10], some part of energy of the ESS is used to provide active power to the grid and rest is used to emulate the virtual inertia using VSG mechanism. EVs battery can act as an ESS in VSG control mechanism. In general, EVs can be used both for transportation as well as for providing the power to the MG through CS.

In VSG mechanism, EVs can be deployed as an ESS by considering a parking lot with inbuilt CS. EVs parked in this parking lot can charge/discharge the required

amount of energy to and fro the CS, as per the frequency regulation requirement of the MG. As the RES are intermittent in nature, continuous supply of electricity to the loads, in MG is not possible. Battery operated EVs connected with the CS can provide the back up power to the loads of MG. So, load demand of the MG is managed by both the CS and DES. Although, EVs parked in parking lot may have different state of charge (SoC) levels but constant supply can be fed to the inverter by using dc-dc converters. Numerous researchers have focused on the participation of EVs in electric power system to illustrate their importance in the grid. Kempton *et al.* [12] reveals that battery operated EVs can provide supply to the grid and can act both as a storage as well as source of power in the system. Tomic *et al.* [13] deliberated that EVs can be used for transportation purpose as well as for providing the power to the grid. Authors described that for EV owners, vehicle to grid (V2G) is a convincing beneficial scheme that would boost the acceptance of EVs in the market. Subotic *et al.* [14] have discussed about the various topologies for charging the EVs. Yilmaz and Krein [15] discussed that the bi-directional flow of power between grid and the EVs can be controlled through V2G strategy. Authors have explained that V2G strategy can enhance the performance of grid in terms of efficiency and generation dispatch. These authors have explained the role of EVs in power system but they haven't discussed on the frequency regulation of MG using EVs. In the conventional grids, the stability of grid depends on the dynamic characteristics of the synchronous generator [16]. However, in the MGs instead of synchronous generators only DES have been preferred to use. Several authors have done the literature survey on EVs and their importance in the MGs to support the frequency using different ways. Literature review on the role of EVs and the different control techniques will be discussed in the next chapter.

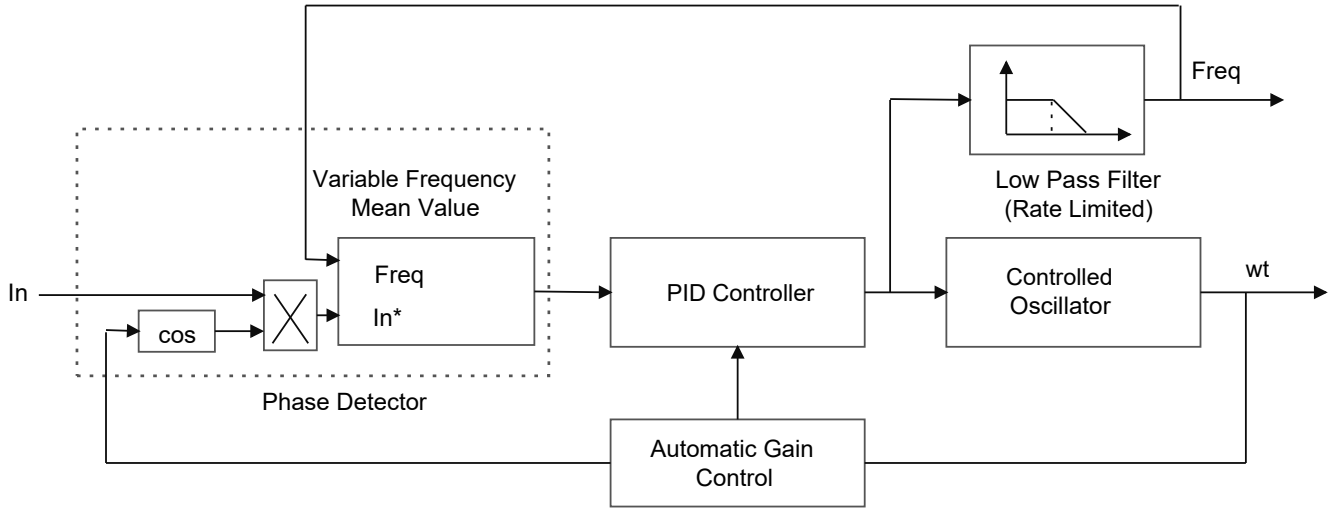

Figure 1.3: Phase locked loop for frequency measurement

1.4 Phase locked loop for measurement of frequency

The phase locked loop (PLL) is used for measuring the frequency in the circuit. PLL is basically a closed loop control system which tracks the frequency and phase of sinusoidal signal with the help of internal frequency oscillator. The internal frequency of the oscillator is adjusted by the control system to maintain the phase difference to zero. Fig. 1.3 depicts the internal diagram of the PLL, as per this figure input signal is mixed with an internal oscillator signal. The DC component of the mixed signal which is proportional to the phase difference between these two signals is extracted with a variable frequency mean value. The PID controller with an automatic gain control keeps the phase difference to zero by acting on a control oscillator. The PID output, corresponding to the angular velocity, is filtered and converted to the frequency, which is used by the mean value.

1.5 Thesis Organization

The thesis has been organized in the following manner.

- Chapter 2: Literature Review

  In this chapter, literature review to illustrate the research work has been pre-

sented. Several authors have focused on the role of EVs to handle the issues of MG and intermittent nature of RES.

- Chapter 3: Frequency control techniques in a microgrid

  In this chapter, droop control and VSG control techniques has been discussed to support the frequency of MG. Further, the comparison of both the techniques has been done while supporting the frequency of MG.

- Chapter 4: VSG based frequency support in MG using EVs

  In this chapter, electric vehicles (EVs) parked at the charging station (CS) has been considered as an energy storage system (ESS) to minimize the gap between load demand and power generation. The concept of VSG mechanism using a CS is proposed to provide the inertia to the system. For simulations, data has been taken from one islanded MG Kynthos in Greece. Through simulation results, it has been verified that the frequency of the system can be supported by the bidirectional flow of power between the CS and MG using VSG control mechanism.

- Chapter 5: VSG mechanism for catering unexpected EVs

  In this chapter, Ingress and egress of EVs at the CS has been catered while maintaining the frequency of the MG. For this purpose, n different type of EVs (EV_1 to EV_n) are considered at the CS. These EVs have a range of battery voltage ratings and are connected in parallel with a common dc bus through bidirectional buck-boost converters. Furthermore, the SoC level of these EVs is considered as different from each other. To accomplish the task of sudden ingress and egress at the CS, EVs are connected with dc bus through controlled switches, which are turned on and off at irregular intervals. The time span for which switches remain open has been considered as EVs are not placed at the CS. The time span for which switches remain closed has been considered as parking period of EVs at the CS. As the battery voltage ratings of these EVs are

different, a constant voltage V_c is obtained at the dc bus through bi-directional buck-boost converters.

- Chapter 6: Handshaking of CSs through VSG

  In this chapter, It has been considered multiple CS in coordination with the power converters behave as a VSG and shares the power with each other through handshaking process to meet the demand of the MG. VSG controls the power converter to manage the bidirectional power flow in the system. Both the PV array and the CS operate in parallel with each other to meet the load demand of the system. In this way, several CS coordinate with each other to support the MG's frequency.

- Chapter 7: Conclusion and Future Scope

  This chapter concludes the thesis work and represents the future work that could be done.

Chapter 2

Literature Review

2.1 Participation of EVs in power system

EVs remain parked in parking lot for most of the time, during that time EVs are in idle state. The duration for which EVs are in idle state can be used for giving power supply to the grid. Many researchers have focused on the participation of EVs in the electrical power system and how EVs can be used for frequency regulation of grids. Kempton *et al.* [17] reveals that battery operated EVs can provide supply to the grid. EVs can act both as a storage and source of generation in the power system. In another work, Kempton *et al.* [18] introduced the concept of vehicle to grid. Authors have discussed that EVs can provide the backup, where RES has been used for the generation of electricity. In this way, reliability and stability of the system can be enhanced. Görbe *et al.* [19] discussed that with the use of EVs and RES the power losses in the smart grids can be reduced to a large extent. Tomic *et al.* [20] deliberates that EVs can be used both for the transportation system as well as for providing the power to the grid. Authors further described that for EVs proprietors this is a convincing revenue stream that would enhance the economics of grid-connected EVs and further boost their acceptance. Yilmaz *et al.* [21] discussed that vehicle to grid concept can be used for the bidirectional flow of power between grid and EVs. Authors also manifest that vehicle to grid approach can enhance the technical achievement of

the grid in the fields such as reliability, stability, efficiency and generation dispatch. Dhanju and Kempton [22] examined that EVs can act as ESS for providing the back-up power to the large scale wind power systems. Authors found that stability of the wind power plant can be enhanced using vehicle to grid concept. Meng *et al.* [23] demonstrates that aggregation of EVs can be used to minimize the frequency deviations for the whole day. Authors have validated the same concept in the Great Britain power system. In another work, Meng *et al.* [24] proposed a dynamic EV frequency regulation scheme, by taking into account the traveling behavior of the EVs proprietors. Authors have implemented the droop control mechanism to regulate the EV charging/discharging power as per the frequency signal. Subotic *et al.* have discussed about the controlled charging of EVs through V2G mode of operation [25]. Saber *et al.* [26] proposed particle swarm optimization technique to generate the successful schedule and control of gridable vehicles (GVs) in a smart grid. Authors verified in a simulation study on 50,000 GVs in grid model that cost and emissions can be reduced to large extent by maximum utilization of GVs and RESs.

2.2 Different techniques for frequency regulation of MG

A lot of techniques have been explored by the researchers for the frequency regulation purpose of the grid. In the conventional grids, dynamic characteristics of the synchronous generator plays a vital role to maintain the stability of grid [16]. However, for the smart grids authors have proposed some techniques to regulate the frequency. Arani *et al.* [27] have proposed the scheme of implementation of power and torque droop control techniques on doubly fed induction generator for frequency regulation purpose. Ramtharan *et al.* have [28] discussed about the droop controller to enhance the inertia provided by the double fed induction generator for frequency regulation purpose. Authors suggested to implement two control loops one to control frequency

deviation and another to control rate of change of frequency. Díaz *et al.* [29] have used the bifurcation theory in order to schedule the droop coefficients and hence to regulate the frequency of the islanded MG. Kottick *et al.* [30] demonstrates that battery energy storage system can be used for the frequency regulation purpose of the islanded MG. Authors have used the 30 MW battery for the validation purpose of this concept. Oureilidis *et al.* [31] demonstrates a control scheme to assure fluctuation of frequency with in the stringent limits of the Standard EN 50160 for supplying a rich quality power to the affiliated loads. In this work, SOC of battery determines the frequency of the main AC bus, in terms of implementing a proposed droop curve. At the same moment, the SOC of the battery is kept under control to prevent the overcharging or deep discharging. Zhang *et al.* [32] discussed that frequency of MG can be regulated, by the bi-directional flow of power between ESS and wind farms using fuzzy logic controller. Authors have discussed that power flow can be controlled based on the frequency fluctuation as well as on its rate of fluctuation.

2.3 Virtual synchronous generator control mechanism

Various authors have used the concept of VSG to stabilize the grid. Authors have implemented this concept using wind generators and energy storage systems. Literature review based on VSG concept to stabilize the grid has been described as follows. Driesen *et al.* [33] examines that frequency of the grid can be regulated by providing the virtual rotational inertia to the DGs. Authors further manifest that DGs in combination with the short term energy storage can behave like VSGs and thus can add the virtual inertia to the system. This virtual inertia can be attained from ESS by controlling the power converter, through proper control mechanism. Zhong *et al.* [34] reveals that inverters can operate as synchronverters by mimicking the behavior of synchronous generators. Authors added that synchronverters can easily operate in

island mode, and hence, can be an optimal solution for MGs. Visscher *et al.* [35] examined that DGs along with the virtual synchronous machines can enhance the frequency stabilization and prevent blackouts due to large short term frequency fluctuations induced by decentralized generation. Torres *et al.* [36] proposed a technique in which inertia can be emulated from the wind diesel power plants by using virtual synchronous machine for the frequency regulation purpose. Wesenbeeck *et al.* [37] discussed that rotor angle stability increases with VSG. Authors further, described that inertia can be emulated by properly selecting the control parameters of phase locked loop. Rathore *et al.* [38] discussed about the VSG control strategy to improve the transient response of the system. Authors have discussed that by changing the parameters of the swing equation frequency deviation in the system can be minimized.

Soni *et al.* [39] demonstrates that transient response of power system can be enhanced by adding the virtual inertia to the system. Torres *et al.* [40] discussed that self tunning virtual synchronous machines reduce the power flow through the ESS up to 58% while giving the similar performance as that of constant parameter virtual synchronous machines. Alipoor *et al.* [41] demonstrates the affect of alternating moment of inertia on power system stabilization. Authors found out that stability of the power system can be improved by altering the moment of inertia.

Morren *et al.* [42] discussed that frequency can be regulated by emulating the virtual inertia from the variable speed wind turbines. Authors added that the required power can be obtained from the kinetic energy stored in the rotating mass of the turbine blades. Bevrani *et al.* [10] proposed the concept of VSG to regulate the frequency of the MG. Authors have proposed that virtual inertia can be emulated from ESS in order to regulate frequency. Karapanos *et al.* [43] demonstrated the VSG hardware in the loop, for the real time simulation of the power system. Authors have implemented the VSG concept in hardware loop for the verification of results. Liu *et al.* [9] discussed the advantages of using VSG control mechanism over droop control. Authors have discussed that frequency can be controlled in a better way using VSG. Shintai *et al.* [8] discussed that oscillations of active and reactive power

can be damped by using the VSG. Authors have linearized the non-linear swing equation of synchronous generator using runga-kutta method to calculate the virtual rotor angle. Further they have used this rotor angle to control the dampings of active and reactive power.

Low inertia or absence of inertia is the main problem in the RES used in the MG. Further, the intermittent nature of RES, may lead to frequency deviation issues in the MG, which can be minimized by providing the virtual inertia to the MG. Number of techniques have been used by the authors to minimize the frequency deviation of MG. Some authors have used the modified droop control technique to regulate the frequency of MG and some have used VSG control technique to overcome this problem by providing virtual inertia to the system. If the virtual inertia is large, the rate of change of frequency can be reduced easily. The main role of VSG is to inherit the dynamic properties of a real synchronous generator so that stability of the system can be improved. VSG technique have already been implemented on wind and diesel generators to emulate the virtual inertia. This technique have also been applied using ESS to emulate the virtual inertia and to stabilize the grid. Some authors have used the battery operated EVs as ESS in MG to regulate the frequency. Bukhari *et al.* [44] have stressed upon the future opportunities for the EVs in tackling the various issues related to MG. Authors have elaborated on the coordination of EVs with MG as a source of power. Ahn *et al.* [45] have discussed that intermittent nature of RES can be catered by adjusting the charging rate of the EVs battery. Honarmand *et al.* [46] discussed about the smart planning of the charging and discharging of EVs while parked in parking lot. Authors have elaborated that both the financial and technical objectives can be achieved by the proper coordination of EVs. These authors have explained the role of EVs in power system but they haven't discussed on the frequency regulation of MG using EVs.

Many of them used different techniques to illustrate the MG's frequency support using CS. Some authors [47] [48] have discussed about the energy management of MG using VSG, where dc voltage source and power converters have been used to manage

the power flow in the system. Almeida *et al.* [49] have elaborated that virtual inertia can be emulated from EVs to maintain MG's frequency. Authors [50] [51] have discussed about the support to MG's frequency using VSG technique. They have elaborated the services which can be provided to the grid through EVs. Fang *et al.* [52] have elaborated the role of virtual inertia in regulating the frequency of weak grids. Authors have done the comparison of virtual inertia with the actual inertia stored in the conventional synchronous generators. Moreover, they verified the superiority of VSG over conventional synchronous generators to provide the virtual inertia to MG. Jin *et al.* [53] have elaborated that EVs can be charged in an optimized way using RES. Authors further described that EVs can be connected at any time with MG system as per the demand of the customer. Roy *et al.* [54] proposed a scheme to charge EVs from office buildings by using the distributed energy sources. Matos *et al.* [55] discussed that power flow between ESS and RES in a MG can be controlled in a better way to manage the SoC of ESS.

Authors [56] [57] have discussed about the parallel operation of inverters which has been controlled by VSG. Authors have explained that both the inverters behave as VSG and play the role to stabilize the steady state performance of MG. Rezkalla *et al.* [58] also discussed about the virtual inertia concept to support grid frequency using EVs. The authors further elaborated that charging of EVs using RES will reduce the dependence on conventional sources. Sakimoto *et al.* [59] have discussed about the VSG control mechanism to stabilize the MG's frequency. Authors have explained the role of phase locked loop in VSG mechanism to control the power converter and hence to stabilize MG frequency. Wang *et al.* [60] discussed about the VSG control mechanism which is based on the voltage control of the system. Authors have elaborated that stability to the PV array and battery based MG can be provided using VSG mechanism. Yan *et al.* [61] discussed about the parallel operation of VSGs to satisfy the load profile of isolated MG. Authors have elaborated that VSGs can share the load of MG in a proportional manner.

Shi *et al.* [62] have explained the importance of virtual inertia to restrain the MG's

frequency during the frequent changes in wind turbine speed and abrupt load change of the system. EV aggregators play a major role in the frequency support mechanism of MG. Aggregator is a combination of CS, which can manage the distribution of power among the EVs. Liu *et al.* [63] have done the comparison of droop and VSG strategy to validate the advantage of VSG over droop control. They further demonstrated that system can be equipped with larger virtual inertia using VSG. Han *et al.* [64] designed an aggregator to regulate the MG's frequency, which further manage the charging and discharging of EVs. Researchers [65] [66] [67] have interpreted the use of EV aggregators in the power system. They have discussed about the energy needs of the MG which can be easily met by using the EV aggregators in the system. Aggregator plays a role to manage the charging and discharging rate of EVs parked at the CS. Few authors [68] [69] have discussed about the prediction of EVs at CS. The authors have elaboarted the stochastic methods to consider the charging and discharging duration of EVs while parked at the CS.

Various researchers have focused on the incentives, which the EV owners can get by allowing the participation of their EVs in the MG support. Aujla and Kumar [70] discussed about the reward points earned by the EV owners by allowing their EVs to participate in charging and discharging process in order to cater the intermittent nature of RES. Ghofrani *et al.* [71] discussed about the incentives earned by EV owners to compensate the fluctuating nature of wind power generation by allowing the charging/discharging of EV batteries through V2G concept. Authors [18] [72] have elaborated that EV owners can earn profit by allowing the discharge of their EV batteries to provide ancillary services to the MG. Authors have further explained that this process can be accomplished when EVs are parked in a parking lot.

2.4 Research Gaps

Number of researchers have focused on the frequency regulation of MG. Some authors have implemented the droop control methods to regulate the frequency of the

MG [27] [73] [74]. Few authors have used vehicle to grid concept for the frequency regulation purpose [20] [24]. Authors have implemented the VSG concept to emulate the inertia from wind turbines and hence, to improve the stability of the MG [39] [42]. Researchers have implemented the VSG concept using ESS also to emulate the virtual inertia and hence to enhance the stability of the MG [37] [41]. The current trends in literature review on ESS in MG lack in many aspects. Some of them are listed below.

- ESS can be used to provide the virtual inertia to the DGs in MG. However, the types of energy sources that can be used as an ESS in MG to emulate virtual inertia is yet to be explored.
- VSG concept have already been implemented using wind turbines and ESS to emulate the virtual inertia, and hence, to regulate the frequency of the MG. Moreover, EVs have already been used as an ESS in the MGs for the frequency regulation purpose. However, VSG concept is not yet explored by considering EVs as an ESS.
- To meet the charging needs while supporting the frequency of MG yet to be explored
- With the increase in penetration of EVs, the possible effect of unexpected ingress and egress of EVs on the CS, is yet to be explored while maintaining the stability of MG.
- Comparison of VSG mechanism, with other control mechanisms is yet to be done, using EVs as an ESS.

In this thesis work, authors have covered the following research gaps: frequency support of MG using VSG mechanism by considering EVs as an ESS, unexpected arrival and departure of EVs at the CS while supporting the frequency of MG and Handshaking among CS to meet the charging and discharging needs of an individual EVs.

Chapter 3

Frequency control techniques in a Microgrid

3.1 Introduction

In the current scenario of power system, deviations in frequency is the main issue in microgrids (MG). These frequency deviations can be eliminated by minimizing the gap between load demand and power generation. DES are playing an important role to manage the load profile of MG. In case, load demand of the MG differs from the power generation then problem of frequency deviation arises in the MG. However, this deviation in frequency can be supported by DES. [1] These sources can deliver or absorb the required power in order to minimize the gap between load demand and generation. Energy storage systems (ESS), diesel generators, fuel cells etc., all act as DES. In case power generation is more than the load demand, excess power can be absorbed by ESS to diminish the gap. On the contrary, ESS and other DES can deliver the power if the generation is less in comparison with the load demand of MG.

[1] The content of this chapter is taken from:

- K. Dhingra and M. Singh, "Comparison of the Virtual Synchronous Generator and Droop Control Techniques to Cater the Unexpected Ingress and Egress of EVs at the CS," International Conference on Automation, Computational and Technology Management (ICACTM), London, United Kingdom, 2019, pp. 539-543, doi: 10.1109/ICACTM.2019.8776772.

However, maintenance cost of the battery's ESS is very high, therefore, alternative solution is required which can act both as load as well as source of power. In the recent trend, electric vehicles (EVs) are behaving as an ESS and act as DES for the MG. Fleet of EVs parked in the parking lot of charging station (CS) can behave as an ESS for the MG. DES and EVs are a perfect combination to accommodate load profile of islanded MG as well as to reduce the emission of gases. However, with the increase in penetration of EVs in the market, unexpected ingress and egress of EVs at the CS will increase. With this increase in unexpected ingress and egress of EVs, it will be difficult to regulate the frequency of MG.

Several investigators have concentrated on the concept of frequency regulation in islanded MGs. They have implemented numerous techniques to regulate the MG's frequency. Out of these techniques, droop control is most commonly used in MG operations to provide the voltage and frequency support [73]. Bevrani and Shokoohi implemented the droop control strategy to regulate voltage and frequency of the MG [74]. However, some authors have implemented the virtual synchronous generator (VSG) control to regulate the MG's frequency [51]. Authors [55] discussed about the power management in islanded MGs using the ESS as well RES. They have explained that ESS deliver or absorb the power to regulate MG's frequency. Serban and Marisnescu [75] have demonstrated that frequency of the islanded MGs can be controlled by including the virtual inertia component with the droop control method.

Soni *et al.* [39] have mentioned the importance of virtual inertia in MG to provide the frequency stability. Katiraei and Iravani [76] demonstrated various techniques to manage the flow of power within MG using droop control technique. Majumder *et al.* [77] have discussed about the sharing of load demand in the rural areas through droop control technique. Usunariz *et al.* [78] have designed a modified droop control method to provide stability to MG. Authors have further described the role of ESS to accommodate the load profile of islanded MG. Reihani *et al.* [79] have applied the droop control method for regulating the frequency of MG by considering batteries as an ESS for the MG. Several authors have opted for droop control and VSG control

to manage MG's frequency. However, the above mentioned researchers have not considered the EVs as an alternative ESS to the battery bank system in MG.

Ma and Mohammed [80] explained that with the use of centralized aggregators of EVs in a proper manner, frequency of MG can be regulated. However, authors have discussed only about the charging process of EV batteries. Gouveia et al. [81] discussed the role of EV batteries to provide primary frequency regulation to MG. Authors have explained the role of EV's battery to support frequency of MG by applying droop control method. Mortaz and Valenzuela [82] have discussed that load demand of the MG can be met by the EVs. Authors have considered the intermittent RES as well as variable load profile of MG to illustrate the importance of EVs as an ESS. In [83] [84] authors have used the combination of battery ESS, EVs and renewable energy sources (RES) to support the MG. Farrokhabadi *et al.* [85] elaborated the frequency regulation of islanded MG by regulating its voltage through droop control technique. Jin *et al.* [86] discussed about the optimized charging of EVs using RES. Several authors have considered EVs as an ESS to provide support to the MG. In this chapter, frequency support to the MG has been provided using two different techniques. One is the VSG control technique and other is the droop control. Two techniques have been applied on same system and comparison of both the techniques has been done.

3.1.1 Motivation

Several researchers have investigated the idea of frequency control of islanded MGs. Some investigators have regulated the frequency using the controlled co-ordination of ESS and RES. Further, for this controlled coordination authors have applied the various types of techniques. Several authors have adopted the droop control strategy for regulating the frequency of MG [73] [79]. Few have implemented the VSG control technique for the same purpose [39] [51] . However, these authors have used battery banks as an ESS for MG to illustrate the frequency regulation process. None of them,

considers the EVs parked at the CS for frequency regulation purpose. In this chapter, EVs parked at the CS have been used as an ESS for the MG. Moreover, unexpected ingress and egress of EVs at the CS has been considered while supporting the MG's frequency. Comparison of the droop control and VSG control techniques has been done while providing the frequency support using EVs as an ESS for the islanded MG.

3.1.2 Contribution

- In this chapter, comparison of droop control and VSG control technique has been done by considering the EV batteries as an ESS for the islanded MG.

3.1.3 Organization

The other sections of the chapter are summarized as follows, Section 3.2 demonstrates the proposed work. Section 3.3 represents the mathematical formulation of the work. Results and discussions have been shown in Section 3.4. Summary of the work is mentioned in Section 3.5.

3.2 Proposed Work

In the proposed work, one CS has been considered to balance the load profile of islanded MG and consequently to regulate the MG's frequency. In the considered system, CS, PV array and diesel generator are connected in parallel to accommodate the load profile of MG. As the power supplied by PV array is irregular and dynamic characteristics of the diesel generator have slow response, EVs parked at the CS can participate to regulate the frequency of MG. Frequency support to the system has been provided by using two different techniques. One is the droop control technique and other is the VSG control. Frequency of the system can be supported by using both the techniques. Although, non-negligible virtual inertia effect can be provided

through droop control technique by modifying the filter time constant used in common power frequency droop based control strategies. However, in this work, authors have used VSG control method in order to emulate the the virtual inertia and hence to regulate the frequency of MG. The VSG concept relies on the emulation of inertial characteristics by the power converter in MG with the coordination of ESS. Using VSG technique, power converter can manage the flow of active power like a synchronous generator. Comparison of both the methods has been done to observe the effectiveness of applied technique to regulate the frequency of MG. The energy stored in the dc link (DL) as well as EV batteries can be used to provide the virtual inertia to the system. This virtual inertia assists to minimize the change in frequency due to sudden changes in load. In this work, EVs parked at CS are assumed as an ESS for MG. In order to manage the load profile of the MG, these EVs can be charged and discharged at the frequent intervals. In case of VSG control, virtual inertia is imitated from the energy stored in the DL capacitor.

Fig. 3.1, illustrates the diagram to accommodate the load profile of islanded MG using CS and PV array, where CS consists of fleet of EVs and buck boost converters. In this work, EVs of various battery voltage ratings has been considered while the output voltage of each buck-boost converter is kept constant. The EV battery charges during the buck mode of dc-dc converter, while it begins to discharge during boost mode. These buck-boost converters are connected with common dc bus.

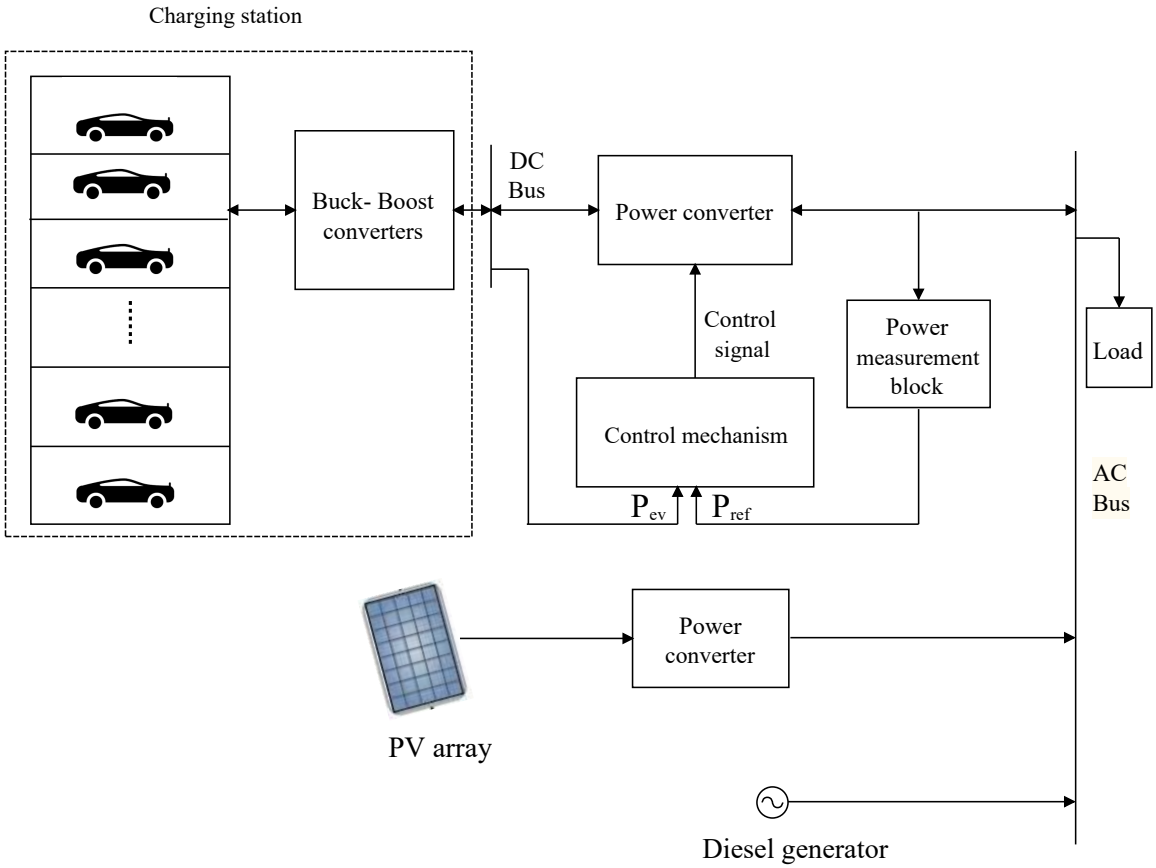

Figure 3.1: Generalized diagram of the proposed system

3.3 Control Strategy

In this work, PV array, CS and diesel generator act as sources of generation, so the total power from all the sources can be written as,

$$P_{total} = P_{pv} + P_{dg} + P_{ev} \tag{3.1}$$

Where, P_{dg}, P_{pv} and P_{ev} represents the power delivered by diesel generator, PV array and by CS respectively and P_{total} indicates the total generated power.

$$\Delta w = -\frac{P_{load} - P_{total}}{\frac{P_{max}^{dg}}{k_p * w_{nom}} + \frac{P_{max}^{pv}}{k_p * w_{nom}} + \frac{P_{ev}}{k_p * w_{nom}}} \tag{3.2}$$

In eq. 3.2, Δw represents the change in angular frequency and P_{load} represents the load of the system. P_{max}^{pv} and P_{max}^{dg} indicates the maximum power that can be delivered by the PV array and diesel generator respectively. k_p and w_{nom} represents the droop gain and nominal angular frequency of the system.

$$P_{dg}^{ref} = P_{dg} + \frac{\Delta w P_{max}^{dg}}{k_p * w_{nom}} \tag{3.3}$$

Eq. 3.3 represents the reference power for the diesel generator. Further, by substituting the Eq. 3.2 into 3.3 the following equation can be obtain as follows,

$$P_{dg}^{ref} = P_{dg} + \frac{(P_{load} - P_{total}) P_{max}^{dg}}{P_{max}^{dg} + P_{ev} + P_{max}^{pv}} \tag{3.4}$$

Eq. 3.4 represents the required power from the diesel generator which needs to be delivered when the frequency of the system changes.

This P_{dg}^{ref} act as reference power for the diesel generator. Fig. 3.2 depicts the frequency droop control mechanism for the diesel generator. Where, T_f indicates the time constant of filter. The P_{dg} is allowed to go through the filter to increase the δP of the system. Further, the integral of the angular frequency response w_r has been taken to obtain the reference voltage phase angle θ from the droop controller.

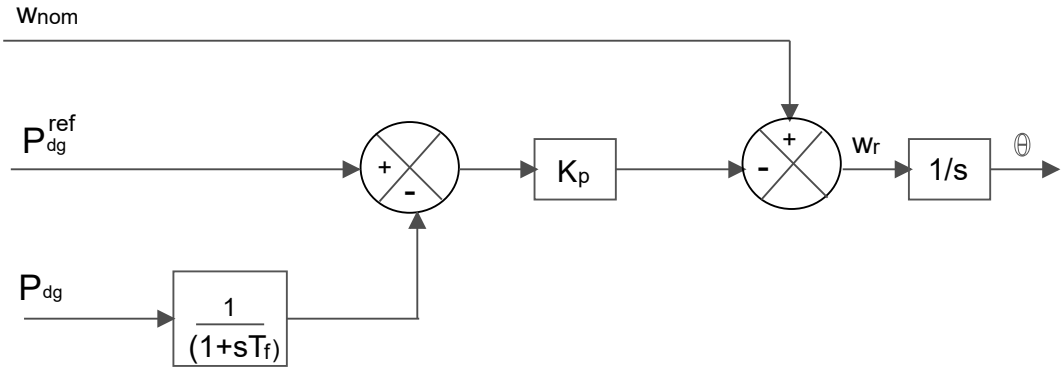

Figure 3.2: Frequency Droop Control for Diesel Generator

Basic motive of applying the VSG technique is to provide the frequency regulation to the system in an effective way. This frequency regulation is provided by minimizing the gap between load demand of islanded MG and power generated by RES. This mismatch is reduced by providing the active power to the MG by emulating the virtual inertia from energy stored in the battery of EVs. Depending on the amount of energy stored in the EVs which are parked in the parking lot of CS, active power can be delivered to the MG. Further, remaining part of the energy stored in the EVs can be used to emulate the virtual inertia. Active power is controlled in a bidirectional way using power converter. VSG mechanism to control the bidirectional flow of power is based on the following swing equation.

$$P_{ref} - P_{ev} = Jw_r \frac{dw_r}{dt} - D\delta w_r \tag{3.5}$$

Where, P_{ref} is the required output power and P_{ev} is power consumed or released by the EVs parked at the CS. J is the virtual inertia of the system and D is the damping factor.

Where, net P_{ev} can be represented by the following equations,

$$P_{ev} = \sum_{k=1}^{r} P_k \tag{3.6}$$

$$P_{ev} = \sum_{k=1}^{l} P_{disc} - \sum_{k=l+1}^{r} P_{char} \tag{3.7}$$

Where, r represents the total number of EVs. l and $r - l$ indicate the number of vehicles in discharging and charging mode respectively.

By taking the Laplace transform of the Eq. (3.5) the following equation can be

obtained as,

$$P_{ref} - P_{ev} = Jsw_r - D(w_o - w_r) \tag{3.8}$$

Further, virtual angular velocity w_r can be calculated by using Eq. 3.8

$$w_r = \frac{Dw_o + (P_{ref} - P_{ev})}{Js + D} \tag{3.9}$$

Using Eq. 3.7, the Eq. 3.9 can be rewritten as follows,

$$w_r = \frac{Dw_o + P_{ref} - (\sum_{k=1}^{l} P_{disc} - \sum_{k=l+1}^{r} P_{char})}{Js + D} \tag{3.10}$$

In case of droop control method, inertia J is not taken into account. So, equation for droop control method will be

$$P_{ref} - P_{ev} = D(w_r - w_o) \tag{3.11}$$

$$w_r = w_o + \frac{P_{ref} - P_{ev}}{D} \tag{3.12}$$

$$w_r = w_o + \frac{P_{ref} - (\sum_{k=1}^{l} P_{disc} - \sum_{k=l+1}^{r} P_{char})}{D} \tag{3.13}$$

w_r is calculated in both the cases, which is further used to obtain the rotor angle. Depending upon the gap between the load demand of MG and power generated by RES, P_{ref} changes. This P_{ref} is managed by the power delivered by the EVs parked at the CS. The w_r is responsible to control the power converter, which further manages

the output power delivered by the CS.

3.4 Results and Discussion

In this section, simulations have been performed by considering the unpredictable load demand of MG as well as unexpected ingress and egress of EVs at the CS.

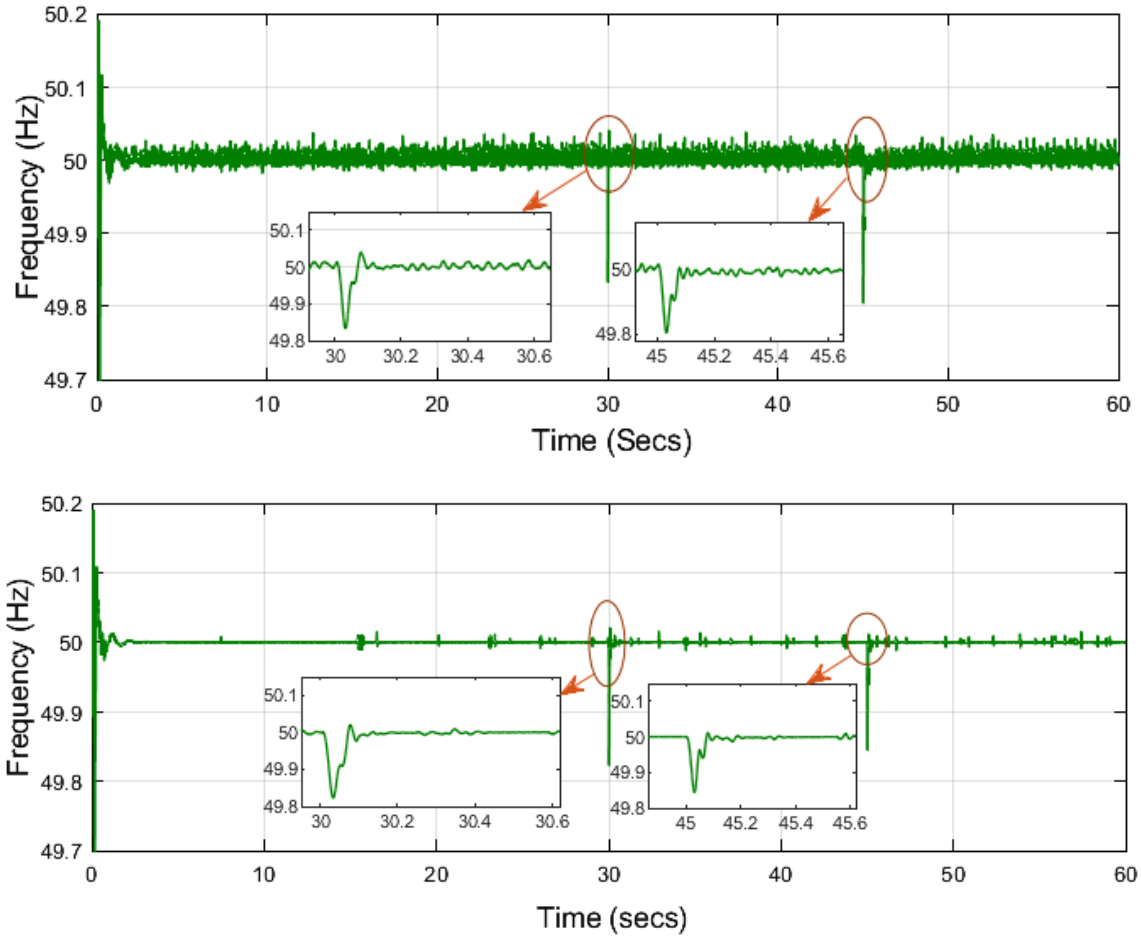

Figure 3.3: Frequency of MG (a) Droop (b) VSG technique

In this system one CS, PV array of 10.7 kW and diesel generator of 5 KVA ratings have been used. Comparison of the droop control and VSG control techniques has been done by considering EVs as an ESS for MG. Where, load demand of the MG is met by both the CS as well RES available at the MG. While doing the comparison between simple droop control and VSG control, zoomed portion of Fig. 3.3(a) shows there is large disturbance in frequency of the system, when droop control technique

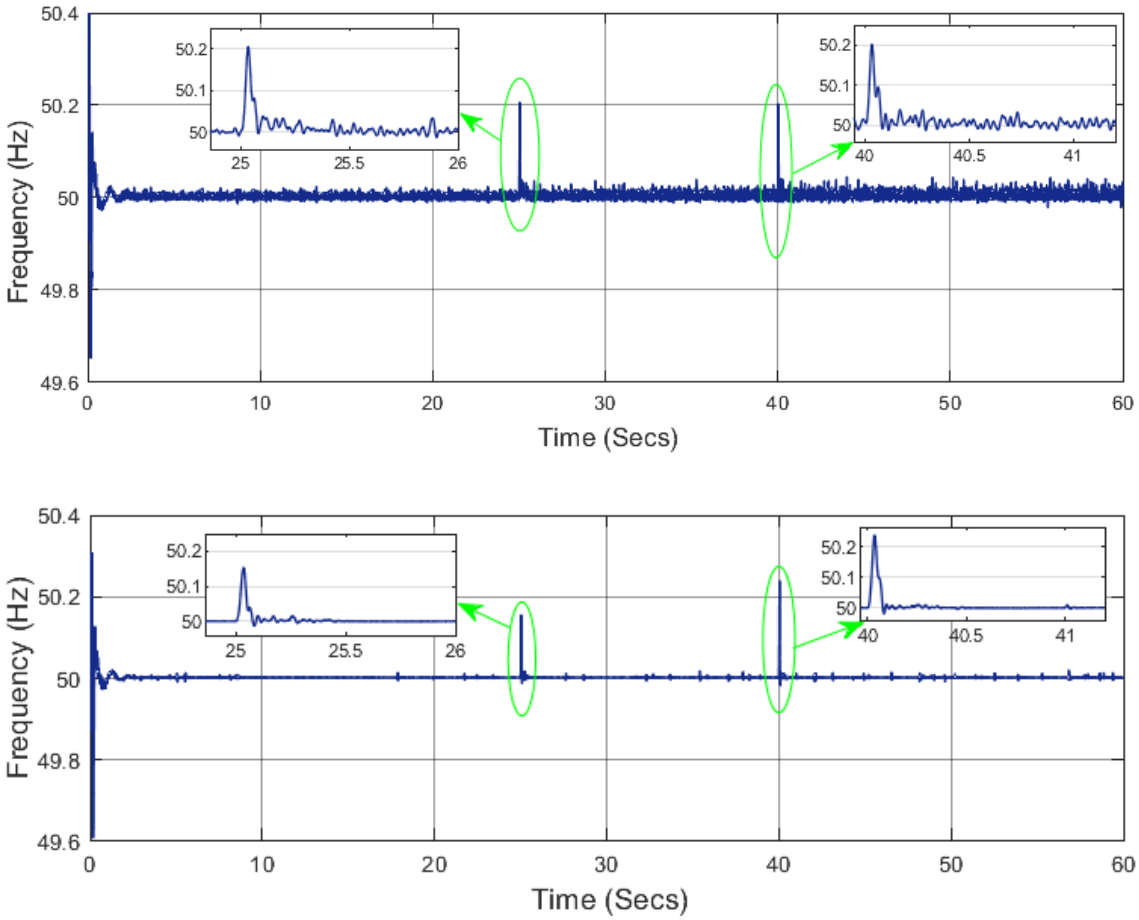

Figure 3.4: Frequency of MG (a) Droop (b) VSG technique

is used to regulate the frequency of MG. However, zoomed portion of the Fig. 3.3(b) shows frequency gets stabilized in an effective way by using the VSG control technique. Further, as per Fig. 3.4(a), there is large deviation in the frequency of system while using the droop control technique. On the other hand, as depicted in Fig. 3.4(b), frequency of the MG gets stabilized easily using VSG control. Based on these results it has been analyzed that VSG control can manage the MG's frequency in a better way.

3.5 Summary

EVs parked at the CS are capable of eliminating the observed deviations in frequency of islanded MG. Moreover, they can be used as movable ESS. It has been observed

from the results that frequency regulation of MG can be obtained through EVs even when they arrive and depart from the CS at unpredictable intervals of time. From the results it is very clear that frequency of islanded MG can be regulated in an effective way by implementing the VSG control technique. It can be concluded that disturbance in MG's frequency is reduced to a large extent through VSG control.

Chapter 4

VSG based frequency support in MG using EVs

4.1 Introduction

A microgrid (MG) is a small scale power grid, consisting of renewable energy sources (RES) and loads that can operate in both grid connected and islanded mode. In grid connected mode, it is synchronized with the main grid and in islanded mode, it provides supply to the loads connected with it.[1] MGs can provide power to the local loads such as military areas, hospitals and even to the remote areas where transmission and distribution of supply from main grid is strenuous [87]. MGs help to enhance the local reliability, support local voltages, voltage sag correction, reduce feeder losses and emission losses. Despite numerous advantages, there are various challenges in the MG operation. Dynamic load change and environment uncertainties are the two main factors that are responsible for making islanded MG operation more challenging. Authors [88] [89] demonstrated that inconsistent behavior of renewable energy sources (RES) during the operation of MG. In addition to low inertia, active

[1] The content of this chapter is taken from:

- K. Dhingra and M. Singh, "Frequency support in a microgrid using virtual synchronous generator based charging station," in IET Renewable Power Generation, vol. 12, no. 9, pp. 1034-1044, 2018, doi: 10.1049/iet-rpg.2017.0713.

and reactive power control are the major issues in MG. Frequency deviation is one of the major issue in islanded operation of an MG.

Many researchers have focused on the MG frequency regulation and have used various methods to regulate the frequency. Few of them discussed about the PV based MGs to provide the stability to the system. Watson *et al.* [90] have described the case of MG that consists of synchronous generator and the PV array connected through single phase inverter. Authors discussed that in case of load variation, the PV array can provide the reserve power through maximum power point tracking mechanism thus can regulate the frequency of the MG. Bacha *et al.* [91] have discussed that in MGs, intermittent nature of the PV array can be compensated by demand side management along with the use of energy storage system (ESS). Some authors have illustrated the various control topologies for PV inverters that can be used in MGs for different range of power and input voltages [92] [93]. Khalil *et al.* [94] have demonstrated about the PV based MG in which two parallel inverters that are connected with the PV arrays operate through different control loops to meet the load demand of the MG. However, the authors have not used any other source of generation in the MG as the PV arrays are intermittent in nature. Chamana *et al.* [95] discussed about the droop control technique in MG having the combination of PV array and the battery energy storage system. Authors described that ESS can provide the reserve power in case of power deficiency by PV array and get charged back in case of surplus power. Ramaiah *et al.* [96] discussed that frequency of the MG can be regulated by operating the PV array using variable rate limited power point tracking (LPPT) technique. Authors have suggested that the required amount of power can be extracted from the PV array using LPPT technique, where reference required power can be set by the droop control technique. However, the authors have not used any ESS as a back up for the MG system. Authors [97] [98] suggested a control system that utilized wind power for regulating the frequency of islanded MG. However, by virtue of seasonal and unreliable nature of wind, this concept was inefficient to regulate the frequency of islanded MGs. Hence, RES alone cannot be used for the purpose

of frequency regulation of the MG. Several authors have used energy storage system (ESS) for the frequency regulation of MG. Han *et al.* [99] discussed that RES in co-ordination with the ESS can be used for the frequency regulation of MG. Li *et al.* [100] deliberated that fuel cells in combination with electrolyzers can be used for the frequency regulation of MG. However, these ESS cannot be used for providing the power for long duration and even maintenance and installation cost of an ESS is very high. Although, various authors have used ESS to regulate the dynamic frequency of a MG yet they have not considered inertia to regulate frequency.

Some authors have demonstrated that the frequency of the MG can be supported by providing some form of inertia to the system. Some RES such as wind turbines have rotational mass, therefore, they can easily provide inertia to the system. On the other hand, RES such as PV system do not have any rotational mass and therefore, unable to provide any inertia to the system for regulating the frequency of MG. In such cases, virtual inertia can be provided to the system to regulate the frequency of the MG. In the case of MGs, distributed generators in combination with power converters have been used to emulate the virtual inertia. Some authors have used variable speed wind turbines to emulate the virtual inertia and hence to regulate the frequency of MG. Soni *et al.* [39] demonstrated that transient response of the power system can be improved by adding the virtual inertia to the system. Authors have applied the modified droop technique on inverters to allow them for bulk power exchange with the system. They have considered inertia as a function of rate of change of frequency to maintain the synchronism of all the connected sources. Morren *et al.* [42] discussed that the frequency can be regulated by emulating the virtual inertia from the variable speed wind turbines. In this concept of emulating inertia, kinetic energy stored in the rotating mass of wind turbine blades provides the required power to support the frequency of the system. However, authors have not considered the intermittent nature of wind turbine and have not used any energy storage device to provide the back up to the system. Alipoor *et al.* [41] demonstrated the effect of alternating moment of inertia on the power system stabilization. Authors have discussed that

in case of VSG transient energy can be eliminated directly by alternating the inertia while in case of real synchronous generator, this energy is dissipated by damping terms. Authors have further described that the stability of the power system can be improved by altering the moment of inertia.

Torres *et al.* [36] discussed a VSG mechanism through which inertia can be emulated from the wind and diesel power plants for the frequency regulation of MG. Authors have demonstrated that maximum deviation of the rotor speed is reduced by emulating the virtual inertia. However, with this inertia emulation response of the system becomes oscillatory and slower. Bevrani *et al.* [10] demonstrated various topologies using VSG to regulate the frequency of the MG. In these topologies, authors have used an ESS to emulate the virtual inertia. Zhong *et al.* [34] discussed that inverters can behave as VSG with proper control mechanism. However, they have not considered any ESS to emulate the virtual inertia. Authors [35] [101] examined that distributed generators along with virtual synchronous machines can be used for frequency stabilization of the grids. Driesen *et al.* [33] described that distributed generators in combination with short term energy storage can behave like VSGs and thus can add the virtual inertia to the system. Tripathy *et al.* [102] have discussed about the calculation of rotor angle using the synchrophasor measurements. Authors have explained that terminal voltage of the generator can be find out using this rotor angle. Mishra *et al.* [103] demonstrated that photo-voltaic based converter can behave as synchronous generator and thus can provide support to the MG during frequency deviation. Karapanos *et al.* [43] demonstrated VSG hardware in the loop and verified the results, in a real time simulation of the power system. Liu *et al.* [9] discussed the advantages of using VSG control mechanism over droop control. Authors have discussed that the frequency can be controlled in a better way using VSG. Shintai *et al.* [8] discussed that oscillations of active and reactive power can be damped by using the VSG. It has been observed that several authors have mentioned the importance of the VSG mechanism in the stabilization of a MG.

Several authors have paid attention on the role of EVs in MG. EVs can act as

an ESS for the MG. Moreover, EVs have the inherent capability to support the MG during peak and off-peak hours. EVs can act both as a source of generation as well as load for the MG. Kempton *et al.* [18] introduced the concept of vehicle to grid. Authors have discussed that EVs can provide the backup, where RES are used for the generation of electricity. In this way, reliability and stability of the system can be enhanced. Bhatti *et al.* [104] have proposed a concept of charging the EVs from MG that consists of PV array and energy storage units. Authors have used the lead acid battery to charge the EVs in case PV array is not able to meet the charging demand of EVs. Mortaz *et al.* [105] described that with the use of EVs as an ESS, operation cost of the MG can be reduced. Authors have explained that longer parking time of EVs leads to higher savings. Authors [81] have demonstrated that during the MG restoration phase, EVs can be used as grid-supporting units to take advantage of their storage capacity and charging flexibility. EVs can manage the frequency deviations of the MG that normally occurs during islanding condition of MG. Rana *et al.* [73] illustrated that frequency of the MG can be supported by using a fleet of EVs. Authors have used the modified droop control technique to provide the frequency support to the MG. However, the authors have not considered the absence of inertia in the distributed energy sources. Yilmaz *et al.* [21] discussed that vehicle to grid concept (V2G) can be utilized for the bidirectional flow of power between grid and EVs, where EVs have been used as an ESS. Authors also manifest that vehicle to grid approach can enhance the technical achievement of the grid in the fields such as reliability, stability and efficiency. Shimizu *et al.* [106] proposed a model for EVs integration in a V2G scenario for frequency regulation. In this model, charging and discharging of participating EVs was regulated based on load frequency control signals. The major shortcoming of this model was its inability to cater for the charging and discharging needs of EVs simultaneously. Lopes *et al.* [107] demonstrated that battery operated EVs can successfully participate in voltage balancing and to control the frequency of the islanded MG. Arani *et al.* [108] described that wind power generators in combination with EVs can contribute to the

frequency regulation of MG. Thus, several authors paid attention to the significance of EVs in frequency regulation of MG.

4.1.1 Motivation

Frequency deviation is one of the major hindrances in stable functioning of MG. It generally occurs due to the dynamic load profile of MG and intermittent nature of RES. Low or absence of inertia in MG is the main reason which further leads to frequency deviation. Several authors have proposed the concept of inertia to regulate the frequency of MG [39] [41]. Few authors have laid emphasis on the role of EVs as an ESS in the MG to support the frequency [73] [108]. Few of them [35] [36] discussed virtual inertia emulation by VSG mechanism to support the frequency of the MG. However, to the best of author's knowledge hardly anyone has implemented the VSG mechanism using EVs parked in charging station (CS) as an ESS. In the proposed work, frequency of the islanded MG is supported by implementing the VSG on EVs parked in the CS. Moreover, the dynamic nature of EVs can be catered by using the VSG mechanism without affecting the rest of the MG system.

4.1.2 Novelty

Novelty of this chapter lies in the following aspects: First, CS is used to support the frequency of the islanded MG. As per the authors best knowledge, no one has used the VSG mechanism in the CS to support the frequency of the islanded MG. Further, considering the future penetration of EVs in large numbers, the proposed method will be a good solution to support the frequency of an islanded MG. Second, from the design point of view, in most of the works till now, battery energy storage system and the PV array are connected through the single dc link and controlled through single dc/dc converter. However, in this work, the CS and the PV array are connected through distinct dc links and are controlled independently, considering the future extension of the MG.

4.1.3 Contribution

The primary contributions of this chapter are as follows:

- In this chapter, bidirectional flow of power between the CS and islanded MG is controlled through the VSG control mechanism.
- Frequency of the system is supported through VSG, while considering the dynamic nature of irradiation level of the PV array and load profile of the MG.
- It has been verified that response time of the CS to any load change or fluctuation in the system is less as compared to the response time of the diesel generator.

4.1.4 Organization

The chapter is organized as follows. Section 4.2 represents the proposed methodology of the work while the VSG mechanism is demonstrated in Section 4.3. Section 4.4 represents the mathematical formulation of control mechanism. Simulations and results are discussed in Section 4.5. The chapter is summarized in the Section 4.6.

4.2 Proposed Methodology

In the proposed work, an islanded MG consisting of PV array, diesel generator and a fleet of EVs is considered. A fleet of EVs parked in the CS is considered as an ESS for the MG. VSG control mechanism is implemented on the considered MG system to support its frequency. Frequency of the system is supported by controlling the bi-directional flow of power between the CS and the MG. The schematic diagram of the proposed scheme has been shown in Fig. 4.1 and explained as given below,

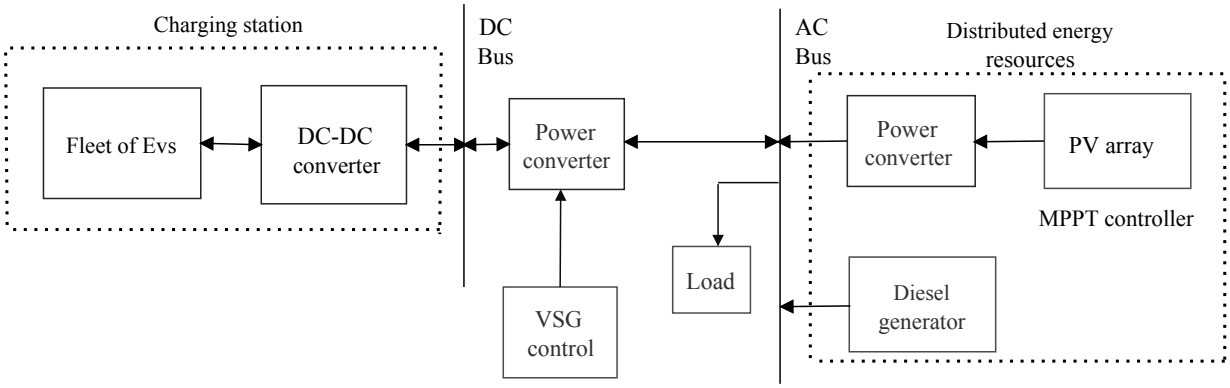

Figure 4.1: Schematic diagram of the proposed islanded microgrid

4.2.1 Charging station

The aim of modelling the CS is to organize the bi-directional flow of power between EVs and MG. As depicted in Fig. 4.1, a fleet of EVs parked in the CS is considered as an ESS. Use of EVs as an ESS has an advantage as they can be used both in transportation as well as to support the MG for balancing the load demand. EVs can act both as a source of power as well as load for MG. In the CS, EVs as an ESS either absorb or deliver the power from or to the MG as per the frequency regulation requirement. EVs parked in the CS may have different state of charge (SoC) levels but constant power can be fed to the power converter through dc-dc converters.

DC-DC converters DC-DC converters act as an interface between a fleet of EVs and power converters, and can be classified either as unidirectional or bidirectional converters. In this work, bi directional dc-dc converters have been used as they can operate in both buck and boost mode [109]. In buck mode of operation, dc-dc converters step down the voltage while in boost mode voltage is stepped up. The fleet of EVs gets discharged during boost mode and is charged back during the buck mode of operation. DC-DC converters, convert the unregulated dc supply to a regulated dc supply. For this purpose, switched mode dc-dc converters store the input energy for short duration and then release that energy to the dc bus at a different voltage level. This energy is stored either in the magnetic field (inductor) or in electric field (capacitor). The released energy appears across the resistor as output voltage. In

this way, the required voltage is provided to the dc bus. The output voltage for buck boost converter is represented by,

$$V_o = -\frac{d}{1-d}V_{in} \tag{4.1}$$

In Eq. 4.1, d is the duty cycle and its value lies between 0 and 1, V_o is the output voltage of the converter and V_{in} is the input voltage to the converter. Duty cycle represents the ratio of turn on time of the switch to the total time.

4.2.2 Design of Buck-Boost Converter

Buck boost converter is designed by selecting the suitable values of L and C. The value of L and C is determined in the following way.

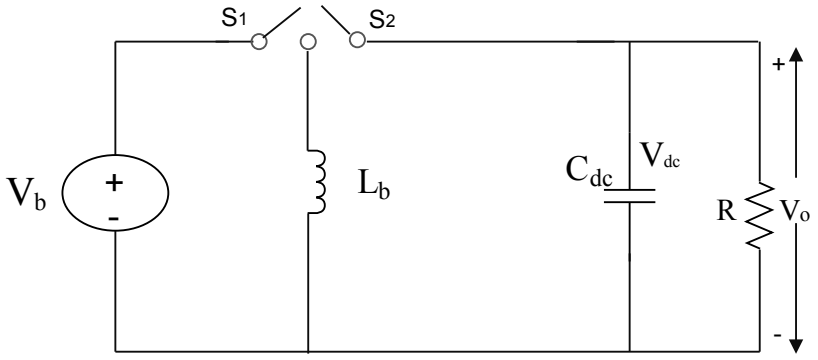

Figure 4.2: Buck Boost converter

Selection of Inductor: The value of inductor for the buck boost converter is estimated as,

$$L_b = \frac{V_b T d}{\Delta I_c} \tag{4.2}$$

where, V_b is the battery terminal voltage, T is the switching time for PWM, d is the duty cycle, I_c is the current through inductor and ΔI_c is the ripple current of inductor. Value of d, V_b and T is considered as 0.6, 400 V and 40 μsec respectively and ripple current is considered as 1% of the actual inductor current. Value of L_b

based on these parameters is calculated as follows,

$$L_b = \frac{(0.6)(400)(40 \times 10^{-6})}{(0.1 \times 120)} = 80\ mH \tag{4.3}$$

Selection of dc link Capacitor: The value of dc link capacitor is estimated as,

$$C_{dc} = \frac{V_{dc} d}{R f_s \Delta V_{dc}} \tag{4.4}$$

where, V_{dc} is the dc link voltage of the capacitor and ΔV_{dc} is the ripple in dc link voltage, R is the resistance at the output terminal. Value of f_s and V_{dc} is taken as 25 kHz and 600 V respectively. Ripple in dc link voltage is considered as 5% of the actual voltage. Value of C_{dc} based on the considered parameters is calculated as follows,

$$C_{dc} = \frac{600 \times 0.6}{0.48 \times 25 \times 10^3 \times (0.05 \times 600)} = 1000\mu F \tag{4.5}$$

4.2.3 Stability analysis of buck boost converter

Stability analysis of the buck boost converter has been done through the state space model. The switches S_1 and S_2 as depicted in Fig. 4.2, are turned on and turned off as per the command obtained through PWM (dc-dc). Fig. 4.3 depicts the circuit diagram of the buck boost converter when the switch S_1 is in on condition.

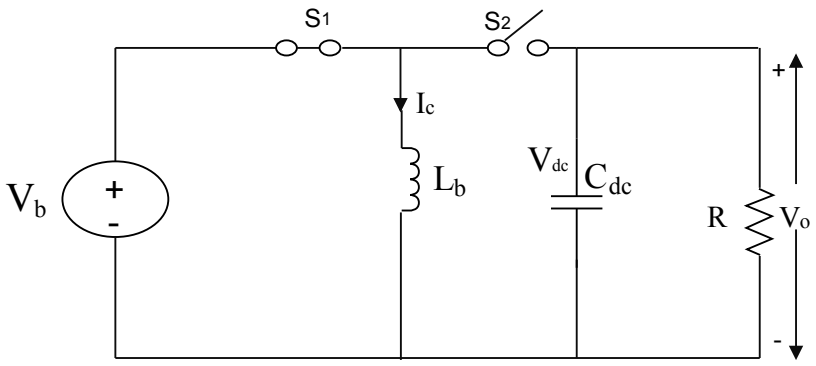

Figure 4.3: Switch S_1 is in on condition

By applying the Kirchoff's voltage and Kirchoff's current law to the circuit shown in Fig. 4.3, the following equations are obtained.

$$V_b - L_b \frac{dI_c}{dt} = 0 \tag{4.6}$$

$$\frac{V_{dc}}{R} + C_{dc} \frac{dV_{dc}}{dt} = 0 \tag{4.7}$$

In state space form, Eq. 4.6 and Eq. 4.7 can be written as,

$$x_1' = A_1 x + B_1 u \tag{4.8}$$

$$y_1 = C_1 x + D_1 u \tag{4.9}$$

where, Eq. 4.8 and Eq. 4.9 represents the state space equation and the output equation of buck boost converter respectively. x represents the state variables I_c and V_{dc} respectively and x' represents the differential form of these state variables. y_1 represents the output variable and u indicates the input state for the buck boost converter. Value of u will be 1 if input is in on condition, else it will be zero. A_1, B_1, C_1 and D_1 are the ABCD parameters of the buck boost converter. The Eq. 4.8 and Eq. 4.9 can be expressed in the form of following equations.

$$\begin{bmatrix} \frac{dI_c}{dt} \\ \\ \frac{dV_{dc}}{dt} \end{bmatrix}_1 = \begin{bmatrix} 0 & 0 \\ 0 & -1/RC_{dc} \end{bmatrix} \begin{bmatrix} I_c \\ V_{dc} \end{bmatrix} + \begin{bmatrix} 1/L_b \\ 0 \end{bmatrix} V_b \tag{4.10}$$

$$V_{01} = \begin{bmatrix} 0 & 1 \end{bmatrix} \begin{bmatrix} I_c \\ V_{dc} \end{bmatrix} \tag{4.11}$$

where,

$$x_1' = \begin{bmatrix} \frac{dI_c}{dt} \\ \\ \frac{dV_{dc}}{dt} \end{bmatrix}_1, x = \begin{bmatrix} I_c \\ \\ V_{dc} \end{bmatrix}, u = V_b, V_{01} = y_1 \tag{4.12}$$

$$A_1 = \begin{bmatrix} 0 & 0 \\ 0 & -1/RC_{dc} \end{bmatrix}, B_1 = \begin{bmatrix} 1/L_b \\ 0 \end{bmatrix}, C_1 = \begin{bmatrix} 0 & 1 \end{bmatrix}, D_1 = 0 \tag{4.13}$$

Fig. 4.4 depicts the circuit diagram of the buck boost converter, when S_2 is in on condition.

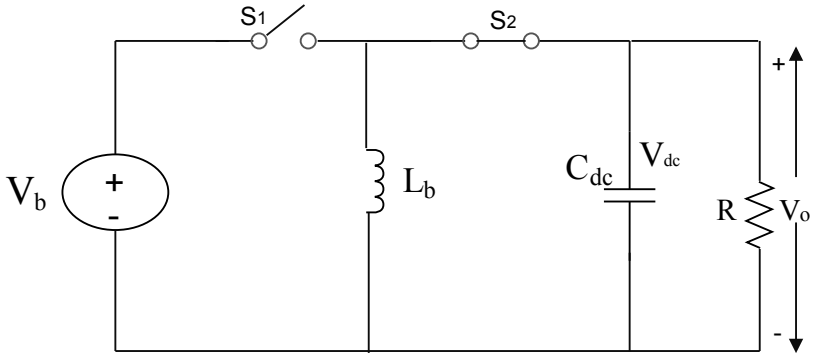

Figure 4.4: Switch S_2 is in on condition

By applying the Kirchoff's voltage and Kirchoff's current law to the circuit as depicted in Fig. 4.4, the following equations are obtained.

$$L_b \frac{dI_c}{dt} + V_{dc} = 0 \tag{4.14}$$

$$I_c - \frac{V_{dc}}{R} - C_{dc} \frac{dV_{dc}}{dt} = 0 \tag{4.15}$$

In state space form, Eq. 4.14 and Eq. 4.15 can be written as below,

$$x_2' = A_2 x + B_2 u \tag{4.16}$$

$$y_2 = C_2 x + D_2 u \tag{4.17}$$

$$\begin{bmatrix} \frac{dI_c}{dt} \\ \\ \frac{dV_{dc}}{dt} \end{bmatrix}_2 = \begin{bmatrix} 0 & -1/L_b \\ 1/C_{dc} & -1/RC_{dc} \end{bmatrix} \begin{bmatrix} I_c \\ V_{dc} \end{bmatrix} + \begin{bmatrix} 0 \\ 0 \end{bmatrix} V_b \tag{4.18}$$

$$V_{02} = \begin{bmatrix} 0 & 1 \end{bmatrix} \begin{bmatrix} I_c \\ V_{dc} \end{bmatrix} \tag{4.19}$$

where,

$$x_2' = \begin{bmatrix} \frac{dI_c}{dt} \\ \\ \frac{dV_{dc}}{dt} \end{bmatrix}_2, V_{02} = y_2 \tag{4.20}$$

$$A_2 = \begin{bmatrix} 0 & -1/L_b \\ 1/C_{dc} & -1/RC_{dc} \end{bmatrix}, B_2 = \begin{bmatrix} 0 \\ 0 \end{bmatrix} \tag{4.21}$$

$$C_2 = \begin{bmatrix} 0 & 1 \end{bmatrix}, D_2 = 0$$

The average state space model of the buck boost converter has been expressed by the

following equations [110].

$$x' = dx'_1 + (1-d)x'_2 \tag{4.22}$$

$$y = dy_1 + (1-d)y_2 \tag{4.23}$$

From Eq. 4.22 and Eq. 4.23, the following expressions can be derived,

$$\begin{bmatrix} \frac{dI_c}{dt} \\ \\ \frac{dV_{dc}}{dt} \end{bmatrix} = \begin{bmatrix} 0 & (d-1)/L_b \\ (1-d)/C_{dc} & -1/RC_{dc} \end{bmatrix} \begin{bmatrix} I_c \\ V_{dc} \end{bmatrix} + \begin{bmatrix} d/L_b \\ 0 \end{bmatrix} V_b \tag{4.24}$$

$$V_0 = \begin{bmatrix} 0 & 1 \end{bmatrix} \begin{bmatrix} I_c \\ V_{dc} \end{bmatrix} \tag{4.25}$$

where,

$$A = \begin{bmatrix} 0 & (d-1)/L_b \\ (1-d)/C_{dc} & -1/RC_{dc} \end{bmatrix}, B = \begin{bmatrix} d/L_b \\ 0 \end{bmatrix} \tag{4.26}$$

$C = \begin{bmatrix} 0 & 1 \end{bmatrix}, D = 0$

As depicted in Fig. 4.5, bode plot has been drawn using the ABCD parameters of the state space model to determine the stability of the buck boost converter. It has been observed from the plot that the system is stable with a phase margin of 132° at a frequency of 1.07 rad/sec.

Control topology of buck boost converter:

In the CS, bidirectional flow of power between an EV's battery and dc bus is controlled through the buck boost converter. The dc link voltage and EV's battery current are

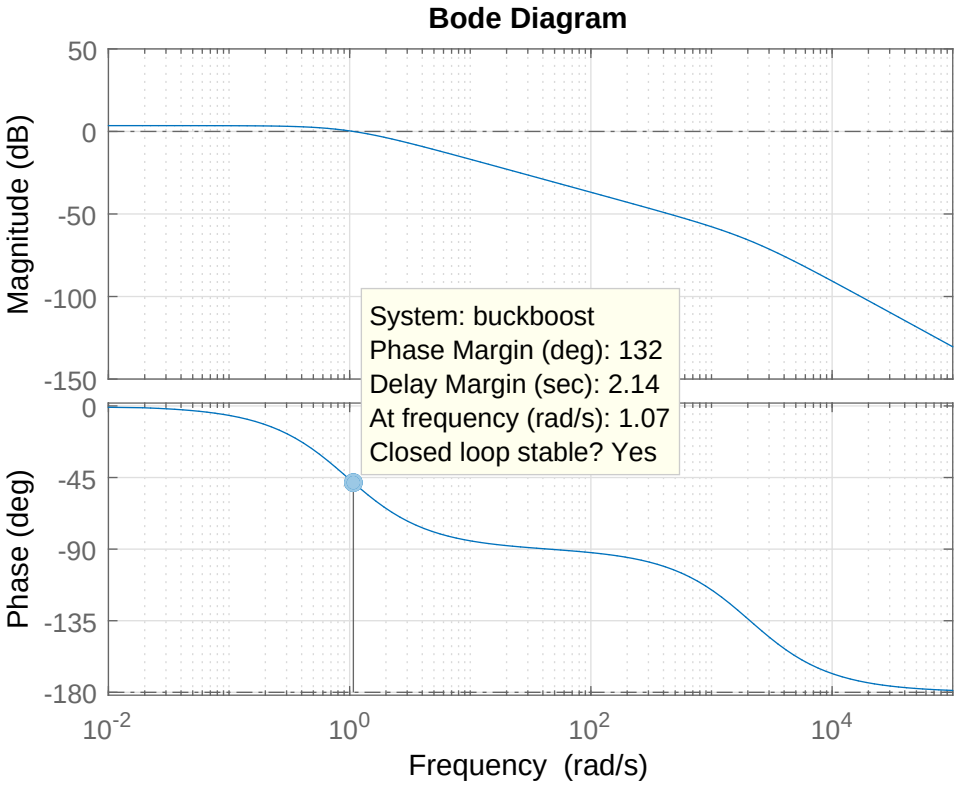

Figure 4.5: Bode plot of the buck boost converter

controlled through two control loops. The outer loop is the voltage control loop and inner loop is the current control loop. As per Fig. 4.6, the actual dc link voltage V_{dc} is compared with the reference dc link voltage V_{dcref} and a reference current signal I_{cref} is generated through the PI controller [111]. This reference current value is further compared with the actual inductor current to generate the control signal for a pulse width modulator (PWM) through the PI controller. This control mechanism is represented by Eq. (4.27) and Eq. (4.28) as shown below.

$$I_{cref} = (V_{dcref} - V_{dc})\frac{K_{pv}.s + K_{iv}}{s} \tag{4.27}$$

$$V_{ref} = (I_{cref} - I_c)\frac{K_{pi}.s + K_{ii}}{s} \tag{4.28}$$

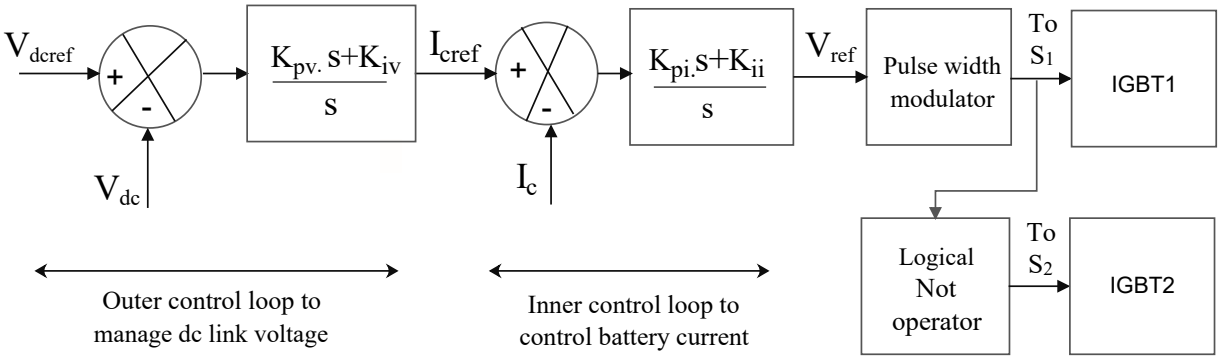

Figure 4.6: Buck-boost converter control strategy

where, K_{pv} and K_{iv} are the proportional and integral gain parameters for the outer control loop and K_{pi} and K_{ii} are proportional and integral gain parameters for the inner current loop. The value of these parameters is given in Table 4.2. I_{cref} is the reference current for inductor which is generated as per Eq. (4.27), I_c is the actual current flowing through the inductor and V_{ref} is the control signal for the PWM (dc to dc). Pulses generated by the PWM are used to fire the IGBTs, one IGBT is fired through S_1 and the other through S_2. Firing of an IGBT is controlled by the duty cycle of the PWM, with this controlled firing, dc-dc converter acts as buck boost converter. Energy stored in the dc link capacitor during this buck boost operation of dc-dc converter act in place of the kinetic energy for the system to provide the virtual inertia to the system.

4.2.4 Power converter (DC-AC)

Power converter converts the dc supply to ac and vice versa. Power converters are mainly of two types, voltage source converter and current source converter. In this work, voltage source converter has been used, where input voltage to the converter from the dc bus is kept constant, while the output power delivered by the converter varies by controlling the switching of PWM [112]. When the power generation is more as compared to the load demand, the frequency of the system increases and power converter delivers the power to the CS. On the other hand, when the load demand is more as compared to the power generation, frequency of the system decreases and the

power converter fetches the required power from the CS to meet the load demand. Thus, bidirectional flow of power takes place between the CS and the MG through power converter to maintain the frequency of the MG. The amount of power flow depends on the deviation of MG frequency from its nominal value. This bidirectional flow of power has been controlled through the VSG mechanism by applying proper control signals to the power converter through PWM. The filter used in the process of conversion of power from dc to ac is low pass RLC filter having values of L and C as $50mH$ and $10\mu F$ respectively.

4.2.5 Distributed energy sources

In the proposed work, a PV array and a diesel generator act as distributed energy sources (DES) and the AC bus behaves as a point of common coupling. As depicted in Fig. 4.1, loads connected with the AC bus are met with the parallel operation of the VSG and DES. The power delivered by the PV array is intermittent in nature and depends on its irradiation level. In the case, when the power delivered by the PV array is insufficient to meet the load demand, the required power is provided by the CS through the VSG control mechanism.

Diesel generator

Diesel generator consists of excitation system, diesel engine governor and alternator. Excitation system, further consists of two elements, voltage regulator and exciter. Voltage regulator, regulates the voltage at the output terminals of rotor. Diesel engine governor model governs the speed of engine. Diesel generator is simulated based on the dynamic equations of the exciter and diesel engine governor model [113].

Dynamic equation of exciter: In the diesel generator, exciter is used to provide the required field current to the rotor winding of the diesel generator. This field current controls the magnetic field of rotor to provide the output voltage. Dynamic

equations of the dc exciter [113] are described below,

$$T_e \frac{dE_{fv}}{dt} = V_p - K_e E_{fv} \tag{4.29}$$

$$T_f \frac{dR_d}{dt} = -R_d + \frac{K_g}{T_f} E_{fv} \tag{4.30}$$

$$T_a \frac{dV_p}{dt} = -V_p + K_c R_d - \frac{K_c K_g}{T_f} E_{fv} + K_c(V_{ref} - V) \tag{4.31}$$

where, T_e represents the time constant of exciter, T_f indicates the stabilizer time constant. K_e is the gain constant of exciter, V_p is the output voltage of the pilot exciter of diesel generator. K_g is the self or separately excited gain constant, R_d represents the rate feedback of the system and E_{fv} is the field voltage. T_a represents the amplifier time constant, K_c indicates the amplifier gain constant, V_{ref} is the reference voltage and V is the voltage magnitude of the diesel generator.

Diesel engine governor model: Governor is used to govern the speed of the diesel engine.

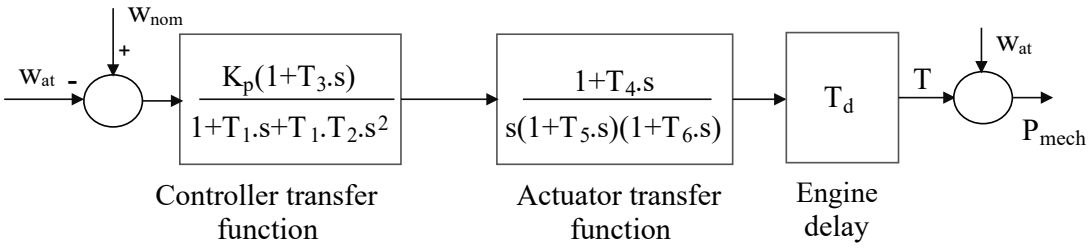

Figure 4.7: Diesel engine governor model

Fig. 4.7, depicts the governor model of the diesel engine, where, w_{at} and w_{nom} represents the actual speed and nominal speed of turbine respectively. K_p indicates the controller gain and T_d represents the engine delay of the system. T_1, T_2 and T_3 are the time constants for controller transfer function and T_4, T_5 and T_6 are the time constants for actuator transfer function. The values of these time constants has been given in Table 4.1. In this model, actual speed of the engine is compared with its

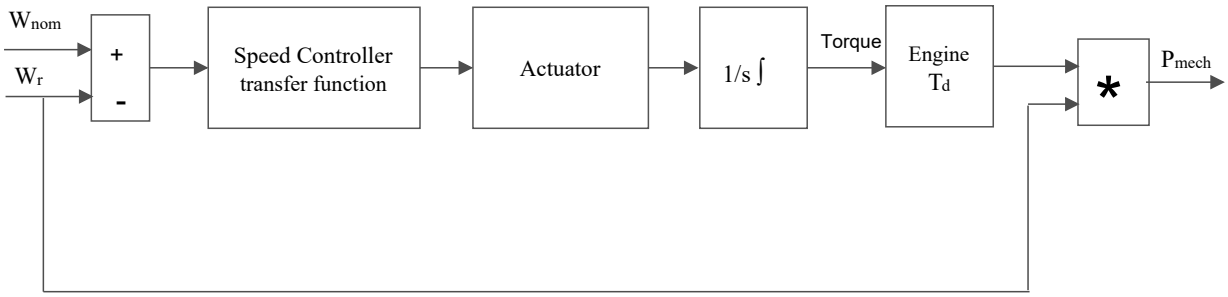

Figure 4.8: Speed Control Model of Diesel Engine

nominal speed and the resulting error signal is given to the controller as an input.

Through this governor model, torque is generated that is further converted to the mechanical power as shown in Fig. 4.7. Further, Fig. 4.8 represents the simplified form of Fig. 4.7. The mechanical power P_{mech} generated through the governor is converted to the electrical power P_{dg} through alternator. Further, the swing equation for diesel generator in Laplace transform can be written as,

$$Js.w_r - K.w_r = P_{mech}(s) - P_{dg}(s) \tag{4.32}$$

By assuming,

$$\delta P(s) = P_{mech}(s) - P_{dg}(s) \tag{4.33}$$

By using eq. 4.32 and eq.4.33, the following equation can be derived as follows,

$$\delta P(s) = Js.w_r - K.w_r \tag{4.34}$$

Further, the eq. 4.34 can be written in the following way,

$$\delta P(s) = (Js - K)w_r \tag{4.35}$$

The value of w_r deceases due to the difference between P_{mech}(s) and P_{dg}(s). Because to this, governor of the diesel engine increases the P_{mech}(s) with relatively high time constant due to the delay of fuel injection process. Further, δP(s) can be gained by allowing the P_{dg}(s) to go through high pass filter. Supporting a first order high pass

filter with time constant T_f, δP(s) can be mathematically modeled in the frequency domain, as follows:

$$\delta P(s) = -P_{dg}(s)(\frac{T_f.s}{1+T_f.s}) \tag{4.36}$$

By substituting the eq. 4.36 into eq. 4.35, the following equation can be obtained as follows,

$$w_r(s) = -P_{dg}(s)(\frac{T_f.s}{(1+T_f.s)(Js-K)}) \tag{4.37}$$

By considering the initial state $w_r(0)$ for $w_r(t)$, the solution of the eq. 4.37 in time domain will lead to the droop curve for the diesel generator.

Table 4.1: Parameters of diesel generator

Parameter	**Value**
Gain constant of exciter K_e	1
Time constant of exciter T_e	0
Amplifier gain constant K_c	300
Amplifier time constant T_a	0.001
Controller gain K_p	29
Time constants of controller (T_1, T_2, T_3)	0.01, 0.02, 0.2 sec
Actuator time constants (T_4, T_5, T_6)	0.25, 0.009, 0.0384 sec
Mechanical torque limits (T_{min}, T_{max})	0, 1.1 N.m
Engine delay T_d	0.024 sec

4.3 Virtual Synchronous Generator

VSG is the combination of ESS, power converter and proper control mechanism. The role of VSG is to exhibit the dynamic properties of a real synchronous generator so that the stability of the system can be improved.

VSG plays a very important role in the islanded operation of MG to balance the load demand. The combination of the CS and VSG control mechanism act as a real synchronous generator for MG in terms of inertia and damping property.

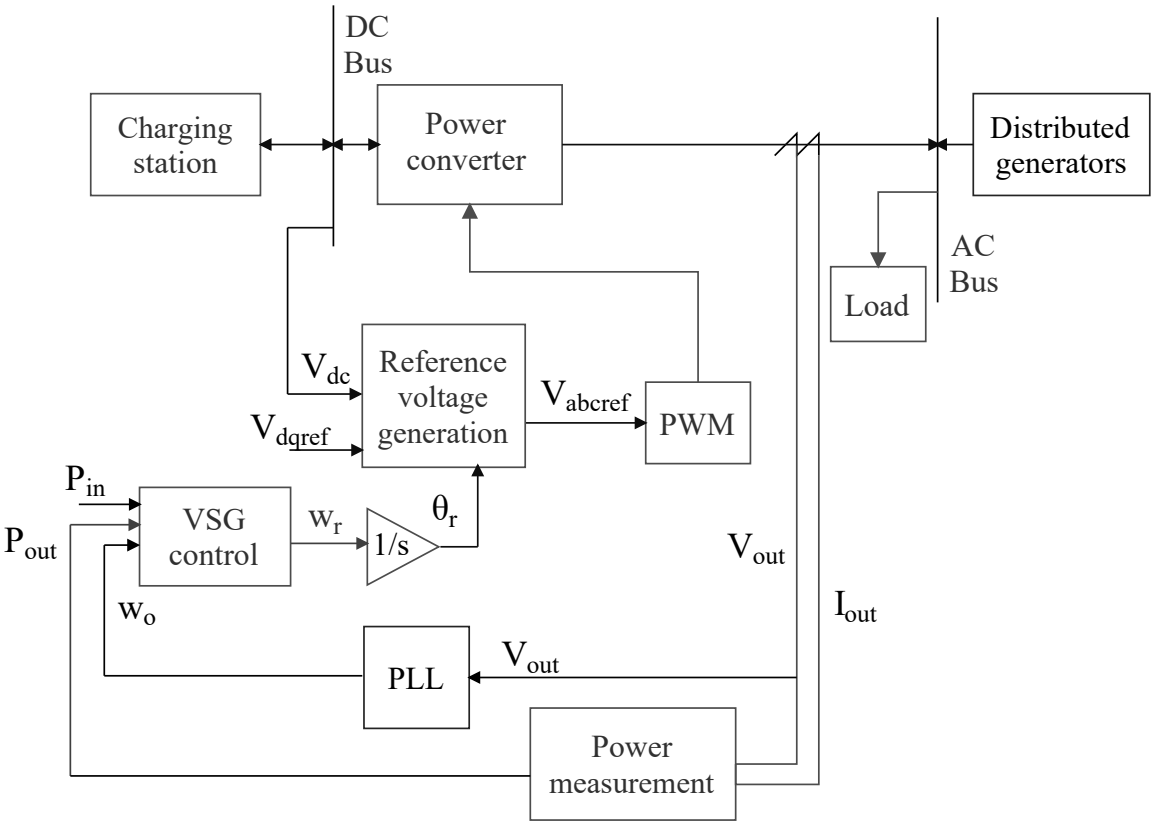

Figure 4.9: VSG control mechanism

The control mechanism of VSG is shown in Fig. 4.9, while Fig. 4.10 illustrates about the generation of V_{dref} and V_{qref}. In Fig. 4.11 the dc link voltage of ESS is used for the generation of control signal for PWM through VSG control. Virtual inertia is emulated from the EV's batteries using VSG control mechanism to minimize the mismatch between power generation and load demand of MG and hence to support the frequency of the system.

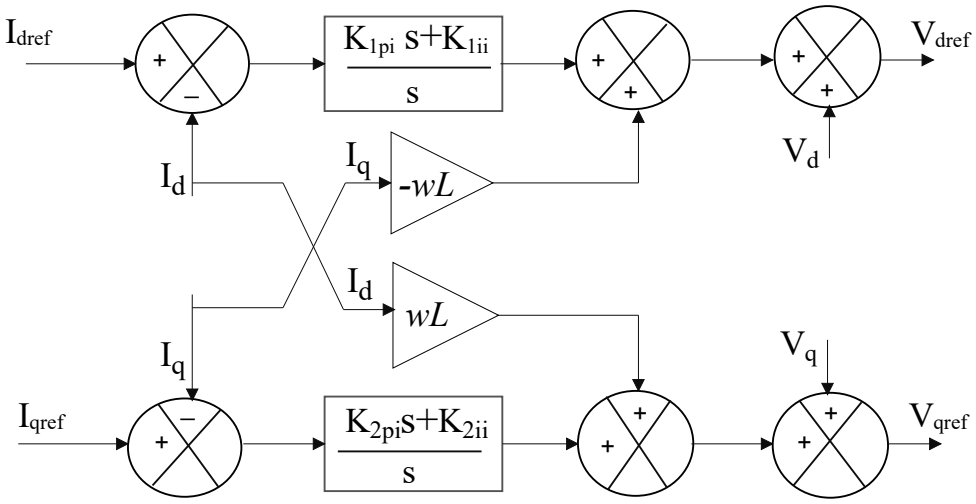

Figure 4.10: Current control scheme

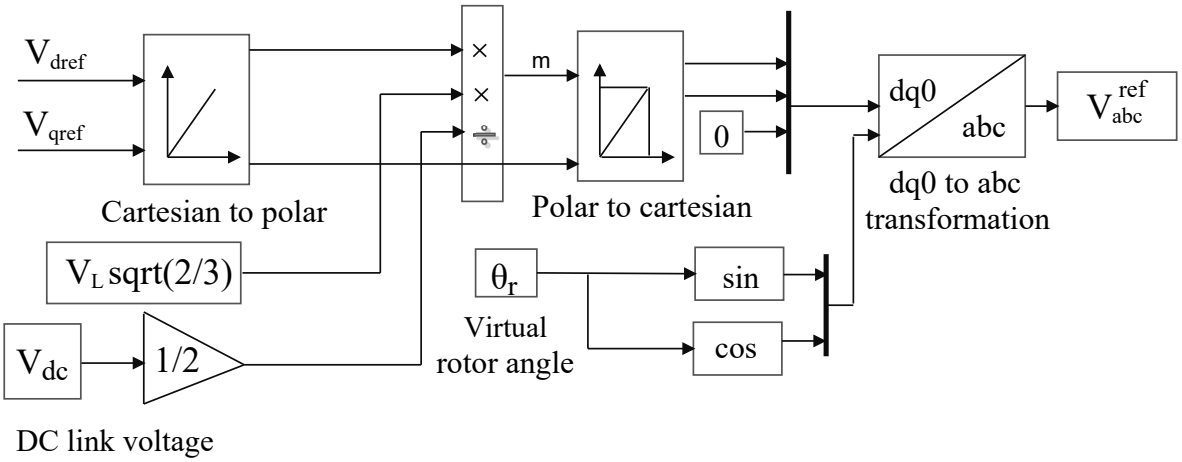

Figure 4.11: Reference signal generation for PWM

In the VSG control mechanism, virtual rotor angle is calculated in order to control the output power of the converter. The dc link voltage of the system is kept constant while the output power delivered by the converter is varied by controlling the switching of PWM. The process of bidirectional flow of power between MG and CS is controlled through VSG mechanism by applying a proper control signal to the converter through PWM. In Fig. 4.9, w_o is the reference angular frequency that is measured through phase locked loop, The virtual angular frequency w_r is calculated through the VSG mechanism which is further integrated to calculate the virtual rotor angle θ_r. This rotor angle acts as a phase signal for PWM to control the output voltage of power converter. Fig. 4.12 represents the block diagram of the swing equation

to determine the virtual rotor angle.

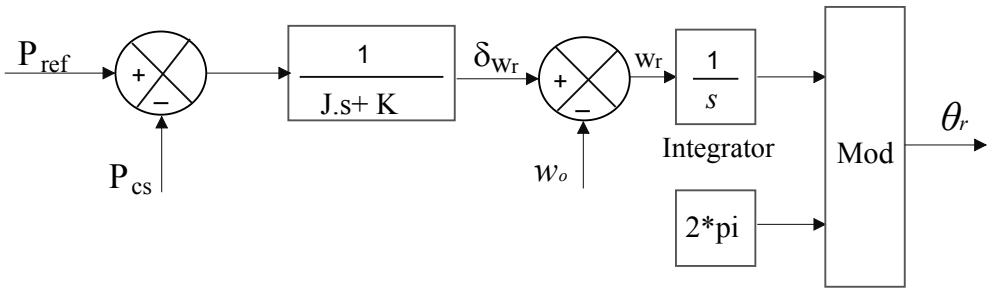

Figure 4.12: Block diagram for swing equation

The swing equation of synchronous generator is represented as follows,

$$P_{ref} - P_{cs} = Jw_r \frac{dw_r}{dt} - K\delta w_r \tag{4.38}$$

where, δw_r is expressed as $(w_o - w_r)$, w_o is the nominal angular frequency, w_r is the angular frequency of the virtual rotor and $\frac{dw_r}{dt}$ represents the rate of change of angular frequency. P_{ref} is the reference power for the VSG and P_{cs} is the power delivered or absorbed by the CS. J is the moment of inertia of rotor which depicts the reserved kinetic energy in the rotor of the synchronous machine. K is a damping factor, required to damp the oscillations that occur due to change of frequency. The moment of inertia J can be expressed as follows,

$$J = \frac{2H}{w_o^2} S_b \tag{4.39}$$

where, H is the per unit inertia constant and S_b is the base power rating of the VSG. H defines the duration for which virtual inertia can be provided to the system

As the swing equation is non-linear in nature, it has to be linearised in order to obtain the angular frequency w_r of the virtual rotor. From Eq. 4.38, the following expression can be derived to calculate the virtual angular frequency of the rotor.

$$\frac{dw_r}{dt} = \frac{P_{ref} - P_{cs} + K\delta w_r}{Jw_o} \tag{4.40}$$

where, P_{ref} is the reference power for the VSG and P_{cs} is the power delivered or absorbed by the CS. The power provided by the VSG can be represented by,

$$\Delta P_{vsg} = P_{ref} - P_{cs} \tag{4.41}$$

Using Eq. 4.41, the Eq. 4.40 can be rewritten as,

$$\frac{dw_r}{dt} = \frac{\Delta P_{vsg} + K\delta w_r}{Jw_o} \tag{4.42}$$

By solving Eq. 4.42, w_r is calculated which is further integrated, as per Eq. 4.43 to compute the virtual rotor angle.

$$\theta_r = \int_0^t w_r dt \tag{4.43}$$

This virtual rotor angle θ_r acts as a phase command for PWM to generate the gate pulses. These gate pulses are further used to control the output power of the converter.

4.4 Mathematical formulation of the Current Controller

In this section, the controller part is discussed to generate the reference signal for PWM which is further used to control the output power of the converter. In the process of reference signal generation for PWM, the virtual rotor angle θ_r and the dc link voltage V_{dc} of the CS have been used. The current control scheme has been implemented to generate the V_{dref} and V_{qref} in dq frame. This control scheme is also designed to protect the power converter from overload and external faults. In this scheme I_d and I_q track their reference current values I_{dref} and I_{qref} respectively and these current reference signals I_{dref} and I_{qref} are obtained by using the voltage

controller. Further, these reference current signals act as an input for the current controller.

In this scheme the current and voltage signals I_d, I_q, V_d and V_q in dq frame are generated through abc to dq transformation.

$$V_{dref} = (I_{dref} - I_d)\frac{K_{1pi}.s + K_{1ii}}{s} - wLI_q + V_d \tag{4.44}$$

$$V_{qref} = (I_{qref} - I_q)\frac{K_{2pi}.s + K_{2ii}}{s} + wLI_d + V_q \tag{4.45}$$

It can be depicted in Fig. 4.10, V_{dref} and V_{qref} are the voltage reference signals generated in dq frame using Eq. 4.44 and Eq. 4.45 respectively, where K_{1pi} and K_{1ii} are the control parameters to generate V_{dref} while K_{2pi} and K_{2ii} are for the generation of V_{qref}. The values of these control parameters are mentioned in Table 4.2. Moreover, the generated voltage reference signals in dq frame are in cartesian form and are converted to the polar form as depicted in Fig. 4.11. V_L is the rms line voltage of the system that is used to find the modulation index (m) for PWM. The value of modulation index is selected in such a way so that the power converter can generate 1 pu voltage. The value of m is calculated as per the following equation,

$$m = \frac{V_L\sqrt{2/3}}{V_{dc}/2} \tag{4.46}$$

where, V_{dc} is the dc link voltage of the CS as mentioned in Section 4.2. This modulation index is further used in the conversion of voltage signal in dq frame from polar to cartesian form. Virtual rotor angle θ_r is used for $dq0$ to abc transformation of voltage signal in dq frame. As depicted in Fig. 4.11, V_{abc}^{ref} is the reference signal generated through $dq0$ to abc transformation. This reference signal act as control signal for PWM to manage the output power of the converter.

4.5 Results and Discussions

This section presents the results of simulations based on the data taken from the MG on the island Kythnos in Greece [114]. This MG consists of PV source of 10.7 kW, diesel generator of 9 kVA and battery of 400 V, 30 Ah as an ESS. Peak load on the system is 12 kW, which is met by the combination of PV array, CS and diesel generator. As the irradiation level of the PV array in the Kythnos MG keeps on changing, the CS can provide the required power to meet the load demand. Moreover, the maintenance required for the battery bank used in the Kythnos MG is very high. To overcome this problem, CS has been considered to deliver or absorb the power, whenever power mismatch arises in the system. Three case studies have been carried out on the MG system to verify the bidirectional flow of power between the CS and the MG through the VSG control mechanism. In the first case study, the load on the system is changed at one instant only at $t = 12$ sec while the irradiation level of the PV array is kept constant. In the second case study, the load is changed at two instants, $t = 8$ and 20 sec respectively, but the irradiation level of the PV array is kept constant. In the third case study, irradiation level of the PV array is changed at $t = 8$ and 20 sec, while the load of the system is kept constant. In the second and third case study, load of the MG and the irradiation level of the PV array have been changed at the same time instant, $t = 8$ and 20 sec respectively.

4.5.1 Case study 1

In this case study, irradiation level of the PV array is kept constant and the load is changed at one instant. As depicted in Fig. 4.13(a), load demand of the system is 12 kW up to 12 sec and after this time instant it changes to 8 kW. Due to this change, power mismatch arises in the system between generation and the load demand that further leads to frequency deviation. Fig. 4.13(b), represents the deviation in frequency of the system from its nominal value, when the load changes from 12 kW to 8 kW. To minimize this frequency deviation, the required load demand is met by the

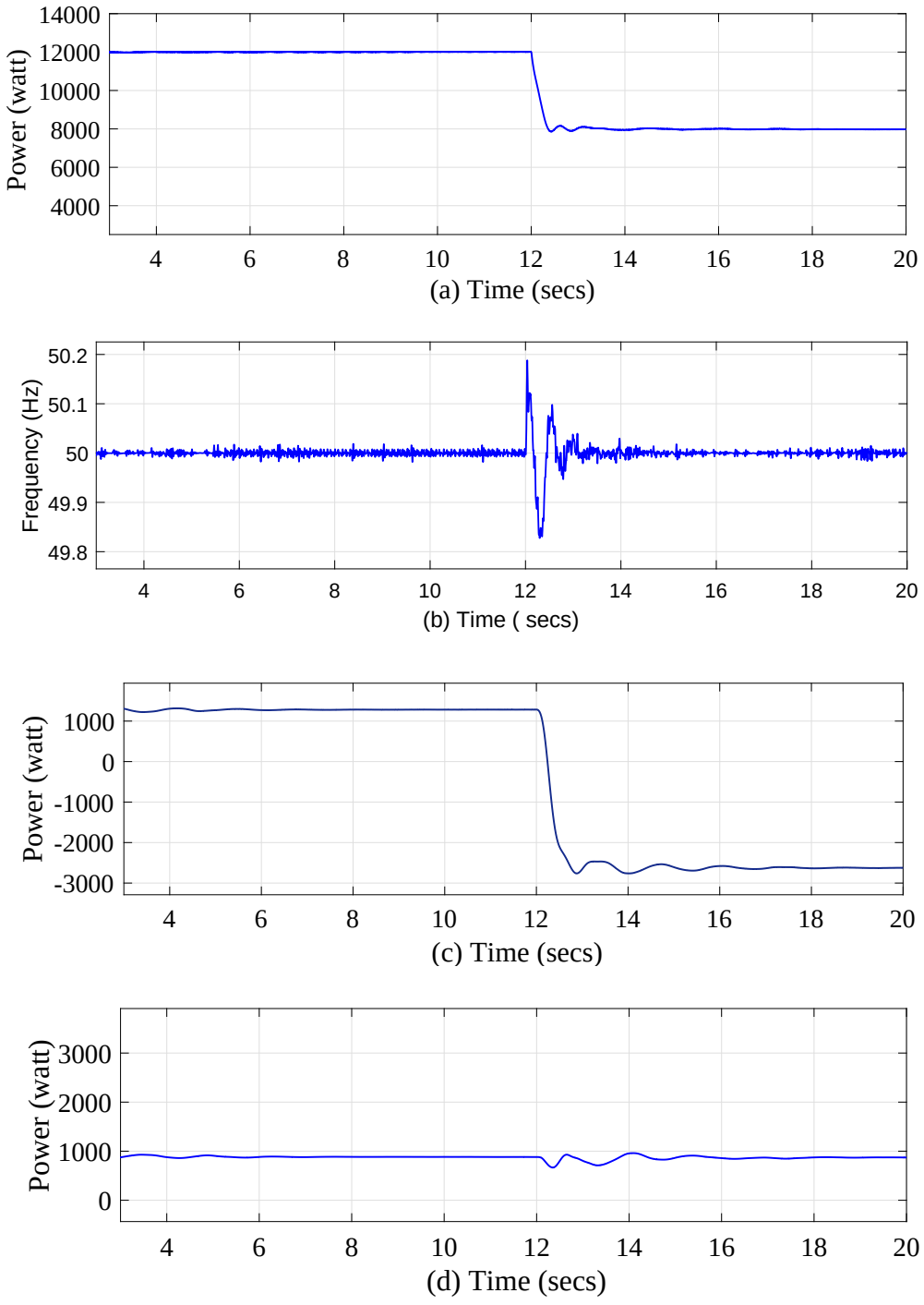

Figure 4.13: (a) Load on the system (b) Frequency of the system (c) Power delivered and absorbed by the CS (d) Power delivered by diesel generator

combination of PV array, CS and the diesel generator. As the irradiation level of the PV array is not changing, it will provide a fixed amount of power. Power delivered by the PV array is 10.7 kW which is less than the load demand 12 kW, therefore the remaining load demand is met by the CS and diesel generator.

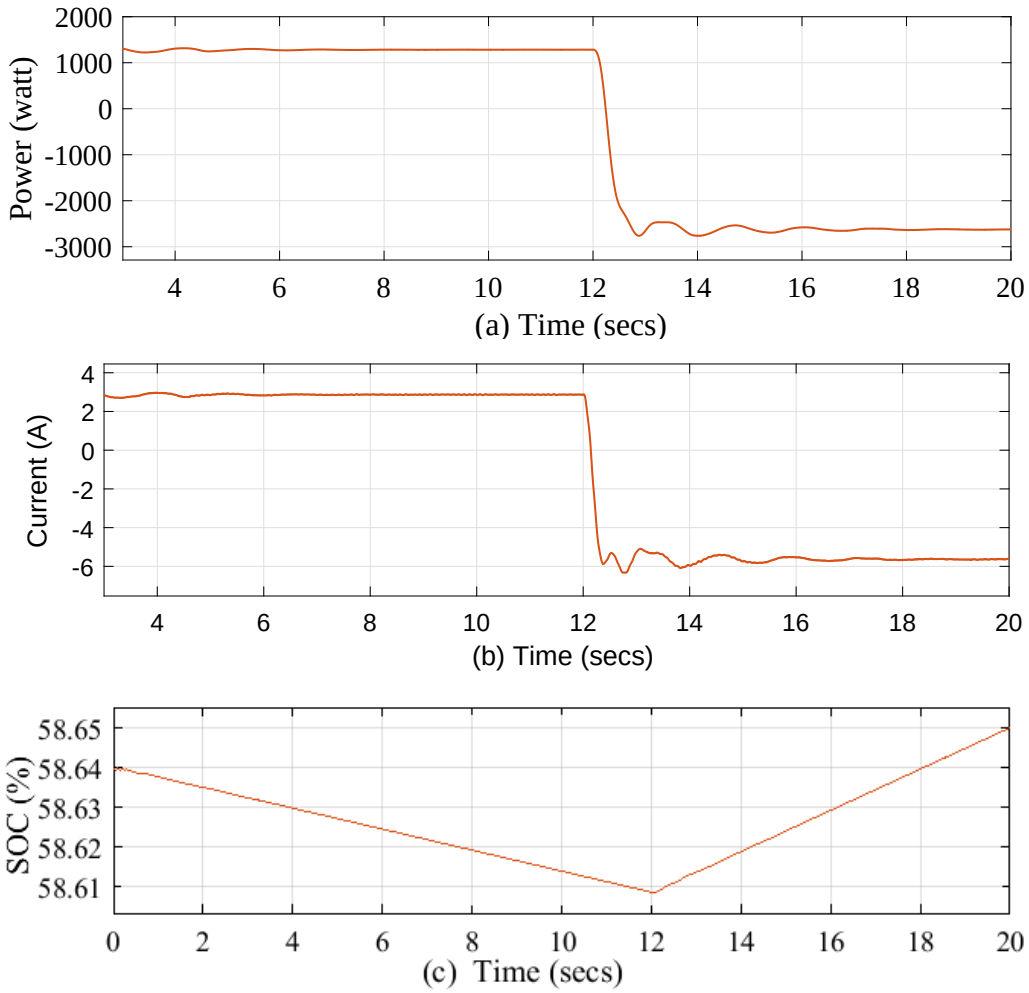

Figure 4.14: (a) Power delivered and absorbed by the CS (b) Charging and discharging current of the EV's battery (c) SoC of the EV's battery during charging and discharging operation

However, the EV's battery parked in the CS has a shorter response time to any load change in the system than the diesel generator. As depicted in Fig. 4.13(c), power delivered by the CS is 1.3 kW till 12 sec and as the load demand changes to 8 kW, CS starts absorbing the power of 2.7 kW from the MG to balance the load demand. This bidirectional flow of power between the CS and the MG is controlled through the VSG control mechanism to support the frequency of the system. On the other hand, power delivered by the diesel generator during this period of change in load demand, hardly shows any deviation as the dynamics of diesel generator are relatively slow. Power delivered by the diesel generator is around 1 kW which can be depicted in Fig. 4.13(d).

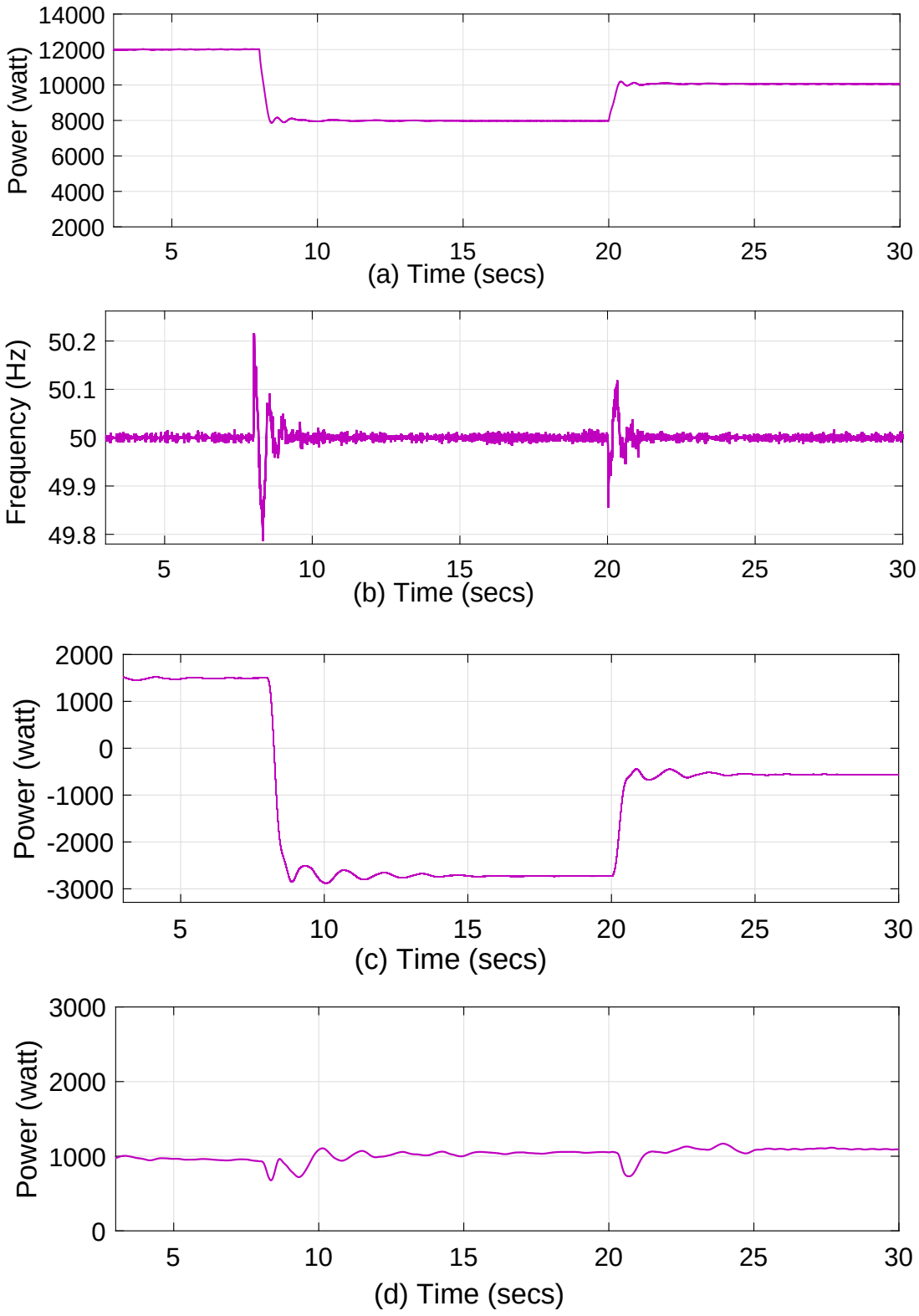

Figure 4.15: (a) Load on the MG system (b) Frequency of the system (c) Power delivered and absorbed by the CS (d) Power supplied by the diesel generator

Fig. 4.14(a), represents the power delivered and absorbed by the CS to or from the MG to balance the load demand of the system. Fig. 4.14(b), indicates the charging and discharging current of the EV's battery during this bidirectional flow of power between the CS and the MG. When the load demand is more as compared to the power delivered by the PV array, EV's battery is in discharging mode and delivers a current of 3 A. On the other hand, as the load demand reduces, EV's battery starts charging with a current of 5.5 A. SoC of EV's battery keeps on changing with the charging and discharging mode of operation. As depicted in Fig. 4.14(c), SoC of EV's battery decreases during discharging mode and starts increasing during charging mode.

4.5.2 Case study 2

In this case, irradiation level of the system is maintained as 1000 W/m^2, while the load demand is changed at two instances. As depicted in Fig. 4.15(a), load demand changes at $t = 8$ sec from 12 kW to 8 kW and then at $t = 20$ sec from 8 kW to 10 kW. With these changes in the load demand, frequency of the system deviates from its nominal value. It can be depicted in Fig. 4.15(b), frequency of the system deviates at $t = 8$ and 20 sec, with the change in load demand. These deviations in the frequency can be minimized by meeting the required load demand of the MG. As the load changes frequently, the CS delivers or absorbs the power quickly to/from the MG through the VSG control mechanism to support the frequency of the system. On the other hand, diesel generator is not able to respond quickly to these sudden load changes.

As shown in Fig. 4.15(c), CS delivers a power of 1.3 kW, when the load demand is more as compared to power generation and as the load demand reduces to 8 kW at $t = 8$ sec, CS starts absorbing power of 2.7 kW. When the load changes again at $t = 20$ sec from 8 kW to 10 kW, CS starts absorbing the power of 0.4 kW. This bidirectional flow of power between the CS and the MG is controlled through VSG

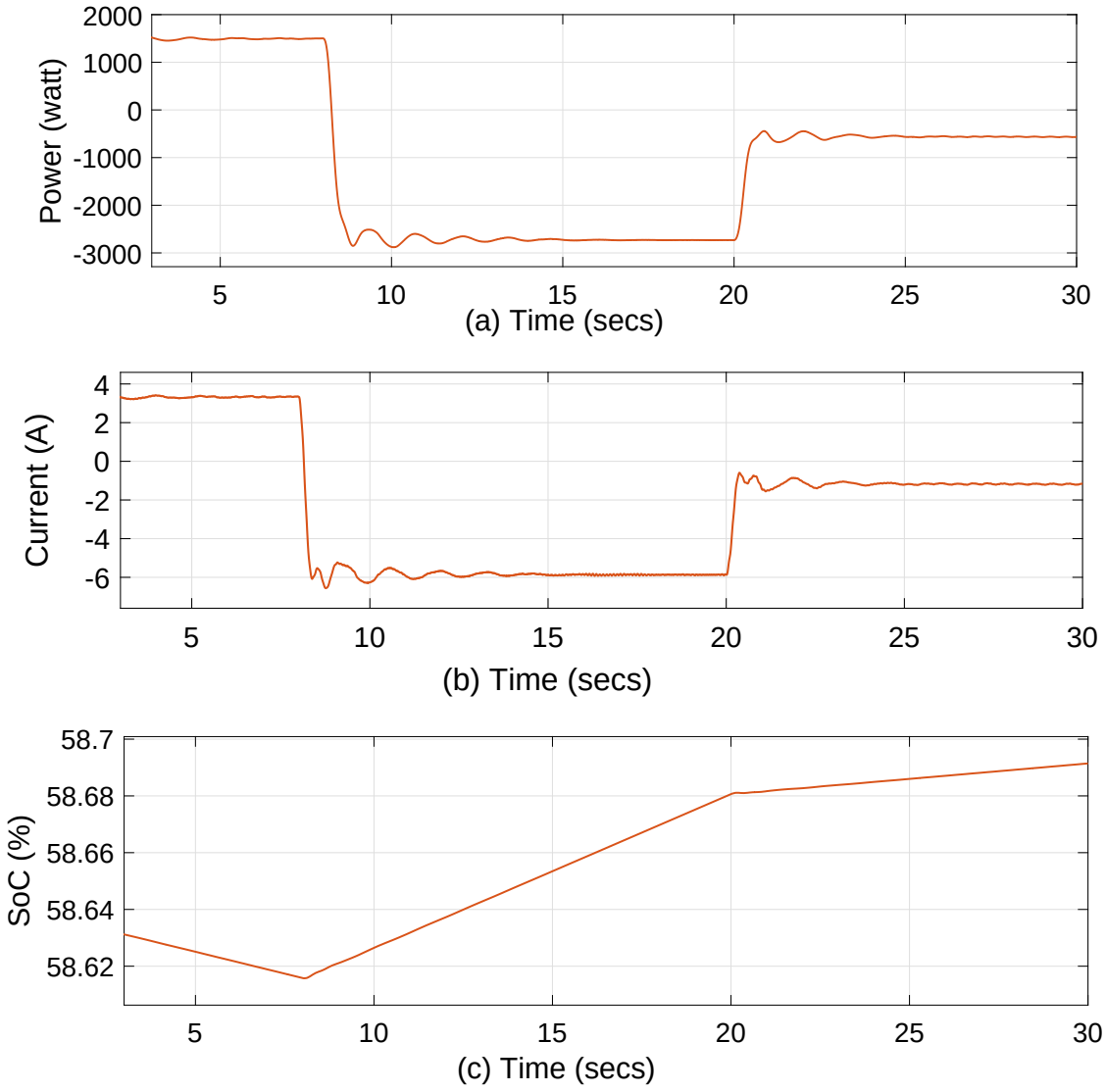

Figure 4.16: (a) Power delivered and absorbed by the CS (b) Charging and discharging current of the EV's battery (c) SoC of the EV's battery during charging and discharging operation

control mechanism to support the frequency of the system. On the other hand, as depicted in Fig. 4.15(d), the power delivered by the diesel generator remains around 1 kW only during this period of change in load demand. As depicted in Fig. 4.16(a), power is absorbed or delivered by the CS to/from the MG. With this bi-directional flow of power between the CS and the MG, the charging and discharging current of the EV's battery varies. Fig. 4.16(b), represents the charging and discharging current of the EV's battery during bidirectional flow of power. At the initial stage,

EV's battery is in discharging mode and delivers a current of 3.8 A, but as the load demand changes at $t = 8$ sec, battery starts charging with a current of 6 A. This change in load demand takes place again at $t = 20$ sec, where the load changes from 8 kW to 10 kW, but as the load demand is less than the power generation, EV's battery remains in charging state with a current of 1.5 A. SoC of EV's battery changes with the change in charging and discharging mode. As depicted in Fig. 4.16(c), SoC of EV's battery decreases at the initial stage, but as the load changes from 12 kW to 8 kW at $t = 8$ sec, SoC of EV's battery starts increasing. Further at $t = 20$ sec, the rate at which SoC was rising is reduced due to the change in the load demand from 8 kW to 10 kW.

4.5.3 Case study 3

In this case, load on the system is kept constant as 8 kW while the irradiation level of the PV array is changed at two time instances. A step change of 200 W/m^2 in the irradiation level is done at $t = 8$ and 20 sec respectively. Firstly, the irradiation level of the PV array is changed from 1000 W/m^2 to 800 W/m^2 at $t = 8$ sec and then again from 800 W/m^2 to 1000 W/m^2 at $t = 20$ sec. As the irradiation level changes, power delivered by the PV array changes in the same manner. It can be depicted in Fig. 4.17(a), at an irradiation level of 1000 W/m^2, power delivered by the PV array is 10.7 kW and as the irradiation level changes to 800 W/m^2, power delivered the PV array reduced to 8.5 kW. Due to these changes in power delivered by the PV array, frequency of the system deviates.

Fig. 4.17(b), illustrates the deviation in the frequency of the system at $t = 8$ and $t = 20$ sec, with the change in the irradiation level of the PV array. This change in frequency of the system is compensated through the VSG control mechanism by controlling the bidirectional flow of power between the CS and the MG. As shown in Fig. 4.17(c), the CS absorbs a power of 2.7 kW, when the power delivered by the PV array is 10.7 kW as the power delivered by the PV array changes to 8.5 kW,

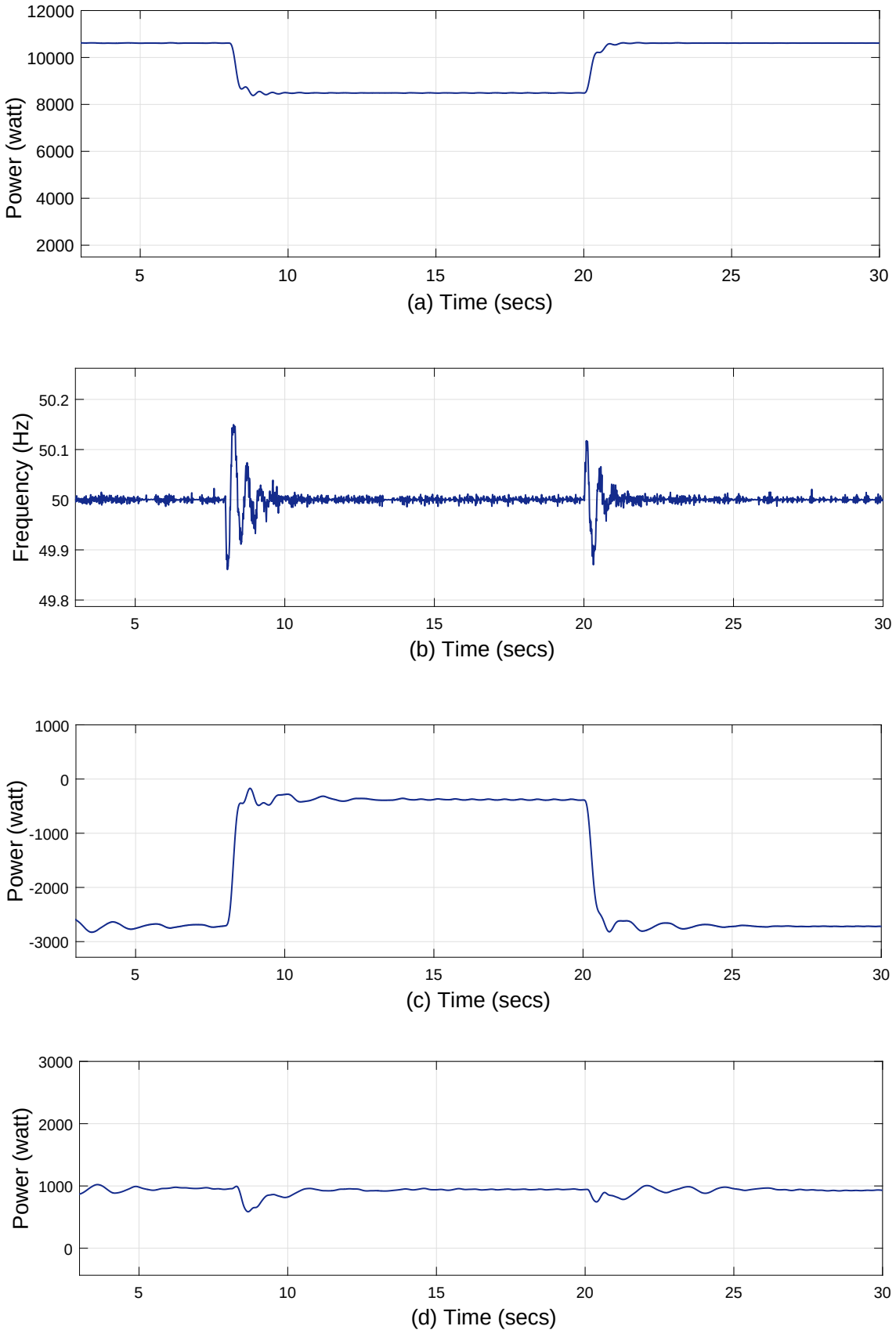

Figure 4.17: (a) Power provided by the PV array (b) Frequency of the system (c) Power delivered and absorbed by the CS (d) Power delivered by the diesel generator

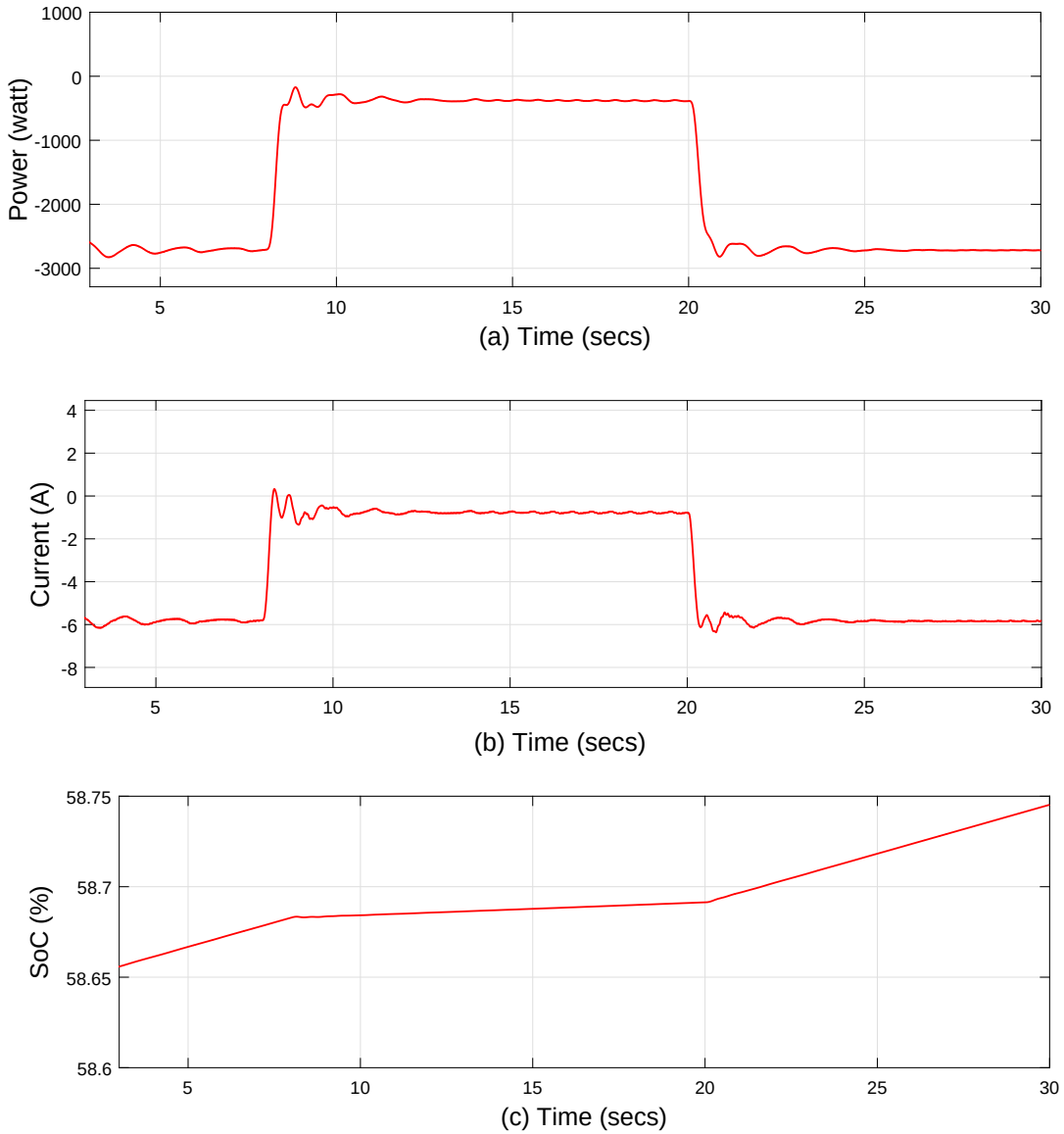

Figure 4.18: (a) Power delivered and absorbed by the CS (b) Charging and discharging current of the EV's battery (c) SoC of EV's battery during charging and discharging operation

the CS starts absorbing a power of 0.4 kW. As the power delivered by the PV array varies again at $t = 20$ sec from 8.5 kW to 10.7 kW, the CS starts absorbing power of 2.7 kW. Fig. 4.17(d) represents the characteristics of the diesel generator, it can be depicted from the figure that there is a small variation in power delivered by the diesel generator when the power produced by PV array changes at $t = 8$ and 20 sec respectively. These characteristics of diesel generator appears to be steady, because whenever any power mismatch arises in the system due to the intermittent nature

of PV array, it is immediately met by the VSG control technique by emulating the virtual inertia from ESS. On the other hand, due to the slow dynamics of the diesel generator, there is hardly any change appear in the power delivery.

Fig. 4.18(a), depicts the power delivered or absorbed by the CS, whenever power mismatch arises in the system. Fig. 4.18(b), depicts that at the initial stage, EV's battery is in charging mode with a current of 6 A. As the irradiation level of the PV array changes from 1000 W/m^2 to 800 W/m^2 at $t = 8$ sec, EV's battery charging current reduces to 1.5 A. However, this charging current is again raised to 6 A, when the irradiation level changes from 800 W/m^2 to 1000 W/m^2 at $t = 20$ sec. Fig. 4.18(c), represents the SoC of EV's battery that changes at $t = 8$ and 20 sec, due to the change in charging or discharging current of EV's battery. Through this change in irradiation level of the PV array it has been verified that frequency of the system can be supported through VSG based CS.

Through these case studies, it has been observed that EV based CS can provide the required power to the MG through the VSG control mechanism. Kythnos MG is selected to perform these case studies, as it consists of PV array, diesel generator and battery bank. One of the main goals of the Kythnos MG is to minimize the usage of diesel generator. This goal, can be achieved through VSG based CS, as it can provide the required power to the MG in a very short span of time. This work is applicable for most of the MGs, as frequency deviation is a common issue in the MGs, so whenever power mismatch arises in the system, the required power can be provided by the CS through the VSG control. Sudden arrival and departure of the EV's at the CS, while supporting the frequency of the MG will be discussed in the next chapter.

4.6 Summary

EVs can act as mobile ESS and have the capability to support the frequency of islanded MG while parked at the CS. This chapter focuses on the role of the VSG

based CS to support the frequency of the islanded MG. To verify the effectiveness of the VSG, three case studies have been carried out on the islanded MG system. In these case studies, load of the islanded MG system and irradiation level of the PV array have been changed arbitrarily to induce the power mismatch in the system. To perform these case studies data is taken from the MG on the island Kythnos in Greece. One CS is considered where a fleet of EVs is parked. This fleet of EVs act as an ESS for the MG. Virtual inertia is emulated from this fleet of EVs through VSG control to support the frequency of the system. Simulations have been performed in Matlab Simulink to validate the case studies. It has been observed from the simulation results that, if power mismatch arises between the generation and load demand in the MG, then the required power is delivered or absorbed by the CS in order to support the frequency of the system. This bidirectional flow of power between the CS and the MG is controlled through the VSG control mechanism. It has also been verified that the CS has less response time to any load change or fluctuation in the system as compared to the response time of the diesel generator. However, the limitation of this proposed system is that sufficient amount of battery ESS must be present at the CS. Because, when EVs are not parked at the CS, the back up power can be provided to the system through battery ESS.

Table 4.2: Simulation parameters

	Parameter	**Value**
Buck-boost converter control	Proportional and integral gains for dc link voltage control	K_{pv}=0.005, K_{iv}=0.004
	Proportional and integral gains for battery current control	K_{pi}=0.0001, K_{ii}=0.0009
	DC link voltage V_{dc}	600V
	DC link capacitor C_{dc}	1000μF
PV panel	Open circuit voltage V_{oc}	85.3V
	Short circuit current I_{sc}	6.09A
	Voltage at maximum power point V_{mp}	72.9V
	Current at maximum power point I_{mp}	5.69A
	Switching frequency f_s	3000Hz
Current controller	Proportional gain K_{1pi}, K_{2pi}	2
	Integral gain K_{1ii}, K_{2ii}	12
	Cross coupling term (wL)	0.9
VSG control	Line voltage V_L	400V
	Base power S_b	10e3
	Moment of inertia J	56.3 $kg\ m^2$
	Damping constant K	4.5

Chapter 5

VSG mechanism for catering unexpected EVs

5.1 Introduction

In today's scenario, electric vehicles (EVs) are playing a significant role in the power system. EVs can reduce the consumption of fossil fuels that further leads to reduction in emission of harmful gases [11]. EVs' battery can be charged through several ways yet charging stations (CS) are recognized as the primary source to satisfy the energy demand of EVs.[1] CS is a place where EVs can accomplish their charging demands and can provide the support to the MG for short duration through plug in and plug out mode. However, the locations of CS should be such that EVs can anywhere locate the CS within its driving circle. CS can be designed at work places and shopping complexes. Most of the EV owners drive the vehicle from residence to work place in the morning and back to residence in the evening. However, the vehicles which are not used in routine by EV owner, can be placed at the CS. The owners of EVs those are going to work place or in shopping complexes can also park their EVs at the CS. The

[1] The content of this chapter is taken from:

- K. Dhingra, M. Singh, "Smart Charging Station to Cater the Sudden Ingress and Egress of EVs while Supporting the Frequency of Microgrid through VSG," Arab J Sci Eng, Springer, vol. 45, pp 6715- 6727, June 2020, https://doi.org/10.1007/s13369-020-04627-y

time span for which the EVs are in idle state while placed in parking lot of work places or shopping complexes can function as an energy storage system (ESS) for microgrid (MG). This time span can be utilized to provide the ancillary services to MG in terms of frequency regulation or voltage support. Numerous researchers have focused on the participation of EVs in electric power system to illustrate their importance in the grid. Kempton *et al.* [12] reveals that battery operated EVs can function as a storage and energy source for the system. Yilmaz and Krein [15] discussed that the bi-directional power flow between grid and the EVs can be controlled through vehicle to grid phenomenon. Authors have explained that vehicle to grid strategy can enhance the performance of grid in terms of efficiency and generation dispatch. These authors have explained the role of EVs in power system but they haven't discussed on the frequency regulation of MG using EVs.

Some researchers have demonstrated the role of EVs in the frequency regulation of MG. Authors [73] have described a modified droop control technique where fleet of EVs act as an ESS to provide support to the frequency of MG. Authors [115] have explained that MG's frequency regulation can be done using EVs, where aggregator acts as a facilitator between the MG and EVs. Dhingra *et al.* [51] have explained about the frequency support of MG using fleet of EVs at the CS through virtual synchronous generator (VSG) control. Authors have compensated the irregular nature of PV array through fleet of EVs at the CS to support the frequency of the system. Roy *et al.* [116] have considered the office building with RES as a MG to charge the EVs. Authors have stressed upon the various charging schemes to charge more number of EVs through limited charging ports. Wi *et al.* [117] demonstrated the concept of smart buildings that consists of PV system to charge the EVs as per customer convenience. Traube *et al.* [118] explained about the role of bidirectional dc-dc charger to cater the charging and dis-charging of EVs in a system where PV is integrated with EVs. However, these studies have hardly examined the control of charging and dis-charging rate of EVs.

Some researchers have elaborated the concept of controlled charging and dis-

charging of EV batteries while meeting the load demand of MG. Authors [119] have discussed that charging and dis-charging of EVs can be governed through droop control while maintaining the power flow in between MG and the CS. Authors have further described that if the generating unit in the MG is not able to provide power supply, CS can meet the load demand by regulating the charging and dis-charging rate of EV batteries. Li *et al.* [120] demonstrated that charging of plug in EVs can be controlled through integrated controller, while maintaining the load demand of the grid. Goli and Shireen [121] designed a smart CS in order to charge the EVs, during the peak load demand on the MG. Zakariazadeh *et al.* [122] deliberated on the importance of EVs to compensate the irregular nature of RES in the future smart grids. Authors demonstrated that the load variation at the distribution side can be minimized by adjusting the C and D of EVs. Liu *et al.* [123] discussed that charging demand of EVs can be met while providing the frequency regulation to the grid using smart CS. Moghaddam *et al.* [124] described a smart charging technique for a plug in EV network, which provides charging alternatives such as quick charging and provision of swapping batteries at the CS. These authors have not considered the real scenario at CS and have not catered the unexpected ingress and egress of different type of EVs at the CS. With the rise in EV's penetration in the market, the chances of sudden ingress and egress of EVs at the CS will enhance. Therefore, in this work, the sudden ingress and egress of the EVs at the CS has been considered by the inclusion of EV's battery through opening and closing of switch at different intervals of time. Here, closing of switch represents the ingress of the EV at the CS, while the opening of switch is considered as the egress of the EV from the CS. However, switch on and switch off intervals of battery operation are considered randomly just to represent the ingress and egress of EVs at different intervals of time. The switching is controlled by using programmable switch in matlab simulink by defining the turn on and turn off time for each switch.

5.1.1 Motivation

Numerous authors have demonstrated the role of EVs in MG. Some of them stressed upon the importance of vehicle to grid concept [13] [15] [125]. Few authors have discussed about the feasibility to regulate MG's frequency using EVs [89] [115]. Some have demonstrated on the charging and discharging control of EVs placed at the CS while meeting the load profile of MG [121] [122]. However, to the best of author's awareness, none of them have considered the sudden ingress and egress of EVs at the CS while providing the frequency support to the MG through VSG mechanism. Further, no one has considered EV batteries of different voltage ratings while providing the support to MG.

5.1.2 Contribution

- In this chapter, sudden ingress and egress of EVs at the CS has been catered while providing the support to the MG's frequency through VSG control mechanism.
- CS has been designed to provide the frequency support to the MG, where EVs having different battery voltage ratings ingress and egress at irregular time intervals.
- Charging and discharging of EVs which are placed at the CS has been controlled simultaneously to meet the load profile of MG.

5.1.3 Organization

Remaining part of the chapter is organized in the following way. Section 5.2 describes the proposed work. VSG control strategy is elaborated in section 5.3 . Results and simulations are discussed in section 5.4. Summary of the chapter is mentioned in section 5.5.

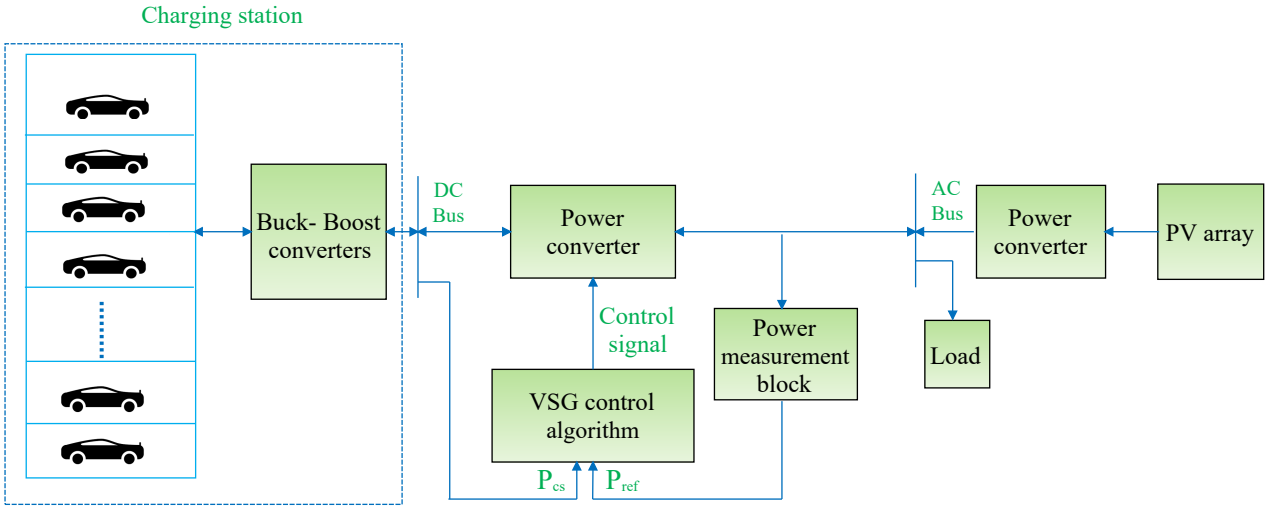

Figure 5.1: Schematic layout of the proposed work

5.2 Proposed Methodology

In the proposed work, support to MG's frequency has been provided while considering the sudden ingress and egress of EVs at the CS. These EVs act as both load and energy source for the MG system. EVs arriving at the CS may have diverse SoC levels and charging requirements of the EV owners may also differ. The EVs which remain placed at CS for longer time span, can contribute as a source of power. On the other hand, some of the EVs ingress and egress from the CS for charging purpose at irregular intervals. Therefore, there is a bidirectional flow of power between CS and MG to charge and discharge the EV batteries. Thus, if the EVs participating in the power flow between CS and MG, ingress or egress from the CS suddenly, it might affect the system. In order to solve this issue, CS has been designed to manage the flow of power between CS and the MG using VSG control strategy. Through this strategy, flow of power between MG and CS has been controlled to support the frequency of MG. If the SoC level of EV's battery is less than the minimum specified SoC level, then battery acts as a load for the system and needs to be charged. On the contrary, if the SoC level of EV's battery is sufficiently high, then it can contribute as a source of power for the MG for the short duration. Buck-boost converters are designed at the CS to meet the charging needs of individual EV batteries and to

provide support to MG by allowing the battery to discharge for a short duration. As depicted in Fig. 5.1, EVs placed at the CS are connected to a common dc bus through dc-dc converters. These converters operate in buck and boost modes respectively to charge and discharge the EVs batteries. However, the limitation of the proposed system is that SoC level of few EVs which are parked at the CS must be high enough so that they can be used to support the MG for short duration.

In this chapter, n different type of EVs (EV_1 to EV_n) are considered at the CS. These EVs have a range of battery voltage ratings and are connected in parallel with a common dc bus through bidirectional buck-boost converters. Furthermore, the SoC level of these EVs is considered as different from each other. As shown in Fig. 5.2, it is being considered that EV_1 to EV_m are the vehicles which are placed at the CS by EV owners which can participate in discharging process to support the MG's frequency. On the other hand, EV_{m+1} to EV_n are the vehicles that ingress and egress at the CS at irregular intervals to charge their batteries. Further, at the initial stage, it is assumed that SoC level of EV_1 to EV_m is high while the SoC level of EV_{m+1} to EV_n is low. This assumption has been made so that EV_1 to EV_m can act as a source of power while EV_{m+1} to EV_n can act as a dc load, which needs to be charged. To accomplish the task of sudden ingress and egress at the CS, EVs are connected with dc bus through controlled switches, which are turned on and off at irregular intervals. Switches S_1 to S_m remain closed throughout the simulation period, whereas switches S_{m+1}, S_{m+2} to S_n open and close at irregular time intervals. The time span for which switches are open, is considered as EVs are not placed at the CS. The time span for which switches are closed is considered as parking period of EVs at the CS. As the battery voltage ratings of these EVs are different, a constant voltage V_c is obtained at the dc bus through bi-directional buck-boost converters. The parameters used for obtaining a constant voltage V_c at the output of buck boost converters are mentioned in Table 5.1. Further, the output of buck-boost converters and input of the bidirectional power converter shares a common dc link (DL). The voltage V_c across the DL capacitor acts as an input for the power converter and

the same act as a dc bus voltage [111]. However, the sudden ingress and egress of EVs, may lead to the variation of DL voltage. This variation in DL voltage can be controlled through virtual inertia, which will be discussed in next section.

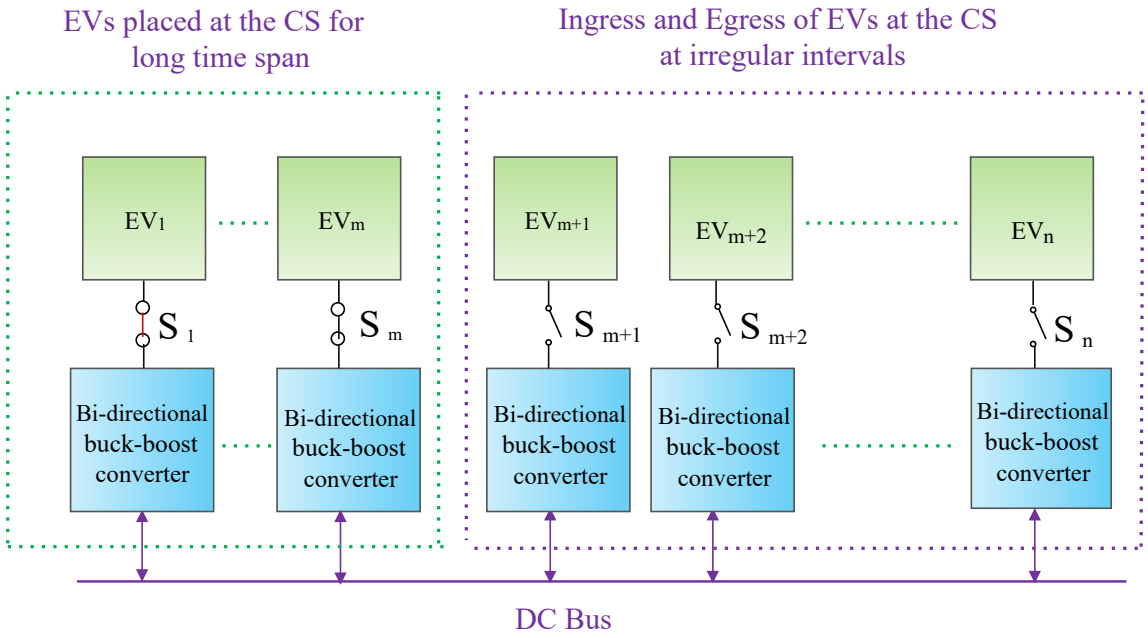

Figure 5.2: Design of charging station

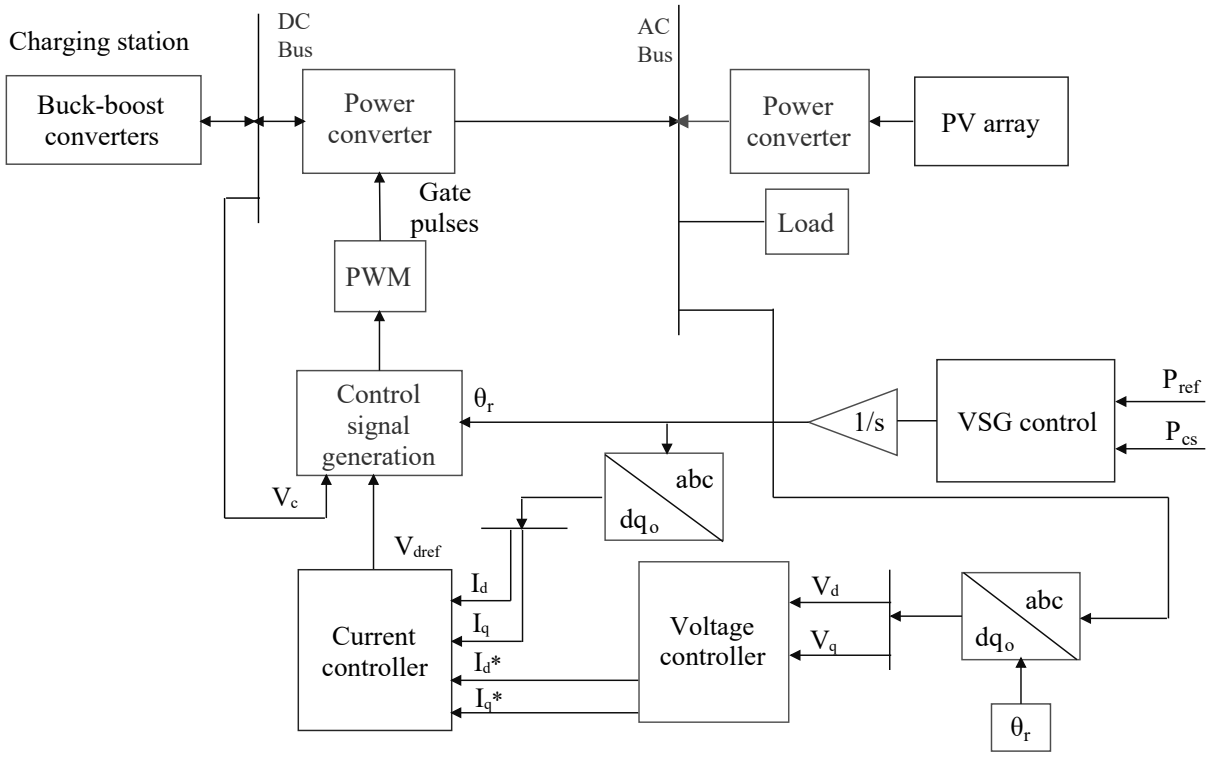

Figure 5.3: Control coordination among buck boost converter and power conveter

Control among the buck-boost converters and the power converter connected between DC and AC bus is coordinated through DC link voltage. All the buck-boost converters are connected in parallel and share a common output voltage with the dc bus. The output voltage of the buck-boost converters and input voltage of the power converter share a common dc link. The coordination between buck boost converters and power converter is shown in Fig. 5.3. As per this figure, the virtual rotor angle θ_r and the dc link voltage V_c participate in the generation of control signal for PWM, which further controls the output power of the converter. The current controller is used to generate the V_{dqref} in dq frame. Based on the generated control signal, the power converter either works as rectifier or inverter. When the load on the MG is more as compared to the power generated by the PV array then power converter acts as an inverter and at the same time buck boost converter works in boost mode to control the discharging rate of EV battery. On the contrary, when power generated by the PV array is more as compared to the load demand then power converter acts as a rectifier and the buck boost converter works in buck mode to control the charging rate of EV battery.

Table 5.1: Design parameters of buck-boost converter

Converter	**Parameter**	**Value**
Buck-boost converter to get 600 V at dc bus	For DL voltage control	K_{pv}=0.02, K_{iv}=3
	For battery current control	K_{pi}=0.2, K_{ii}=110
	DL voltage V_c	600 V
	DL capacitor C_d	2500 μF

5.3 Control Strategy

VSG is used as a control strategy to adjust the power flow in the system. VSG consists of energy storage system (ESS), power converter and its control algorithm. Bi-directional power flow between CS and the MG is managed by VSG. EVs which ingress and egress at the CS at irregular intervals and which are placed at the CS act as an ESS for the MG. The VSG control strategy is based on the following equation [126].

$$Jw_r \frac{dw_r}{dt} = P_{ref} - P_{cs} \tag{5.1}$$

where, P_{ref} is the reference power and P_{cs} is the net power supplied or fetched by the CS. J is the moment of inertia of the rotor and w_r is the angular frequency of the virtual rotor.

Net power supplied or fetched by EVs which are placed at the CS is given by the following equation,

$$P_{cs} = \sum_{j=1}^{n} P_j \tag{5.2}$$

where, P_j is the power supplied or fetched by individual j^{th} EV battery and n is considered as number of EVs at the CS. As the EVs are connected in parallel with a common dc bus, voltage across them will be same. However, current supplied or fetched by them varies from each other. Let I_j be the current supplied or fetched by j^{th} EV battery. So, net current delivered or absorbed by EV batteries is mentioned by the following equation,

$$I_{tot} = \sum_{j=1}^{n} I_j \tag{5.3}$$

The current, delivered and absorbed by the EV battery is assumed to be positive and negative respectively. In this work, it is assumed that EV_1 to EV_m are delivering the

power while EV_{m+1} to EV_n are absorbing the power. Net power supplied or fetched by the CS can be written as,

$$P_{cs} = \sum_{l=1}^{m} P_{disc} - \sum_{j=m+1}^{n} P_{char} \tag{5.4}$$

where, m is the number of EVs dis-charging and $(n-m)$ is charging respectively at the CS. P_{disc} and P_{char} represent the net power supplied and fetched by the batteries. P_{char} is the power fetched by $(n-m)$ EV batteries and P_{disc} represents the power supplied by m EVs which remain placed at the CS for long time span. During the charging and dis-charging process of EV batteries, if Q_c is the charge stored in the DL capacitor then current across it can be described as mentioned below,

$$\frac{dQ_c}{dt} = I_{tot}(t) - I_l(t) \tag{5.5}$$

where, $I_{tot}(t)$ is the net current supplied or fetched by EV batteries and $I_l(t)$ is the remaining current flowing towards the power converter at time sudden t respectively. The charge stored in the DL capacitor can be described as below,

$$Q_c = C_d V_c \tag{5.6}$$

where, C_d is the capacitance and V_c is the voltage of the DL capacitor. As the C_d is fixed and V_c is variable in nature, the Eq. (5.7) can be formulated using Eq. (5.5) and Eq. (5.6).

$$C_d \frac{dV_c}{dt} = I_{tot}(t) - I_l(t) \tag{5.7}$$

From Eq. (5.7), the dynamic equation of the DL voltage can be written in the following way,

$$C_d V_c \frac{dV_c}{dt} = (I_{tot}(t) - I_l(t))V_c = P_{cs} - P_{out} \tag{5.8}$$

where, P_{out} is the power supplied by converter to the load at AC side. Eq. (5.8) is similar to the Eq. (5.1) and by comparing these two equations the Eq. (5.9) is obtained as follows,

$$C_d V_c \frac{dV_c}{dt} = J w_r \frac{dw_r}{dt} \tag{5.9}$$

where, C_d and V_c correspond to J and w_r respectively. By integrating both sides of Eq. (5.9), the Eq. (5.10) and Eq. (5.11) can be obtained as follows,

$$\int C_d V_c \frac{dV_c}{dt} = \int J w_r \frac{dw_r}{dt} \tag{5.10}$$

$$\frac{1}{2} C_d V_c^2 + K_1 = \frac{1}{2} J w_r^2 \tag{5.11}$$

Value of K_1 can be find out by considering the initial states of V_c and w_r respectively.

$$K_1 = \frac{1}{2} J w_o^2 - \frac{1}{2} C_d V_{co}^2 \tag{5.12}$$

where, w_o and V_{co} is the reference angular frequency and required DL voltage respectively. By substituting the value of K_1 in Eq. (5.11), the expression for virtual inertia can be obtained using following equations,

$$\frac{1}{2} C_d V_c^2 + \frac{1}{2} J w_o^2 - \frac{1}{2} C_d V_{co}^2 = \frac{1}{2} J w_r^2 \tag{5.13}$$

Further by rearranging Eq. (5.13), the new equation can be obtained as follows,

$$C_d (V_c^2 - V_{co}^2) = J (w_r^2 - w_o^2) \tag{5.14}$$

From Eq. (5.14), the expression for J can be written as,

$$J = \frac{C_d (V_c^2 - V_{co}^2)}{(w_r^2 - w_o^2)} \tag{5.15}$$

Eq. (5.15) indicates that V_c varies in the same proportion as w_r. J indicates the amount of virtual inertia required to maintain the DL voltage.

Due to the sudden ingress and egress of EVs at the CS, DL voltage may vary. Variation in DL voltage further leads to change in frequency of the system [127]. This variation in DL voltage can be controlled through virtual inertia. Based on the virtual rotor angle θ_r which can be obtained by solving the Eq. (5.15), and dc link voltage V_c, a control signal is generated for PWM for controlling the power converter in both inverter and rectifier mode.

5.4 Results and Discussion

This section illustrates the simulation results, which are based on the bi-directional flow of power between CS and MG. EVs parked at CS has been used for charging and to provide support to the MG when transients arise in the frequency of the system. In this work, total number of EVs considered are $n = 6$. Out of these, the number of EVs that remain parked at the CS for long duration are considered as $m = 2$. However, the number of EVs that ingress and egress from the CS at regular intervals are $n - m = 4$. Further, one PV array is considered that can deliver a peak power of 10.7 kW. Load profile of the MG is met by both CS and the PV array.

Battery voltage rating of these six EVs (EV_1, EV_2, EV_3, EV_4, EV_5 and EV_6) is considered as 375 V, 330 V, 300 V, 275 V, 230 V and 300 V respectively. Voltage of 600 V is obtained the dc bus using buck-boost converters. Moreover, it is assumed that EV_1 and EV_2 are the vehicles which are parked at CS by EV owners which can be used for providing the energy for short duration. Whereas, EV_3, EV_4, EV_5 and EV_6 are the vehicles that ingress and egress at the CS at regular intervals. SoC level of these EVs is different with respect to each other. Further, it is assumed that SoC level of EV_1 and EV_2 is higher than the EVs that ingress at the CS. However, SoC levels of EV_3, EV_4, EV_5 and EV_6 is considered as 20%, 30%, 40% and 45% respectively. This assumption has been made so that EV_1 and EV_2 can participate in

the frequency support process of MG when it is required, while EV_3, EV_4, EV_5 and EV_6 can act as a load and needs to be charged. Case studies have been performed to observe the effect of load change in MG and ingress/egress of EVs at the CS, on the frequency of the system. Further, it has been discussed that the frequency of system can be supported by adjusting the charging and discharging rate of EVs parked at the CS. The time interval of ingress and egress of EVs at the CS is mentioned in Table 5.2 and Table 5.3. The parameters of the considered system are given in Table 5.4.

5.4.1 Case 1: Change of load on MG while catering the ingress/ egress of EVs at the CS

In this case, ingress and egress of EVs at the CS has been catered while maintaining the frequency of the MG. For this purpose, six EVs are considered at the CS, out of which two EVs (EV_1 and EV_2) having high level of SoC are assumed to be parked at the CS to participate in MG frequency support. Whereas, EVs having low SoC levels ingress at the CS to charge their batteries. In the considered case, EV_1 and EV_2 having SoC level of 95% and 90% respectively remain parked at the CS for long duration. However, EV_5 and EV_6 having SoC level of 40% and 45% ingress at the CS at $t = 0$ sec while EV_3 and EV_4 having SoC level of 20% and 30% ingress at $t = 5$ and $t = 10$ sec respectively. Moreover, EV_5 and EV_6 egress from the CS at $t = 25$ and $t = 20$ sec respectively. As depicted in Fig. 5.4, as the EV_3 and EV_4 having low SoC levels ingress at the CS they start charging. However, their charging rate gets affected at $t = 15$ sec when the load on MG varies from 6 kW to 11 kW.

Due to the load profile of MG, its frequency differs from the reference value. As shown in Fig. 5.5a, at $t = 15$ sec, frequency of the system deviates. However, this deviation in frequency is minimized using VSG mechanism by extracting power from the CS. As shown in Fig. 5.4, the rate at which EV_1 and EV_2 were discharging is increased at $t = 15$ sec to meet the load demand of MG. Concurrently, the rate at

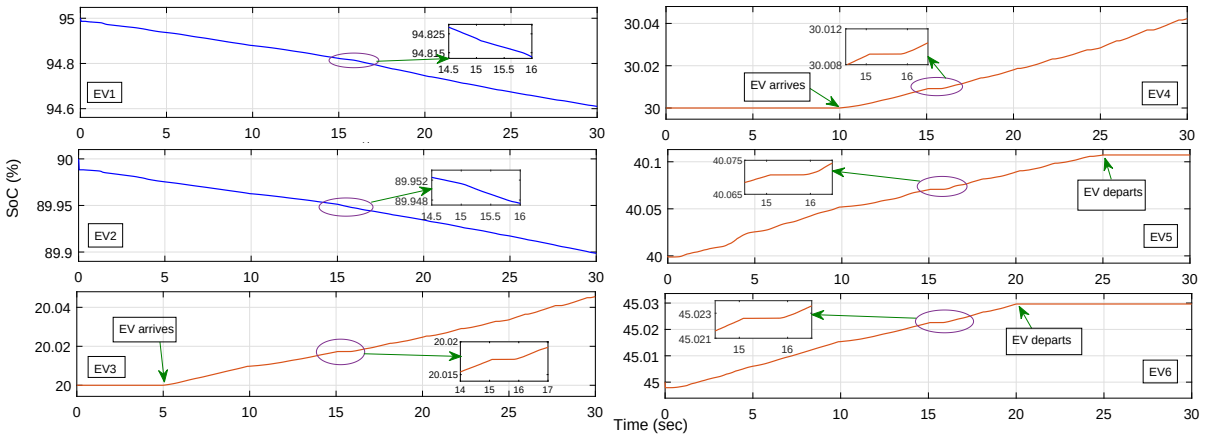

Figure 5.4: Charging and discharging of EVs during their ingress and egress at the CS

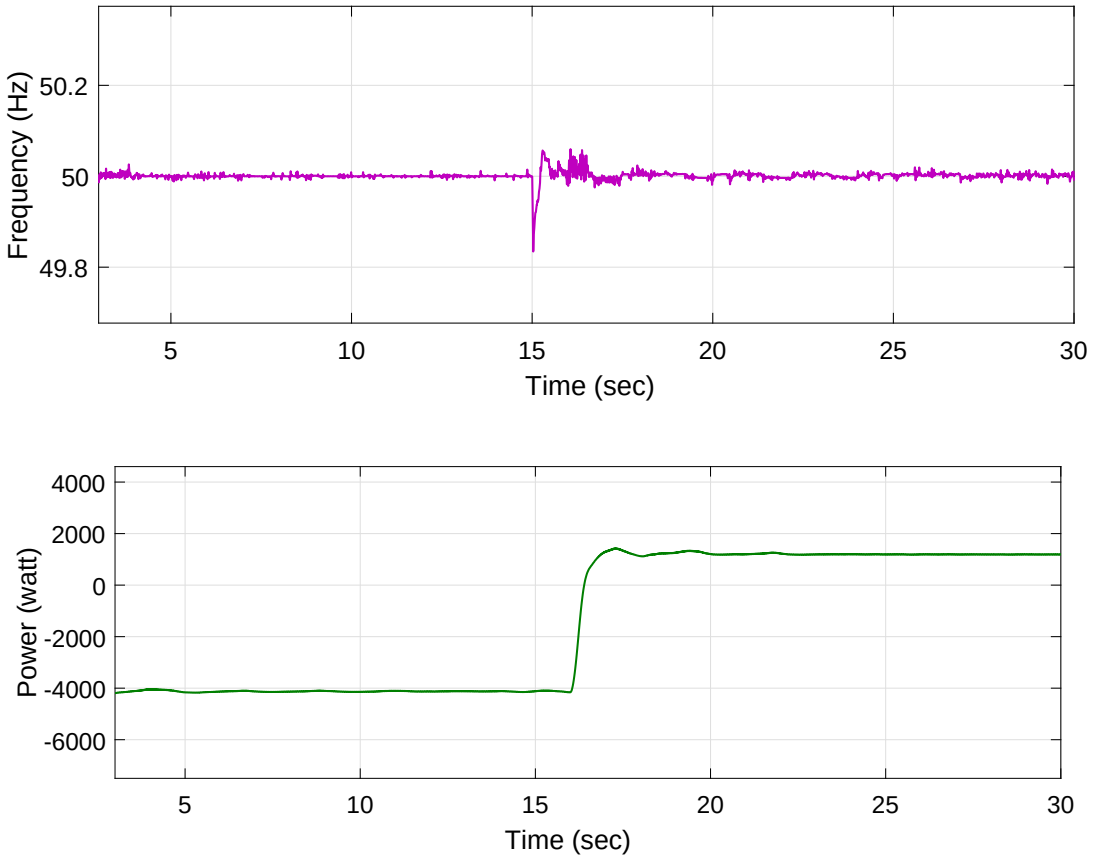

Figure 5.5: (a) Frequency deviation in the MG. (b) Power released or consumed by the CS

which EV_5 and EV_6 were charging also gets affected. As a result, CS delivers the required power to the MG by adjusting the charging and discharging rate of EVs. As per Fig. 5.5*b*, power consumed by the CS is 3.6 kW when load on the MG is 6 kW.

As the load on MG is increased to 11 kW, EV_1 and EV_2 start discharging at a faster rate and CS delivers a power of 1.2 kW. Hence, the power requirement of loads on the MG and EVs at the CS has been managed simultaneously.

5.4.2 Case 2: Change in load on MG while considering no movement of EVs at the CS

In this case, load on the MG is changed at regular intervals while EVs are considered to be remain parked at the CS. As depicted in Fig. 5.6, EV_1 and EV_2 are considered as vehicles which can participate in the frequency support process of MG. On the other hand, EV_3, EV_4, EV_5 and EV_6 having different SoC levels, ingress at the CS at $t = 0$ sec and act as a dc load for the system. Load on the MG varies at $t = 12$ and $t = 20$ sec from 6 kW to 8 kW and from 8 kW to 10 kW respectively. Due to these variations in load demand on MG, frequency of the system differs from its reference value. As illustrated in Fig. 5.7*a*, frequency of the system tends to deviate from its reference value at $t = 12$ and $t = 20$ sec respectively. However, these deviations in frequency are minimized by adjusting the charging and discharging rate of EVs. As depicted in Fig. 5.6, with the increase in load at $t = 12$ and $t = 20$ sec, EV_1 and EV_2 start discharging at a faster rate while charging rate of EV_3, EV_4, EV_5 and EV_6 is reduced at the same instant. However, charging and discharging rate of EVs attain the steady state after a minor change in their charging and discharging slopes.

Fig. 5.7*b*, represents the power released or consumed by the CS due to load variations in the MG. In the beginning, when the load on the MG is of 4 kW and the power generated by PV array is of 10.7 kW, CS absorbs a power of 6 kW. However, when the load on MG varies at $t = 12$ sec from 4 kW to 6 kW, power consumed by the CS is reduced to 4 kW. Further, as the load on MG varies from 6 kW to 8 kW, power consumption by the CS is reduced to 1.9 kW to provide the frequency support to the system.

Table 5.2: EV specifications at CS for Case 1

Vehicle	**Initial SoC of battery**	**Battery voltage rating**	**Ingress and egress interval of EV at CS**
EV_1	95%	375 V	Parked at CS for long duration
EV_2	90%	330 V	Parked at CS for long duration
EV_3	20%	300 V	Ingress at CS after 5 sec
EV_4	30%	275 V	Ingress at CS after 10 sec
EV_5	40%	230 V	Egress from CS after 25 sec
EV_6	45%	300 V	Egress from CS after 20 sec

Table 5.3: EV specifications at CS for Case 3

Vehicle	**Initial SoC of battery**	**Battery voltage rating**	**Ingress and egress interval of EV at CS**
EV_1	90%	375 V	All the EVs ingress after 16 sec
EV_2	85%	330 V	
EV_3	20%	300 V	
EV_4	25%	275 V	
EV_5	30%	230 V	
EV_6	40%	300 V	

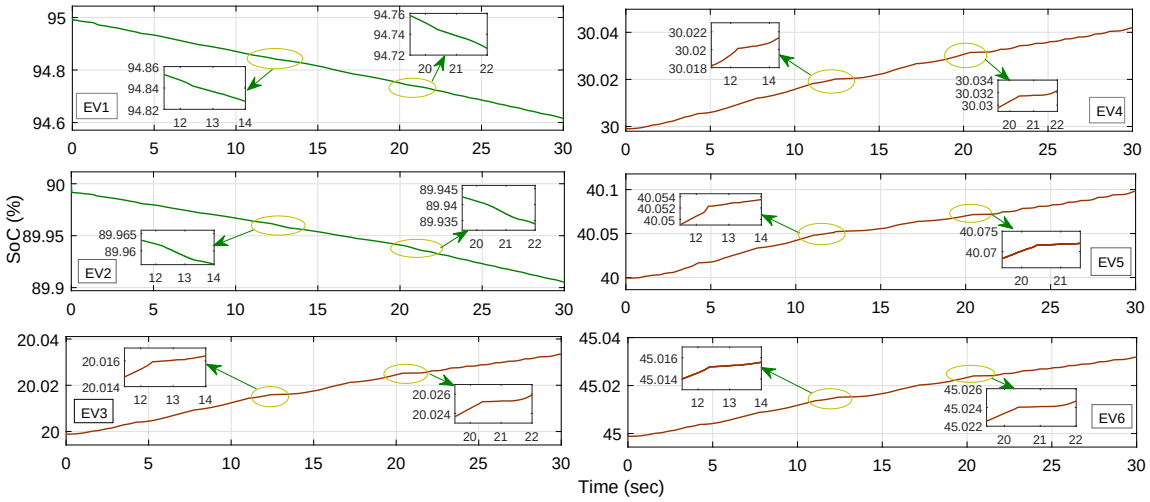

Figure 5.6: Charging and discharging of EV batteries during change in load on MG

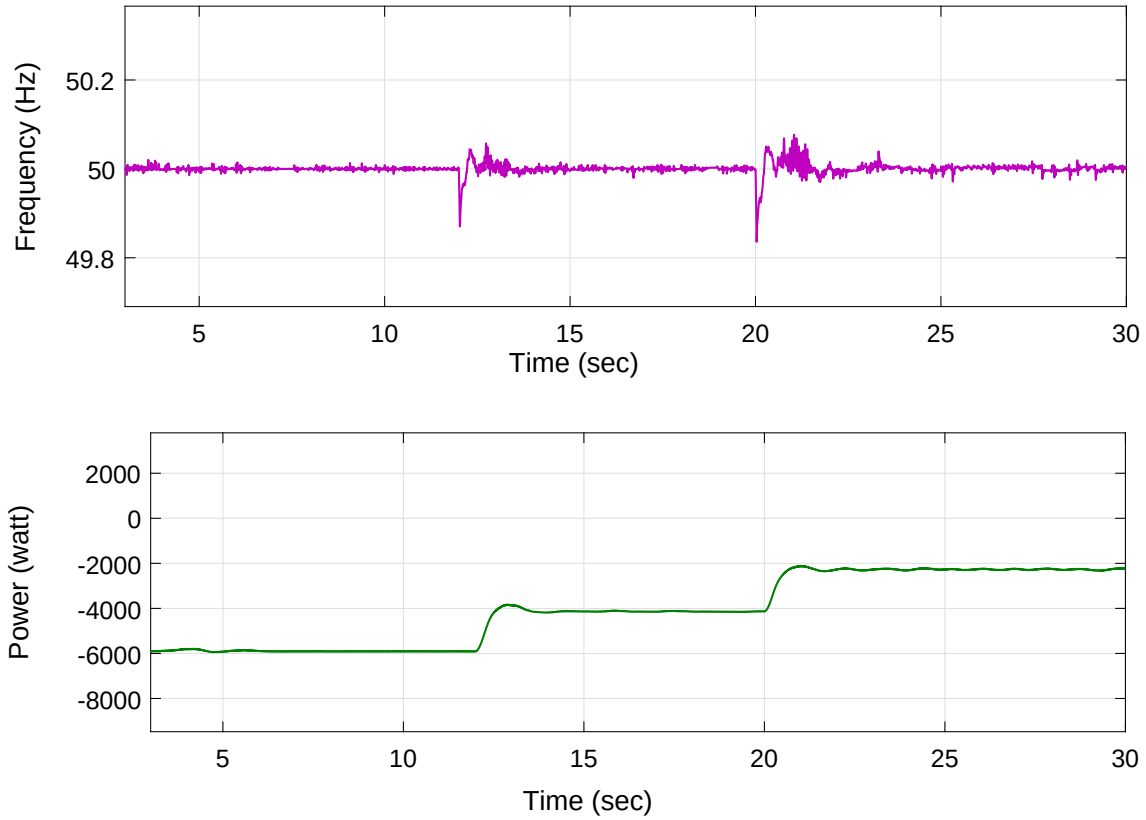

Figure 5.7: (a) Frequency deviation in the system due to load change on MG. (b) Power released or consumed by the CS

5.4.3 Case 3: Sudden ingress of EVs at the CS

In this case, it has been considered that two EV are parked at the CS. which are not participating in the MG support at the initial stage. Moreover, at this stage,

Table 5.4: Parameters of the considered system

Parameter	**Value**
Line voltage V_L	400 V
Base power S_b	10 kW
Frequency f	50 Hz
Switching frequency f_s	10 kHz

load demand of the MG is balanced by the power delivered by the PV array only. However, after some time, few EVs, having different SoC levels, suddenly ingress at the CS. These EVs having low SoC levels and ingress at the CS for charging purpose. Due to the sudden ingress of all these EVs at the CS for charging purpose, frequency deviation occurs in the system.

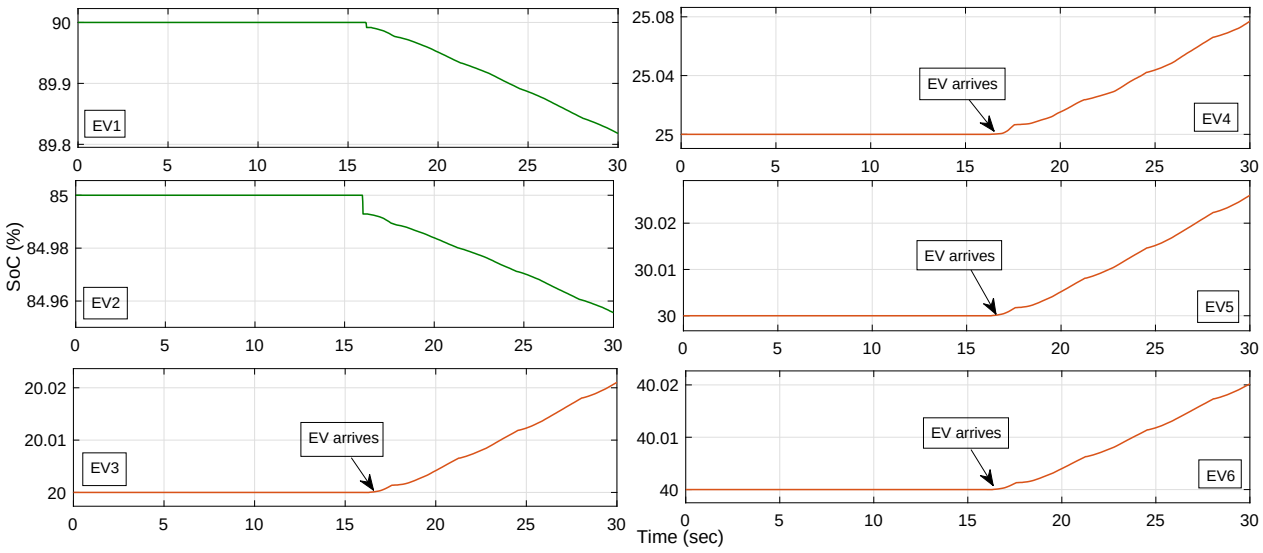

Figure 5.8: Sudden ingress of EVs at the CS

This deviation in frequency is minimized through VSG mechanism by extracting power from the EVs which are already parked at CS and have high SoC levels. As depicted in Fig. 5.8, EV_1 and EV_2 having SoC of 90% and 85% are parked at the CS but not participating in discharging process of EV batteries because the load demand of MG is already balanced by the PV array. Whereas, few EVs like EV_3, EV_4, EV_5 and EV_6 having SoC levels of 20%, 25%, 30% and 40% respectively suddenly ingress at the

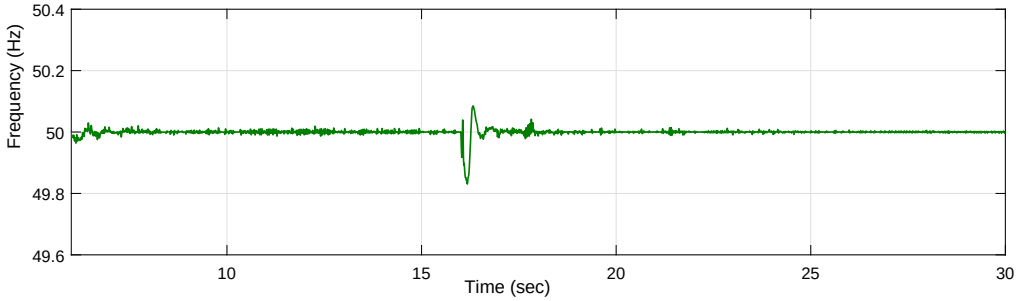

Figure 5.9: Frequency deviation in the system due to sudden ingress of EVs at the CS

CS at the same time instant $t = 16$ sec. As depicted in Fig. 5.9, this sudden ingress of all EVs at the same time leads to frequency deviation in the system. However, this change in frequency is minimized through VSG mechanism by extracting the power from EVs which are already parked at the CS. Thus EVs parked at the CS participates in the MG's frequency regulation process by behaving as a source of power.

5.5 Summary

This chapter focuses on the concept to cater the sudden ingress and egress of EVs at the CS while supporting the MG's frequency. Some EVs are assumed to be parked at the CS. On the other hand, few EVs are considered to ingress and egress at the CS at irregular intervals. Smart CS has been designed, where EVs having a range of battery voltage ratings with diverse SoC levels are parked at the CS. The EVs which are parked at the CS for long duration by EV owners are participating in the charging and discharging process of their batteries to support the frequency of MG. In this work, six EVs have been considered at the CS. Out of these, two EVs are parked at CS which participate in charging and discharging process and rest of the EVs ingress and egress to charge their batteries. VSG control strategy has been adopted to balance the load demand of MG by adjusting the charging and discharging rate of EVs present at the CS. Three case studies have been performed to justify the

frequency support to MG using EVs that are parked at CS and which ingress and egress at irregular intervals. From the results it has been concluded that frequency support to MG can be provided by managing the charging and discharging rate of EV batteries through VSG mechanism.

Chapter 6

Handshaking of CSs through VSG

In today's scenario, frequency regulation is the main concern in islanded Microgrids (MG). This concern of frequency in MG can be sorted out in various ways. Several authors have used different strategies to support the MG's frequency. Handshaking of charging stations (CS) among each other through proper control mechanism can be one of the approach to sort out fluctuation of frequency in MG. This process of handshaking resembles with the interconnected two or multi area system, where different interconnected systems co-ordinate with each other to maintain the frequency of the system [128]. In this chapter, novel handshaking process among multiple CS has been carried out by using virtual synchronous generator (VSG). These multiple CS co-ordinate with each other to accomplish the handshaking process by controlling the charging and discharging of electric vehicle (EV) batteries through VSG mechanism. Fleet of EVs placed at these CS act as an energy storage device for MG. Aggregator plays a role to collect the information from multiple CS about the charging requirements of the EVs. [1]To accomplish the process of handshaking, simulations have been carried out in MATLAB simscape by considering the different case studies. In these case studies, diverse fleet of EVs are assumed to be deployed at the CS. From the

[1]The content of this chapter is taken from:

- K. Dhingra, M. Singh, "Handshaking of VSG with charging station to support the frequency in microgrid," in Electrical Engineering, Springer, vol. 102, pp 2349-2362, June 2020, DOI: 10.1007/s00202-020-01029-z

simulation results, it has been observed that each individual EV deployed at the CS participate in the charging and discharging of their batteries to achieve the process of handshaking and hence to provide the support to MG's frequency through VSG mechanism.

6.1 Introduction

Nowadays, intake of EVs in the market is increasing day by day. Even governments are providing sufficient amount of incentives to the customers to promote the growth of EVs. However, most of the time they remain in idle state. Moreover, in day to day life they remain parked in the shopping malls, cinema halls and office buildings. This parking duration of EVs for which they are in idle state can be used for providing energy to the MG. These vehicles can be used for the energy management schemes [129] [130] [131] by integrating them with the commercial buildings, houses and CS. With the use of EVs, emission of harmful gases can be reduced to a large extent in both the transportation and power sector. Batteries of EV can be used in a bidirectional way through vehicle to grid (V2G) and grid to vehicle (G2V) techniques. EVs as an ESS can be used for the power management [82] in MG , thus they can be used for providing the ancillary services to the MG.

Several authors have explored the concept of charging of EVs using RES. Moreover, burden on the conventional sources can be reduced by charging the EVs using PV arrays. Traube *et al.* [132] proposed a scheme through which power fluctuation in MG due to intermittent nature of PV array can be minimized using the EV battery. Authors have designed a buck-boost converter connected with the dc bus and an EV battery to control the output power of inverter and to support MG's frequency. Bhatti *et al.* [104] have explained about the day time charging of EVs using the PV array in case of stand alone MGs. Sujitha *et al.* [133] have discussed about the different type of power converters which can be utilized in stand alone and grid connected

MGs for the coordination between RES and EVs. Gao *et al.* [134] have demonstrated vehicle to grid concept for energy management between EVs and RES. Authors have elaborated, the gap between power generation and load demand can be minimized at a quick rate by deploying EVs in the system. Zhu *et al.* [135] discussed about the role of EV aggregator in regulating the MG's frequency. Authors have considered the large penetration of EVs in the frequency regulation process of MG. However, authors have not considered the EVs as a load while regulating the frequency of MG. Yao *et al.* [80] have elaborated the real time charging of EVs placed at the parking station. Kaur *et al.* [136] have demonstrated on the use of aggregator to provide support to the grid frequency using EVs. Authors have explained, that the charging and discharging rate of EVs can be controlled while providing the frequency support to grid. Some authors have focused on the mobile behavior of EVs as a flexible load as well as the source of power, these authors have talked about the role of CS in the system. Authors suggested that by deploying EVs at the CS, power fluctuations in the MG can be reduced to a large extent which arises due to the intermittent nature of RES.

Some authors have illustrated the importance of CS in maintaining the MG's frequency to its actual value. Sometimes, it may be difficult to meet the load demand of MG by using EVs parked at single CS, in such a case multiple CS can be used to balance the load demand of MG. Energy can be withdrawn or delivered to the CS as per the requirement of the MG. Thus, EVs placed at the CS can participate in the frequency regulation process of MG by balancing the load demand [137]. EVs placed at the CS can be charged to a high value during off peak hours of the MG and can deliver the energy back to MG during peak hours. In this way, EVs can be utilized to balance load demand and hence, to regulate the MG's frequency.

6.1.1 Motivation

Several authors have discussed about the power management of MG using CS. Some authors have elaborated the PV assisted CS to meet the load demand of commercial buildings [138] [139]. Some of the contributors have illustrated the importance of CS to support the frequency of stand alone MGs. Various researchers [125] [140] have used EV based droop control techniques to support MG's frequency. Few researchers [62] [141] have implemented VSG control on single power converter to regulate MG's frequency. However, none of them considered the handshaking of CS with VSG to support the MG's frequency. In this work, handshaking of VSG with multiple CS has been proposed to maintain the MG's frequency and to meet the charging needs of EVs. Multiple CS share the power with each other through VSG mechanism to accomplish the process of handshaking and hence to support the MG's frequency.

6.1.2 Contribution

- Multiple CS co-ordinate with each other through VSG mechanism to meet the charging needs of EVs.
- Frequency of the MG has been supported through handshaking process of CS among each other.
- Reliability of the system does not get affected even if one of the power converter fails to operate due to any fault.

6.1.3 Organization

This chapter is organized in the following way. Section 6.2 elaborates the proposed methodology. Control strategy of the work is mentioned in Section 6.3. Obtained results are analyzed in Section 6.4. Summary of the chapter is described in Section 6.5.

6.2 System Framework

In the proposed work, a system is considered, which consists of multiple CS, power converters and PV array. CS considered in the system is a combination of buck boost converters and fleet of EVs. Three different CS have been considered in the system and each CS is connected with a common dc bus. CS is a venue where EVs can meet their charging requirements. Furthermore, the owners of EVs can allow the participation of their vehicles in discharging process also for short duration to satisfy the load profile of MG in peak hours. The owners of EV can get various incentives for allowing their vehicles to participate in discharging process at the CS [70]. Buck-boost converters present at the CS can allow the EV battery to charge or discharge by working in buck and boost mode respectively. In this way, EVs can behave both as load as well as source of energy for the MG. CS can be installed at various locations like parking of industries, basement of shopping complexes and office buildings. Moreover, at these locations vehicles are parked in abundance so charging and discharging operation of EVs can be easily performed to provide the support to the MG. However, the limitation of the proposed system is CS must not be located too far from each other to ensure the proper handshaking process among them.

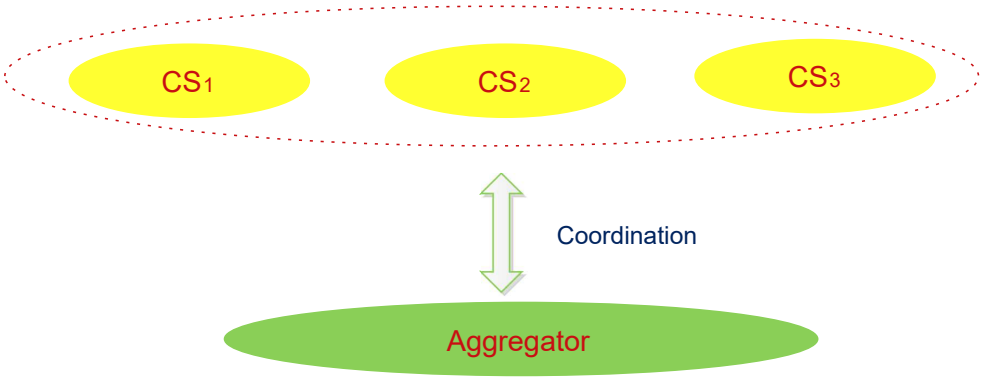

Figure 6.1: Coordination of charging station with aggregator

6.2.1 Coordination of Charging Station with Aggregator

Aggregator behaves as an interface between CS and the MG. EVs parked at CS behave as flexible loads and work in close coordination with aggregators and CS. The information related to the state of charge (SoC) of the EVs parked at the CS is provided to the aggregator to meet their charging and discharging demands. Further, as per the SoC value of EV, it is analyzed that what amount of power can be taken from the EVs parked at the CS. These fleet of EVs accomplish the charging and discharging operations as per the requirements of MG. As per Fig. 6.1, each CS exchanges the information with aggregator about their charging requirements. Aggregators plays a role to regulate the charging (C), and discharging (D) rate of EVs while accommodating their energy demands. Aggregator sends a signal among the CS to receive or deliver the power as per the requirement of the system. CS shares the load among each other to satisfy the load demand of MG.

6.2.2 Control mechanism

In this system, it has been considered that multiple CS in coordination with the power converters behave as a VSG. As depicted in Fig. 6.2, all the VSGs are connected with a single AC bus to accommodate the load demand of the system. VSG controls the power converter to manage the bidirectional power flow in the system. Both the PV array and the CS operate in parallel with each other to meet the load demand of the system.

As per the considered system, buck boost converter and power converter behaves as an intermediate between PV array and CS. PV array delivers the fixed amount of power, however due to the change in load on the considered system, power delivered by the CS keeps on changing. When there is a mismatch between the power generated by the RES and load demand of the MG then frequency deviation in the system will occur. This frequency deviation is compensated through aggregator by sending a signal to the CS to supply or fetch the power. When the MG's frequency increases

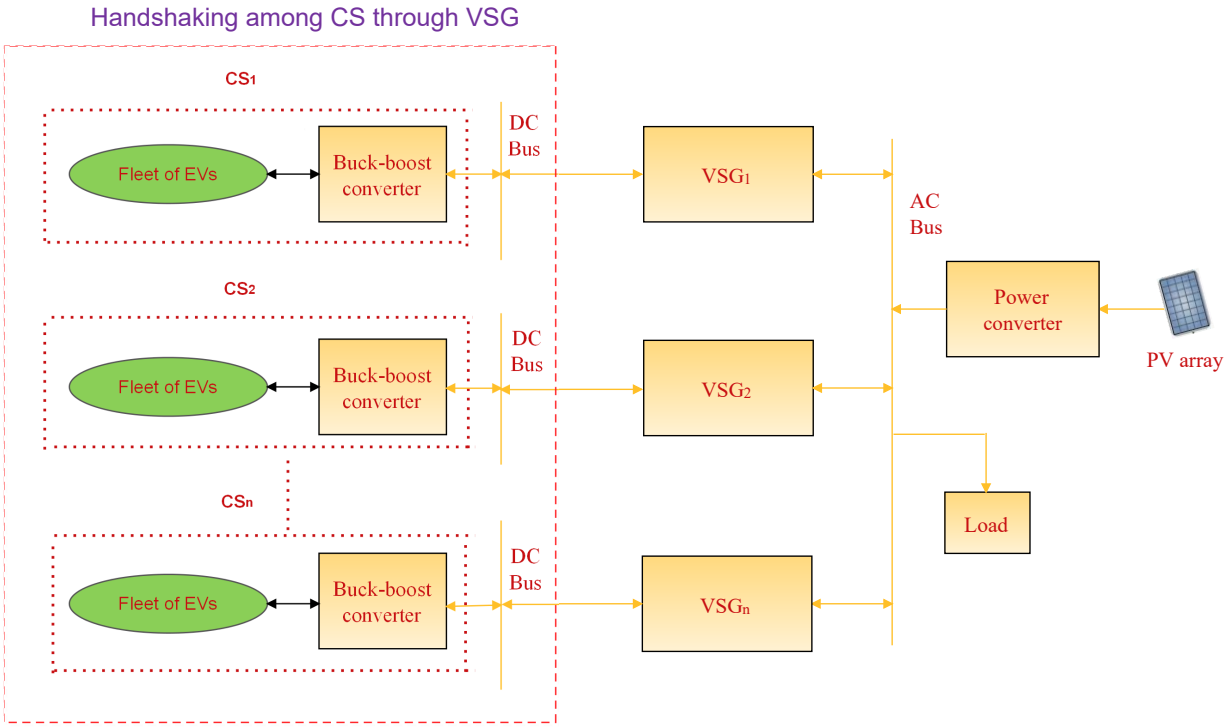

Figure 6.2: Schematic diagram of the proposed system

from its nominal value then the aggregator sends a signal to the CS to fetch the surplus power and charge the EV batteries. On the other hand, when MG's frequency decreases to a value less than the nominal value then aggregator sends a signal to the CS to supply the power and to accommodate the load profile of MG.

The logic behind the power management in MG is the virtual inertia which is extracted in the form of energy through dc link capacitors. However, while considering the parallel operation of the VSG for each CS, equivalent inertia for the whole system is taken into account. On the other hand, angular frequency for each VSG is considered to remain same. In case, there is a difference between load profile of the system and power produced by PV array then CS supplies/fetches the power to/from the MG. Buck-boost converter operate in both the buck mode and boost mode to charge and discharge the battery respectively. VSG control mechanism governs the power converter to manage the flow of power in both the directions. Power converter acts both as a rectifier and an inverter. As a rectifier, power converter charges the battery, on the other hand as an inverter, power converter helps the battery to op-

erate in discharge mode. With the variation in the load demand of MG, the power delivered or fetched by CS changes. Charging and discharging of EVs has been taken care of through the coordination of multiple CS among each other. As the EVs are mobile in nature they can serve the MG both as load and source of power. Based on SoC level of each EV it can participate to provide support to MG's frequency. The owners of EVs can get incentives for the participation of their vehicles to provide power to MG during peak hours. Handshaking process works as a distributed control strategy where, number of power converters operate in parallel with each other. Each power converter behaves as a VSG. Moreover, it can be described as a system where number of VSG operate in parallel with each other. The main advantage of the proposed system is that the reliability of the MG will not be affected even if one of the VSG fails to operate. If any power converter gets faulted then the other power converters keep on sharing the power to maintain the frequency of MG.

Control strategy of the considered system has been represented by Fig. 6.3. As per this figure, current controller, voltage controller and droop control perform various functions. Whereas droop control generates the reference V_d^* and V_q^*, voltage controller produces reference I_d^* and I_q^*. For the current controller I_d^*, I_q^*, I_d and I_q are used as an input parameters. The signal V_{dq} is generated by using current controller, which is further used as an input to generate control signal for PWM. Virtual rotor angle θ_α is generated by using the VSG control strategy, the dc link voltage V_{dc} and V_{dq} generated using current controller, all these parameters act as an input signal for the generation of control signal for PWM. Further, the PWM controls the power converter based on the input parameters of control signal generation. In this way the dc link voltage of the CS coordinates with the VSG control to manage the flow of power in the system. The generation of virtual rotor angle θ_α has been explained in the mathematical formulation section of this chapter.

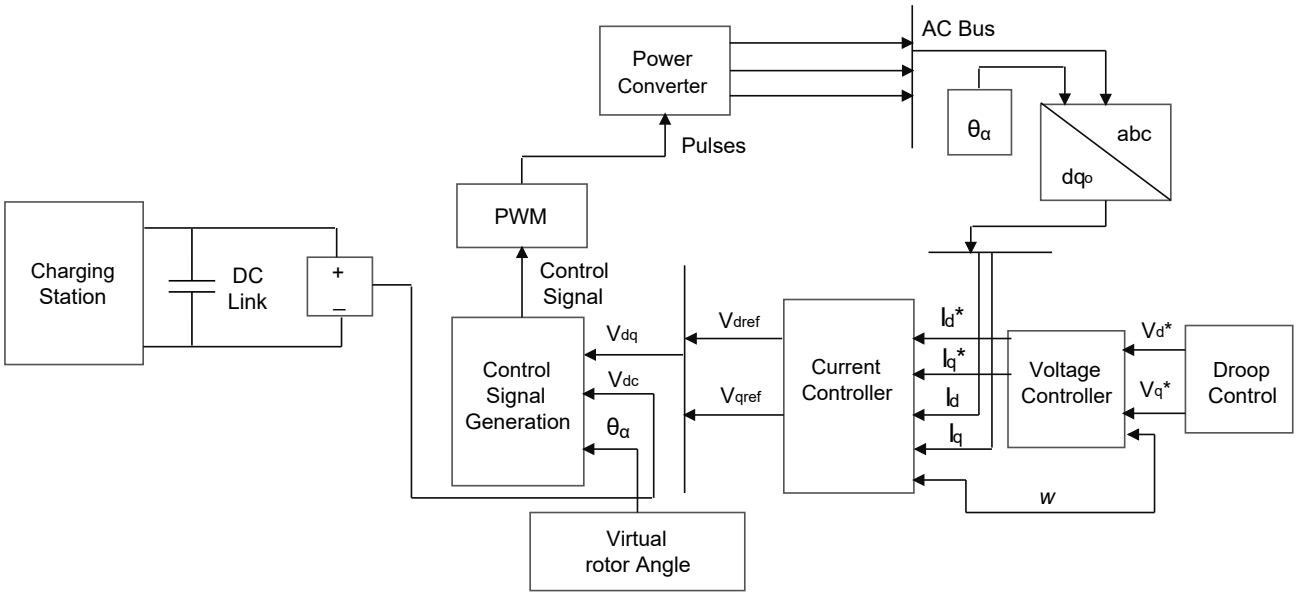

Figure 6.3: Control strategy of power converter

6.3 Mathematical formulation

In this section, control mechanism related to charging and discharging of EVs has been discussed while maintaining the load demand of the considered system. This strategy can be applied on n number of VSG operating in parallel and share the power distribution among CS and the MG. VSG behaves as an intermediate between EVs and MG. Handshaking of the VSG with CS has been taken into account to support the MG's frequency. Virtual inertia to the system has been provided by using the swing equation as follows, which is written separately for each CS.

Swing equation for the system related to the CS_1 is illustrated as,

$$P_{cs_1} - P_{ref} = \Delta P_{vsg_1} = J_1 w \frac{dw}{dt} \tag{6.1}$$

For CS_2

$$P_{cs_2} - P_{ref} = \Delta P_{vsg_2} = J_2 w \frac{dw}{dt} \tag{6.2}$$

For CS_n

$$P_{cs_n} - P_{ref} = \Delta P_{vsg_n} = J_n w \frac{dw}{dt} \tag{6.3}$$

Where, P_{cs_1}, P_{cs_2} and P_{cs_n} is the power delivered by the CS_1, CS_2 and CS_n respectively. P_{ref} is the reference power for each converter. J_1, J_2 and J_n is the virtual inertia for each VSG and $\frac{dw}{dt}$ is the rate at which angular frequency changes.

The net active power shared by CS through handshaking with VSG to balance the load demand of MG is expressed in the following way,

$$\Delta P = \Delta P_{vsg_1} + \Delta P_{vsg_2} ..... + \Delta P_{vsg_n} \tag{6.4}$$

Further, Eq. (6.4) can be written in the following way,

$$\Delta P = J_1 w \frac{dw}{dt} + J_2 w \frac{dw}{dt} ..... + J_n w \frac{dw}{dt} \tag{6.5}$$

Eq. (6.5), can be further rearranged as,

$$\Delta P = (J_1 + J_2 ..... + J_n) w \frac{dw}{dt} \tag{6.6}$$

From Eq. (6.6), the following expression can be written as,

$$\Delta P = P_{cs} - P_{ref} = J_{eqv} w \frac{dw}{dt} \tag{6.7}$$

From Eq. (6.7), the expression for the rate of change of angular frequency can be written as,

$$\frac{dw}{dt} = \frac{P_{cs} - P_{ref}}{J_{eqv} w} \tag{6.8}$$

Where, P_{cs} is the net power supplied or fetched by the EVs placed at the CS which

can be positive or negative. Virtual angular frequency w is calculated from the above mentioned equation. Emulation of virtual inertia means the power converter to hold or deliver the required amount of energy based on the fluctuations in frequency from its base value. Where, J_{eqv} can be represented as,

$$J_{eqv} = \frac{2H}{w^2} S_n \tag{6.9}$$

Where, H can be represented as an inertia constant while S_n represents the rated power of system. Reference power of the system can be represented by,

$$P_{ref} = \begin{cases} P_{cs} - \frac{(\Delta f) P_{cs}}{f_{nom}}, & \text{If } P_{cs} \text{ is negative.} \\ P_{cs} + \frac{(\Delta f) P_{cs}}{f_{nom}}, & \text{If } P_{cs} \text{ is positive} \end{cases} \tag{6.10}$$

Where,

$$\Delta f = -\frac{P_{load} - P_{pv}}{P_{cs} + P_{load}} \tag{6.11}$$

Let us assume, P_{cs} is the amount of power required from the CS to minimize the frequency fluctuation Δf. This P_{cs} can be either positive or negative. If it is positive, then aggregator will send the signal to the CS to fetch the power, otherwise to deliver the power. P_{ref} is the amount of power to be delivered by the power converter in either direction to minimize the fluctuation in frequency. Where, Δf is the deviation in frequency due to the change in load demand of the system, f_{nom} is the nominal frequency of the system. P_{load} is the load on the system, P_{cs} and P_{pv} is the power released by CS and PV array respectively.

Using Eq. (6.8) and Eq. (6.10), the expressions for two cases can be derived.

Case A. When power is delivered by the CS, the expression for change in angular frequency can be written in the following way,

$$\frac{dw}{dt} = \frac{P_{cs} - (P_{cs} - \frac{\Delta f P_{cs}}{f_{nom}})}{J_{eqv} w} \tag{6.12}$$

Further, simplified form of Eq. (6.12) can be expressed in the following way,

$$\frac{dw}{dt} = \frac{\Delta f * P_{cs}}{J_{eqv} w * f_{nom}} \tag{6.13}$$

Case B. When power is fetched by the CS, the expression for change in angular frequency can be written as,

$$\frac{dw}{dt} = \frac{P_{cs} - (P_{cs} + \frac{\Delta f P_{cs}}{f_{nom}})}{J_{eqv} w} \tag{6.14}$$

Further, Eq. (6.14) can be rearranged in the following way,

$$\frac{dw}{dt} = -\frac{\Delta f * P_{cs}}{J_{eqv} w * f_{nom}} \tag{6.15}$$

The main parameter on which the power sharing among VSG depends is angular frequency w. With the change in Δf the rate of angular frequency changes, due to which power delivered by the converter also changes. By solving Eq. (6.15), w is obtained, which is further used to find out the virtual rotor angle θ_α of the system as per the following equation

$$\theta_\alpha = \int_0^t w dt \tag{6.16}$$

This virtual rotor angle is further used to control the power converter to manage the bi-directional movement of power in the system. However, the considered system is just an approach for the analysis purpose.

6.4 Results and Discussion

In this work, the proposed system consists of multiple CS, where each CS shares the power to minimize the frequency fluctuation of MG. Handshaking among CS takes place through VSG to balance the MG's load profile. EVs parked at these CS play a crucial role to balance the MG's frequency. These EVs with the help of VSG control either contribute or fetch the power to and from the MG to minimize the gap between power generation and load demand. Through VSG mechanism, EVs send the power to MG during peak hours and absorb the power from MG during off peak hours respectively. Simulations have been carried out in MATLAB Simulink to analyze the results. Through these simulations, it has been observed that each CS contributes for power management through VSG control to stabilize the MG's frequency. For the simulation purpose, three CS have been considered, further diversity of EVs is assumed at the CS. Two case studies have been performed to observe the participation of CS to support the MG's frequency through VSG control.

6.4.1 Case 1

In this case, it has been assumed that the four EVs are parked at each CS which can participate in the frequency support of MG. The EVs which have less SoC, arrived at the CS for charging purpose. On the other hand, EVs which are already parked at the CS and have high SoC contribute as an energy source to balance the load demand of MG. Here, in this case EV_1 to EV_4 are the EVs which are parked at CS_1. Moreover, EV_1'' to EV_4'' are parked at CS_2 and EV_1''' to EV_4''' are parked at CS_3. These three CS co-ordinate with each other to meet the charging needs of their respective EVs. The EVs those have low SoC level can charge their batteries on the other hand, EVs having high SoC participate in discharging process to meet the load demand on the MG side. As depicted in Fig. 6.4, EV_1, to EV_3 have SoC level of 92%, 85% and 90%, deployed at the CS_1 participates in the power sharing process. On the other hand, EV_4 having SoC of only 20% starts charging at the same time.

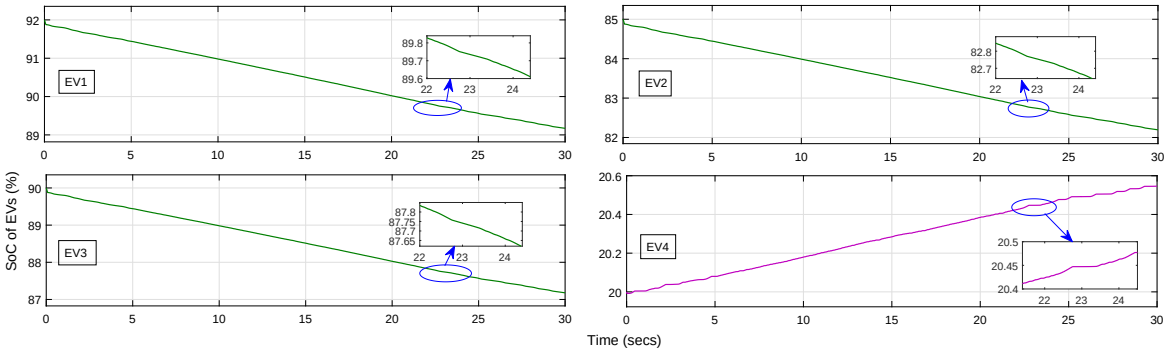

Figure 6.4: EVs deployed at the CS_1 for participation in charging and discharging process

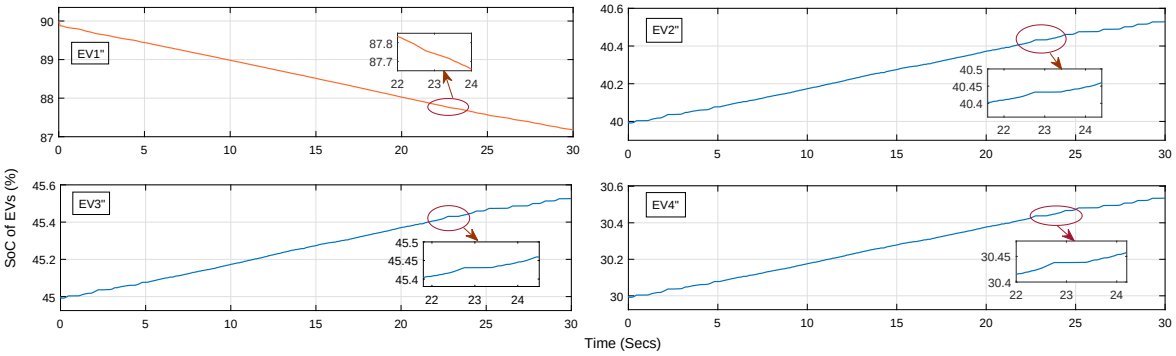

Figure 6.5: EVs deployed at the CS_2 for participation in charging and discharging process

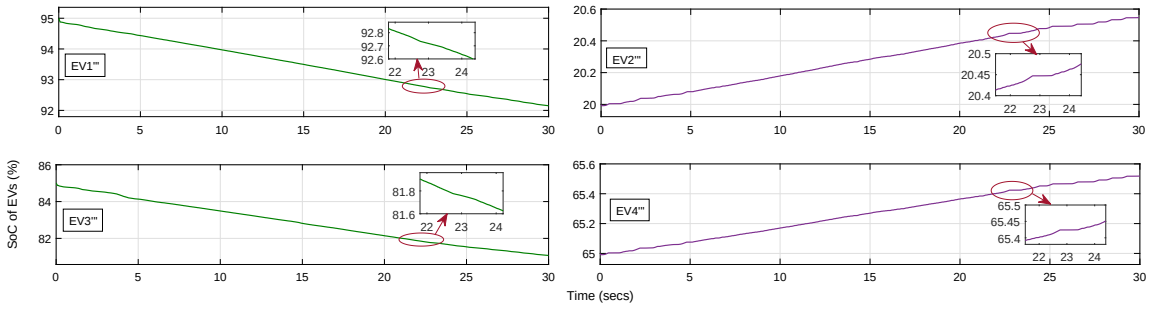

Figure 6.6: EVs deployed at the CS_3 for participation in charging and discharging process

Similarly, as illustrated in Fig. 6.5 and Fig. 6.6, the charging and discharging of the EVs commences which are parked at CS_2 and CS_3. EV_2'' to EV_4'' and EV_2''', EV_4''' having low SoC level of 40%, 45%, 30%, 20% and 65% starts charging. On the other hand, EV_1'', EV_1''' and EV_3''' having high SoC level of 90%, 95% and 85%

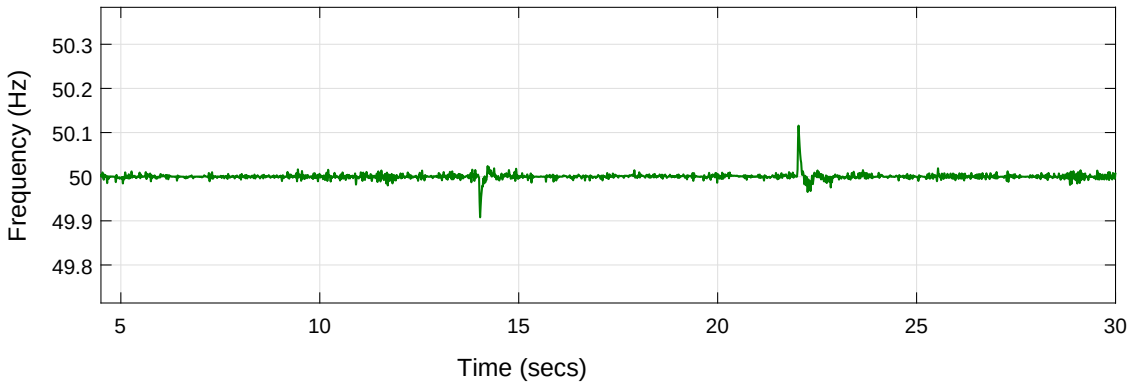

Figure 6.7: **Frequency of the system**

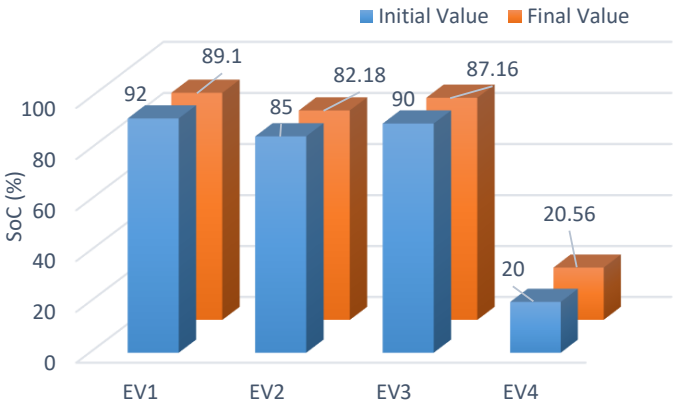

Figure 6.8: SoC of EVs at CS_1 during change in load of MG

starts discharging to accommodate the sudden increase in load demand of MG. As depicted in Fig. 6.4, Fig. 6.5 and Fig. 6.6, due to the change in load demand of MG, there is slight reduction in the charging rate of EV_4, EV_2'' to EV_4'', EV_2''' and EV_4''' respectively. However, D rate of EV_1 to EV_3 and EV_1'', EV_1''' and EV_3''' increases at the same time. Zoomed portion of Fig. 6.4, Fig. 6.5 and Fig. 6.6, clearly shows the change in C and D rate of the EVs which are parked at the CS. From these results, it is very clear that, EVs deployed at the multiple CS co-ordinates the power exchange through VSG mechanism, while meeting the load demand of MG.

Fig. 6.8, Fig. 6.9 and Fig. 6.10, shows the change in SoC levels of EVs when different CS coordinate with each other through VSG mechanism. As per Fig. 6.8, the SoC level of EV_1 parked at CS_1 changes from 92% to 89.10% within 30 secs of

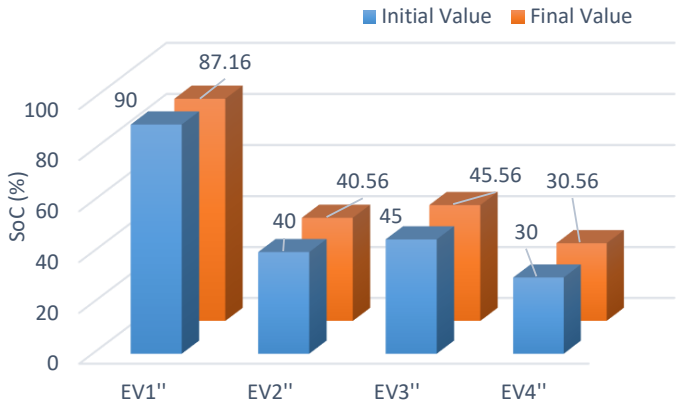

Figure 6.9: SoC of EVs at CS_2 during change in load of MG

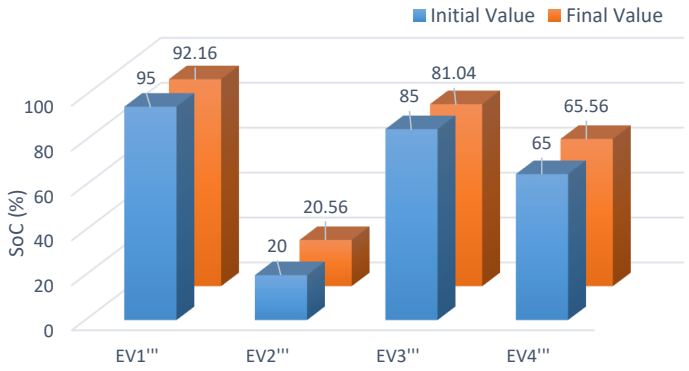

Figure 6.10: SoC of EVs at CS_3 during change in load of MG

simulation, whereas the SoC level of EV_2 and EV_3 changes from 85% to 82.18% and from 90% to 87.16% respectively. On the other hand, SoC level of EV_4 is increased from 20% to 20.56%. This change in SoC takes place to satisfy the load demand of MG during load change and to meet the the charging needs of EVs which have low SoC levels. Similarly, as per Fig. 6.9, the SoC levels of EVs parked at CS_2 change in the following way. SoC level of EV_1'', changes from 90% to 87.16% while the SoC level of EV_2'', EV_3'' and EV_4'' change from 40% to 40.56%, 45% to 45.56% and 30% to 30.56% respectively within 30 secs of simulation. Further, Fig. 6.10, represents the change in SoC levels of EVs parked at the CS_3. As per this figure SoC level of EV_1''' and EV_2''' decreases from 95% to 92.16% and 85% to 81.04% respectively. On the other hand, SoC level of EV_3''' and EV_4''' increases from 20% to 20.56% and 60%

Table 6.1: Parameters of the system

Parameter	**Value**
DC bus voltage for CS	600 V
Line to line voltage V_L	400 V
Battery voltage rating of EV	230 V
Maximum power delivered by PV emulator	10.7 KW
Frequency f	50 Hz

to 60.56% respectively. These changes in SoC levels of EVs at the CS represent the handshaking of CS among each other to support the MG's frequency through VSG mechanism.

6.4.2 Case 2

In this case, dynamic behavior of EVs at the CS is considered while the handshaking process takes place among CS. Switching of EVs has been done for considering the dynamic behavior of EVs. Here, EVs parked at the different CS, arrive and depart from the CS at random intervals of time. It is assumed that some EVs remain parked at the CS for long duration while others arrive and depart at random intervals. From the results, it has been verified that all the three CS do handshaking among each other through VSG mechanism to meet the load demand of MG and satisfy the charging needs of other EVs. In this case, four EVs are assumed to be deployed at each CS. However, it is assumed that for CS_1, EV_1, remains deployed at the CS upto 26^{th} sec of simulation time and departs after that.

On the other hand, EV_2 to EV_4 arrive at the CS at different intervals of time. EV_2 arrives at the beginning, while EV_3 and EV_4 arrive at 2^{nd} sec and 10^{th} sec of

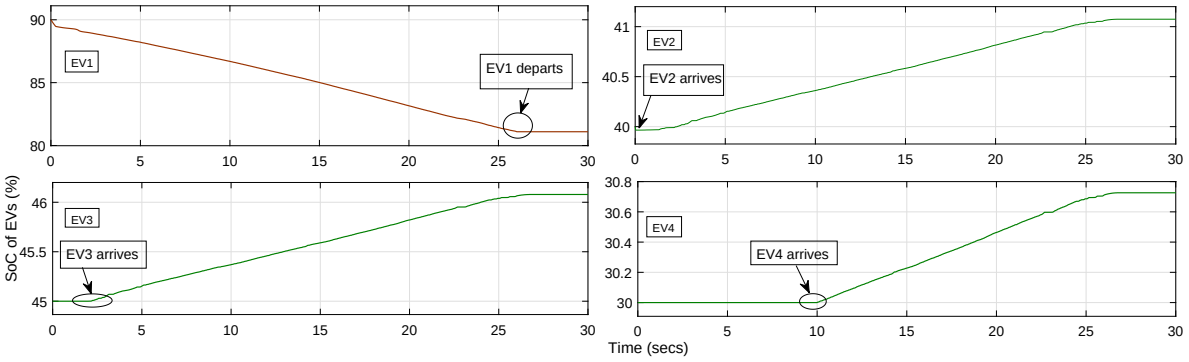

Figure 6.11: Dynamic behavior of EVs at the CS_1

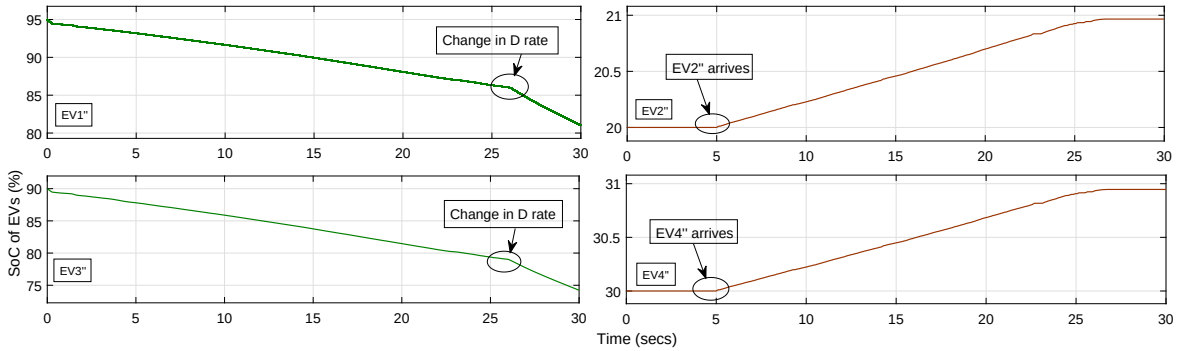

Figure 6.12: Dynamic behavior of EVs at the CS_2

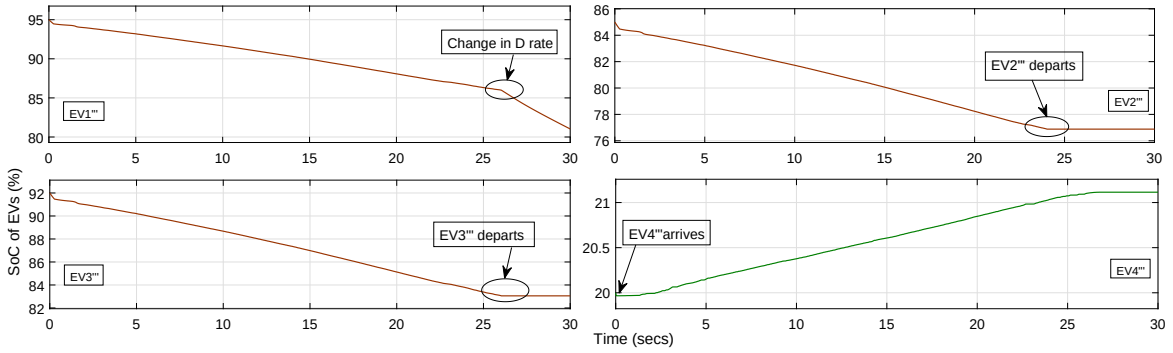

Figure 6.13: Dynamic behavior of EVs at the CS_3

simulation time respectively. Similarly for CS_2 and CS_3, EV_1'' and EV_3'', EV_1''' and EV_4''' remain deployed at the CS for all the time, while EV_2'' and EV_4'' both arrive at the CS at 5^{th} sec of simulation time. Moreover, EV_2''' and EV_3''' depart at 24^{th} and 26^{th} sec respectively.

During the handshaking process of CS among each other through VSG mechanism, all the CS share the flow of power in the system. As depicted in Fig. 6.11, when one

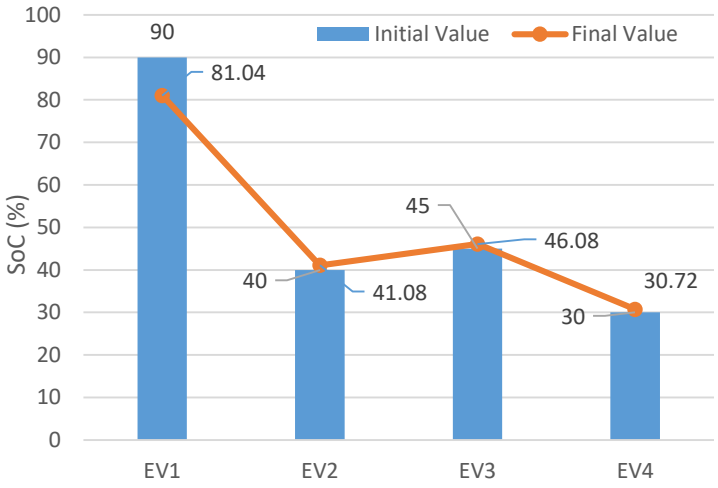

Figure 6.14: SoC of EVs considering their dynamic movement at CS_1

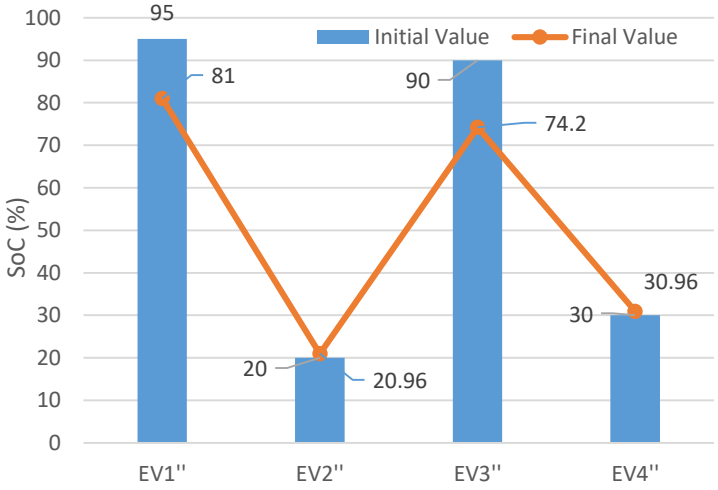

Figure 6.15: SoC of EVs considering their dynamic movement at CS_2

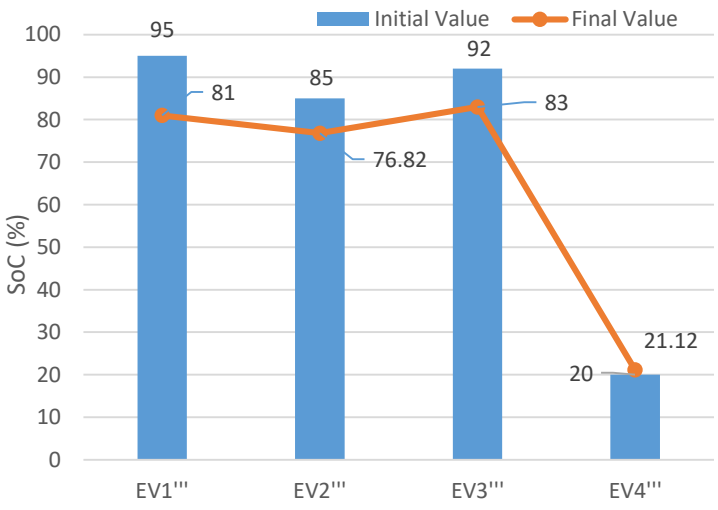

Figure 6.16: SoC of EVs considering their dynamic movement at CS_3

EV having high SoC level is departed from the CS_1 at the 26^{th} sec, then more power is shared by the EVs which are parked at CS_2 and CS_3. As shown in Fig. 6.11, Fig. 6.12 and Fig. 6.13, when the EV_1, which is in discharging state and deployed at CS_1 departs from the CS at the 26^{th} sec then the discharging rate of $EV_1^{''}$, $EV_3^{''}$, $EV_1^{'''}$ gets increased at the same time to balance the load demand of MG. This management of change in discharging rate occurs due to handshaking process of CS among each other through VSG mechanism. Further, as depicted in Fig. 6.11, when the EV_3 and EV_4 arrives at the CS_1, at 2^{nd} sec and 10^{th} sec of simulation time, the charging of their battery commences. Similarly, as shown in Fig. 6.12 and Fig. 6.13, when the $EV_2^{''}$, $EV_4^{''}$ and $EV_4^{'''}$ arrive at the CS_2 and CS_3, the batteries of these EVs starts charging. It can be depicted from Fig. 6.7 that frequency of the system changes due to the change in load demand of the system. However, this fluctuation in frequency is minimized through handshaking process of multiple CS by sharing the power among each other. This process of power sharing takes place through VSG mechanism by managing the charging and discharging rate of EVs which are parked at different CS.

Fig. 6.14, Fig. 6.15 and Fig. 6.16, represents the value of SoC at the arrival time and at the departure time of EV. During the considered simulation period, some EVs gets discharged to meet the load demand of MG, while other EVs which arrive at the CS for charging purpose, charge their batteries. These figures represent the initial and final value of SoC of EV battery. Fig. 6.14, indicates the charging of three EVs, EV_2 to EV_4 respectively. Whereas initial and final SoC value of EV_2 varies from 40% to 41.08%, for EV_3 it varies from 45% to 46.08% and for EV_4 it varies from 30% to 30.72% respectively. On the other hand, EV_1 participates in the frequency support process and its SoC changes from 91% to 81.04%. Similarly as depicted in Fig. 6.15, SoC of $EV_1^{''}$ and $EV_3^{''}$ decreases to 81% from 95% and to 74.2% from 90% respectively. On the other hand, SoC of $EV_3^{''}$ and $EV_4^{''}$ increases from 20% to 20.96% and from 30% to 30.96% respectively. Fig. 6.16, shows the participation of $EV_1^{'''}$ to $EV_3^{'''}$ in handshaking process while providing the support to MG's frequency. Whereas, $EV_4^{'''}$ parked at the CS for charging the battery, gets charged upto 21.12%

from 20% within 30 seconds of simulation time. As per this figure, the SoC of $EV_1^{'''}$ to $EV_3^{'''}$ decreases while the SoC level of $EV_4^{'''}$ increases.

Table 6.2: Specifications of EVs For Case 2 at CS_1

EV	**Initial SoC of EV**	**Status of EV**
EV_1	90%	Depart from CS_1 at 26^{th} sec
EV_2	45%	Arrive on CS_1 at 2^{th} sec
EV_3	40%	Remain parked at the CS_1
EV_4	30%	Arrive on CS_1 at 10^{th} sec

Table 6.3: Specifications of EVs For Case 2 at CS_2

EV	**Initial SoC of EV**	**Status of EV**
$EV_1^{''}$	95%	Remain parked at the CS_2
$EV_2^{''}$	85%	Remain parked at the CS_2
$EV_3^{''}$	20%	Arrive at CS_2 at 5^{th} sec
$EV_4^{''}$	30%	Arrive at CS_2 at 5^{th} sec

Table 6.4: Specifications of EVs For Case 2 at CS_3

EV	**Initial SoC of EV**	**Status of EV**
$EV_1^{'''}$	95%	Remain parked at CS_3
$EV_2^{'''}$	92%	Remain deployed at CS_3
$EV_3^{'''}$	85%	Depart from CS_3 at 24^{th} sec
$EV_4^{'''}$	20%	Remain parked at CS_3

6.4.3 Case 3

In this case, the variation in irradiation level of the PV array has been considered to observe its effect on the charging and discharging behavior of EVs while parked at the CS. As illustarted in Fig. 6.17, the irradiation level of the PV array has been changed from 1000 w/m^2 to 600 w/m^2 at 18^{th} sec and again from 600 w/m^2 to 1000 w/m^2 at 22^{th} sec. In the considered case, load of the system is assumed as constant and only the irradiance level of the PV array has been varied. From the results, it has been observed that the D rate of EVs changes at 18^{th} and 22^{th} sec, when the irradiation level of PV array changes. As depicted in Fig. 6.18, Fig. 6.19 and Fig. 6.20 the charging rate of EV_4, EV_2'', EV_3'', EV_4'', EV_2''' and EV_4''' reduces at 18^{th} sec when the irradiation level changes from 1000 w/m^2 to 600 w/m^2. Further, at 22^{th} sec when the irradiation level changes again from 600 w/m^2 to 1000 w/m^2, the C rate of the EVs rises again.

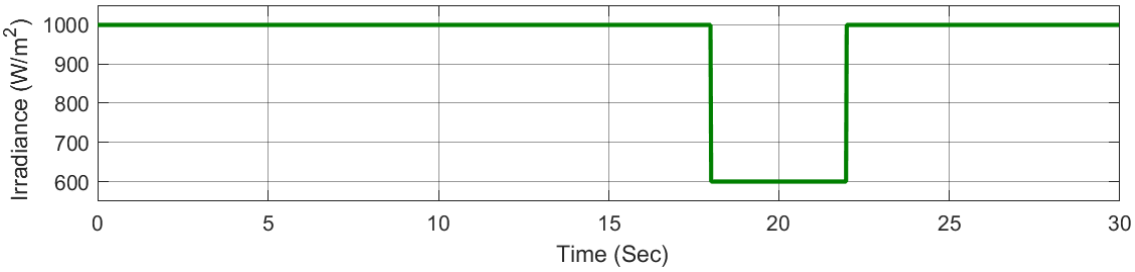

Figure 6.17: Change in the Irradiance of PV array

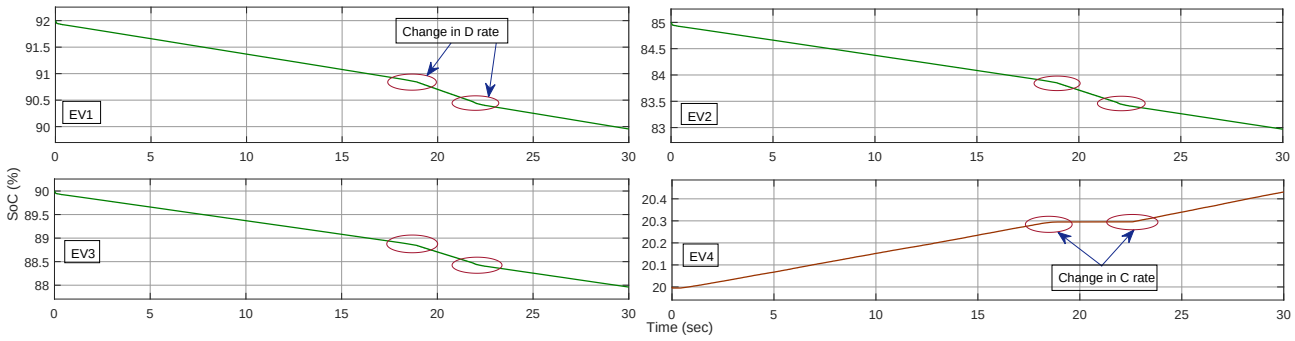

Figure 6.18: Effect of change in Irradiation level of PV array on the EVs parked at CS_1

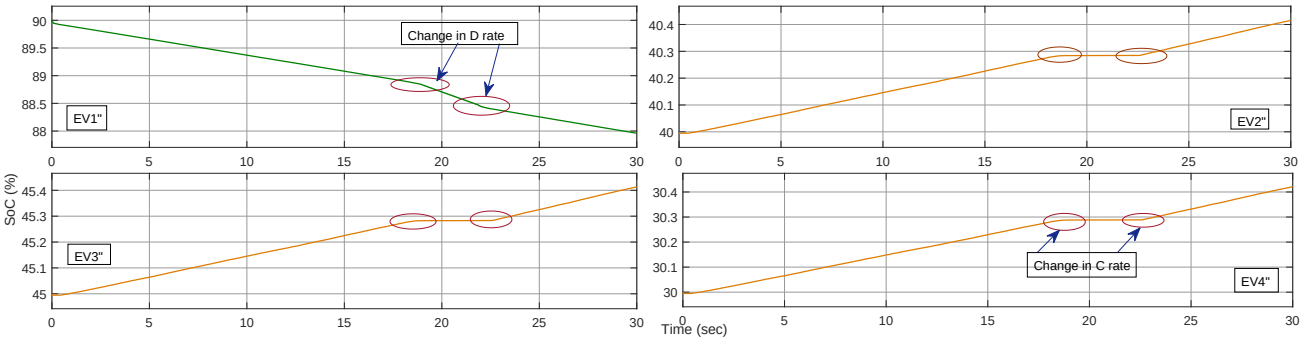

Figure 6.19: Effect of change in Irradiation level of PV array on the EVs parked at CS_2

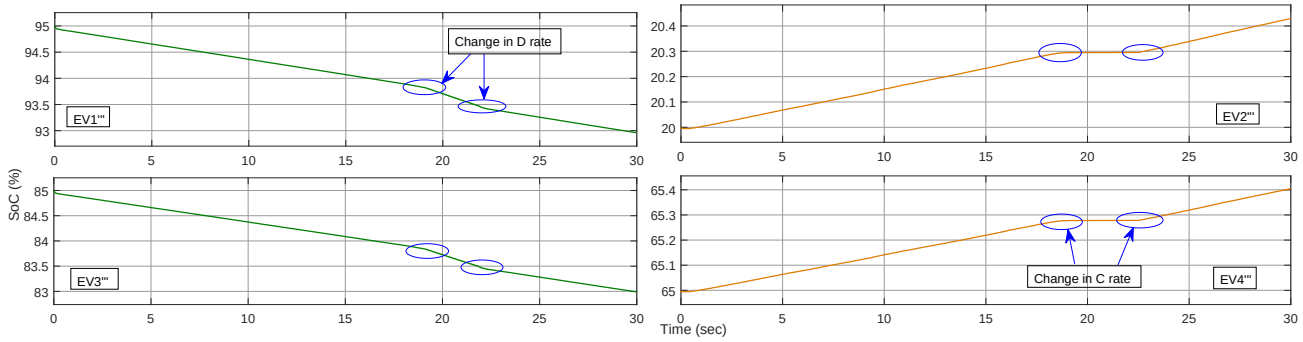

Figure 6.20: Effect of change in Irradiation level of PV array on the EVs parked at CS_3

Fig. 6.21, Fig. 6.22 and Fig. 6.23, illustrates the variation in SoC of EVs parked at the CS during change in the irradiation level of PV array. As illustrated in Fig. 6.21, the SoC level of EV_1, EV_2 and EV_3 changes from 92% to 89.97%, 85% to 83.04% and 90% to 87.97% respectively. On the other hand, the EV_4 changes from 20% to 20.44%. Similarly, Fig. 6.22 and Fig. 6.23, depicts the changes in SoC levels during handshaking process among CS, while considering the variation in irradiation level of PV array.

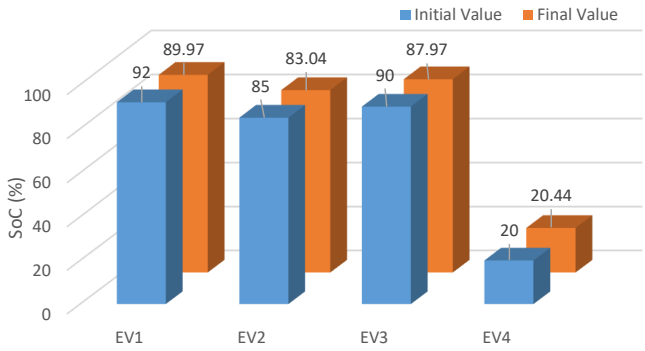

Figure 6.21: SoC of EVs parked at CS_1 during change in irradiation level of PV array

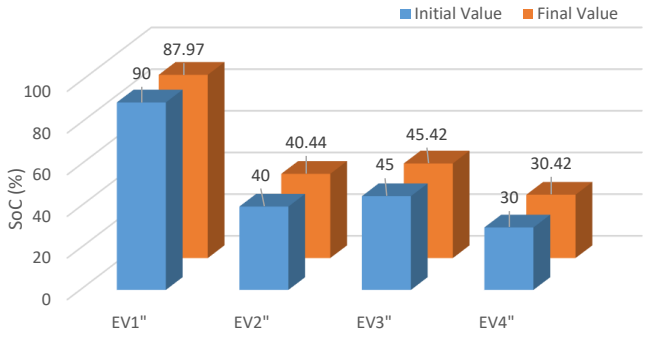

Figure 6.22: SoC of EVs parked at CS_2 during change in irradiation level of PV array

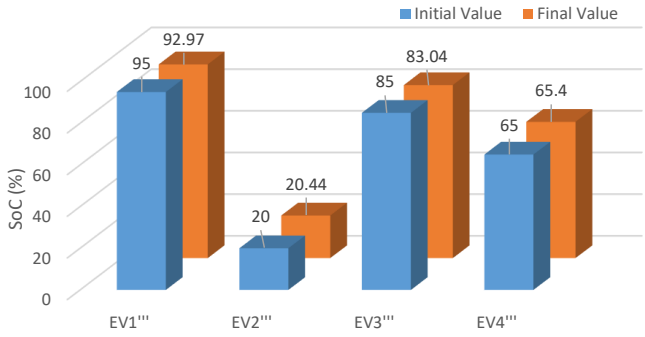

Figure 6.23: SoC of EVs parked at CS_3 during change in irradiation level of PV array

6.5 Summary

This chapter focuses on the power sharing among different CS through VSG control mechanism. The CS co-ordinate among each other through VSG control to regulate

the frequency of MG. It is being concluded that EVs parked at the different CS can participate in power sharing through handshaking of CS among each other. Moreover, this handshaking process is achieved through the parallel operation of VSG and many CS co-ordinate with each other to balance the load demand of MG. It has been found that even if one of the power converter fails to operate then other power converters share the power to support the frequency of MG and hence, to make the system more reliable. Novelty of this chapter lies in the fact that handshaking among CS takes place through VSG mechanism. Moreover, this process of handshaking leads to the exchange of power among CS to support the MG's frequency. Irradiance level of the PV array has been varied to observe its effect on the charging and discharging of EVs during handshaking process of CS. Reduction in irradiance level shows that the rate at which the battery was charging decreases slightly and at the same time the rate at which battery was discharging got increased. Results show the effective handshaking among the CS even during the fluctuation in the power delivered by the PV array. Further, in the case of multiple MG, centralized handshaking between MGs is another option to support the frequency.

Chapter 7

Conclusion and Future Scope

7.1 Conclusion

Frequency of the MG usually fluctuates due to the power mismatch between generation and load demand. This fluctuation in frequency can be minimized by providing the inertia to the system. However, RES are not capable enough to provide inertia to the system so, there is need of virtual inertia to be provided to the system to maintain the MG's frequency. To achieve this requirement of virtual inertia, VSG control mechanism has been implemented. Virtual Inertia is provided to the system through VSG mechanism which helps to support the frequency of MG. Moreover, virtual inertia can be extracted from the ESS. In this work, fleet of EVs parked at the CS has been used to provide the virtual inertia to the MG through VSG control. The designed CS meet the charging needs of the EVs while managing the frequency support of the MG. CS provides the constant DL voltage to the input of three phase power converter terminals even if the EVs parked at the CS are of different voltage ratings. The buck boost converters designed at the CS are responsible for the charging and discharging operation of EV batteries. These converters charge the EV batteries during buck mode and discharge them during boost mode. Mismatch in power at the MG is countered by the energy stored in the EVs which are parked at the CS.

Moreover, sudden ingress and egress of the EVs at the CS has been catered while providing the frequency support to the MG. From the coordination between batteries parked at the CS it has been observed that the multiple CS can do the handshaking among each other through VSG mechanism. In this process of handshaking frequency support to the MG has been provided while meeting the charging needs of the EVs at the same time.

Although, these proposed systems will be quite useful to support the frequency of the islanded MG, but high penetration of EVs in the market will be required so that EVs can participate in frequency regulation process. Moreover, proper infrastructure of the CS will be a challenge for the implementation of these proposed systems.

7.2 Future Scope

The future directions in the area of EVs in MG can be focused on the following aspects.

- With the increase in penetration of EVs in the market, charging of EVs can be done using the RES, while providing the ancillary services to the MG during peak and off peak hours.
- The charging rate of EV batteries can be controlled at the CS to provide the support to the MG.
- The pollution in the environment can be reduced to a large extent with the use of EVs as an ESS for the MG. For instance, in future, ancillary services to the MG can be provided by a fleet of EVs parked at the CS by which dependence on diesel generators and other fuel based energy sources can be reduced to large extent. This will lead to the reduction in emission of harmful gases to the environment.
- With the proper infrastructure, large number of CS can interact with each other

to satisfy the demands of MG. These CS can share the load demand of MG just for short duration

- The impact on the main grid can be reduced by developing smart onboard or offboard charging facilities in residential and office areas.
- In addition to MG, VSG control technique can also be applied to aircraft, rails, ships, submarines and in other forms of electrified transportation sectors.

Bibliography

[1] P. Basak, S. Chowdhury, S. H. Dey, and S. Chowdhury, "A literature review on integration of distributed energy resources in the perspective of control, protection and stability of microgrid," *Renewable and Sustainable Energy Reviews*, vol. 16, no. 8, pp. 5545–5556, 2012.

[2] A. Kulasekara, K. M. Hemapala, and R. Gopura, "Dual layered architecture for multi agent based islanding and load management for microgrids," *Journal of Power and Energy Engineering*, vol. 3, no. 05, pp. 29–42, 2015.

[3] M. S. Ariyasinghe and K. M. Hemapala, "Microgrid test-beds and its control strategies," *Smart Grid and Renewable Energy*, vol. 4, pp. 11–17, 2013.

[4] M. Hasanuzzaman, U. S. Zubir, N. I. Ilham, and H. Seng Che, "Global electricity demand, generation, grid system, and renewable energy polices: a review," *Wiley Interdisciplinary Reviews: Energy and Environment*, vol. 6, no. 3, p. e222, 2017.

[5] R. Mohanty and A. K. Pradhan, "Protection of DC and hybrid AC-DC microgrids with ring configuration," in *7th International Conference on Power Systems (ICPS)*. IEEE, 2017, pp. 607–612.

[6] V. Nougain, S. Mishra, and A. K. Pradhan, "MVDC microgrid protection using a centralized communication with a localized backup scheme of adaptive parameters," *IEEE Transactions on Power Delivery*, vol. 34, no. 3, pp. 869–878, 2019.

[7] H. Zhao, M. Hong, W. Lin, and K. A. Loparo, "Voltage and frequency regulation of microgrid with battery energy storage systems," *IEEE Transactions on smart grid*, vol. 10, no. 1, pp. 414–424, 2017.

[8] T. Shintai, Y. Miura, and T. Ise, "Oscillation damping of a distributed generator using a virtual synchronous generator," *IEEE transactions on power delivery*, vol. 29, no. 2, pp. 668–676, 2014.

[9] J. Liu, Y. Miura, and T. Ise, "Comparison of dynamic characteristics between virtual synchronous generator and droop control in inverter-based distributed generators," *IEEE Transactions on Power Electronics*, vol. 31, no. 5, pp. 3600–3611, 2015.

[10] H. Bevrani, T. Ise, and Y. Miura, "Virtual synchronous generators: A survey and new perspectives," *International Journal of Electrical Power and Energy Systems*, vol. 54, pp. 244–254, 2014.

[11] A. Y. Saber and G. K. Venayagamoorthy, "Plug-in vehicles and renewable energy sources for cost and emission reductions," *IEEE Transactions on Industrial electronics*, vol. 58, no. 4, pp. 1229–1238, 2011.

[12] W. Kempton and S. E. Letendre, "Electric vehicles as a new power source for electric utilities," *Transportation Research Part D: Transport and Environment*, vol. 2, no. 3, pp. 157–175, 1997.

[13] J. Tomić and W. Kempton, "Using fleets of electric-drive vehicles for grid support," *Journal of power sources*, vol. 168, no. 2, pp. 459–468, 2007.

[14] I. Subotic and E. Levi, "A review of single-phase on-board integrated battery charging topologies for electric vehicles," in *IEEE Workshop on Electrical Machines Design, Control and Diagnosis (WEMDCD)*. IEEE, 2015, pp. 136–145.

[15] M. Yilmaz and P. T. Krein, "Review of the impact of vehicle-to-grid technologies on distribution systems and utility interfaces," *IEEE Transactions on power electronics*, vol. 28, no. 12, pp. 5673–5689, 2013.

[16] A. Fodor, A. Magyar, and K. M. Hangos, "Dynamic modeling and model analysis of a large industrial synchronous generator," in *International Conference on Applied Electronics*. IEEE, 2010, pp. 1–6.

[17] W. Kempton and S. E. Letendre, "Electric vehicles as a new power source for electric utilities," *Transportation Research Part D: Transport and Environment*, vol. 2, no. 3, pp. 157–175, 1997.

[18] W. Kempton and J. Tomić, "Vehicle-to-grid power fundamentals: Calculating capacity and net revenue," *Journal of power sources*, vol. 144, no. 1, pp. 268–279, 2005.

[19] P. Görbe, A. Magyar, and K. M. Hangos, "Reduction of power losses with smart grids fueled with renewable sources and applying EV batteries," *Journal of cleaner production*, vol. 34, pp. 125–137, 2012.

[20] J. Tomić and W. Kempton, "Using fleets of electric-drive vehicles for grid support," *Journal of power sources*, vol. 168, no. 2, pp. 459–468, 2007.

[21] M. Yilmaz and P. T. Krein, "Review of the impact of vehicle-to-grid technologies on distribution systems and utility interfaces," *IEEE Transactions on power electronics*, vol. 28, no. 12, pp. 5673–5689, 2012.

[22] A. Dhanju and W. Kempton, "Electric vehicles with V2G storage for large-scale wind power," *Windtech International*, vol. 2, no. 1, pp. 18–21, 2006.

[23] M. Jian, M. Yunfei, W. Jianzhong, J. Hongjie, D. Qian, and Y. Xiaodan, "Dynamic frequency response from electric vehicles in the Great Britain power system," *Journal of Modern Power Systems and Clean Energy*, vol. 3, no. 2, pp. 203–211, 2015.

[24] J. Meng, Y. Mu, H. Jia, J. Wu, X. Yu, and B. Qu, "Dynamic frequency response from electric vehicles considering travelling behavior in the Great Britain power system," *Applied Energy*, vol. 162, pp. 966–979, 2016.

[25] I. Subotic, N. Bodo, and E. Levi, "An EV drive-train with integrated fast charging capability," *IEEE Transactions on Power Electronics*, vol. 31, no. 2, pp. 1461–1471, 2015.

[26] A. Y. Saber and G. K. Venayagamoorthy, "Plug-in vehicles and renewable energy sources for cost and emission reductions," *IEEE Transactions on Industrial electronics*, vol. 58, no. 4, pp. 1229–1238, 2010.

[27] M. F. Arani and Y. A. I. Mohamed, "Analysis and impacts of implementing droop control in DFIG-based wind turbines on microgrid/weak-grid stability," *IEEE Transactions on Power Systems*, vol. 30, no. 1, pp. 385–396, 2014.

[28] G. Ramtharan, N. Jenkins, and J. Ekanayake, "Frequency support from doubly fed induction generator wind turbines," *IET Renewable Power Generation*, vol. 1, no. 1, pp. 3–9, 2007.

[29] G. Diaz, C. Gonzalez-Moran, J. Gomez-Aleixandre, and A. Diez, "Scheduling of droop coefficients for frequency and voltage regulation in isolated microgrids," *IEEE Transactions on Power Systems*, vol. 25, no. 1, pp. 489–496, 2009.

[30] D. Kottick, M. Blau, and D. Edelstein, "Battery energy storage for frequency regulation in an island power system," *IEEE transactions on energy conversion*, vol. 8, no. 3, pp. 455–459, 1993.

[31] K. O. Oureilidis, E. A. Bakirtzis, and C. S. Demoulias, "Frequency-based control of islanded microgrid with renewable energy sources and energy storage," *Journal of Modern Power Systems and Clean Energy*, vol. 4, no. 1, pp. 54–62, 2016.

[32] S. Zhang, Y. Mishra, and M. Shahidehpour, "Fuzzy-logic based frequency controller for wind farms augmented with energy storage systems," *IEEE Transactions on Power Systems*, vol. 31, no. 2, pp. 1595–1603, 2015.

[33] J. Driesen and K. Visscher, "Virtual synchronous generators," in *2008 IEEE Power and Energy Society General Meeting-Conversion and Delivery of Electrical Energy in the 21st Century*. IEEE, 2008, pp. 1–3.

[34] Q. Zhong and G. Weiss, "Synchronverters: Inverters that mimic synchronous generators," *IEEE transactions on industrial electronics*, vol. 58, no. 4, pp. 1259–1267, 2010.

[35] K. Visscher and S. W. H. De Haan, "Virtual synchronous machines (VSG's) for frequency stabilisation in future grids with a significant share of decentralized generation," in *CIRED Seminar: SmartGrids for Distribution*. IET, 2008, pp. 1–4.

[36] M. Torres and L. A. Lopes, "Virtual synchronous generator control in autonomous wind-diesel power systems," in *IEEE Electrical Power and Energy Conference (EPEC)*. IEEE, 2009, pp. 1–6.

[37] M. Van Wesenbeeck, S. De Haan, P. Varela, and K. Visscher, "Grid tied converter with virtual kinetic storage," in *2009 IEEE Bucharest PowerTech*. IEEE, 2009, pp. 1–7.

[38] B. Rathore, S. Chakrabarti, and S. Anand, "Frequency response improvement in microgrid using optimized VSG control," in *National Power Systems Conference (NPSC)*. IEEE, 2016, pp. 1–6.

[39] N. Soni, S. Doolla, and M. C. Chandorkar, "Improvement of transient response in microgrids using virtual inertia," *IEEE transactions on power delivery*, vol. 28, no. 3, pp. 1830–1838, 2013.

[40] M. A. Torres L, L. A. Lopes, L. A. Moran T, and J. R. Espinoza C, "Self-tuning virtual synchronous machine: A control strategy for energy storage systems to support dynamic frequency control," *IEEE Transactions on Energy Conversion*, vol. 29, pp. 833–840, 2014.

[41] J. Alipoor, Y. Miura, and T. Ise, "Power system stabilization using virtual synchronous generator with alternating moment of inertia," *IEEE journal of Emerging and selected topics in power electronics*, vol. 3, no. 2, pp. 451–458, 2014.

[42] J. Morren, S. W. De Haan, W. L. Kling, and J. Ferreira, "Wind turbines emulating inertia and supporting primary frequency control," *IEEE Transactions on power systems*, vol. 21, no. 1, pp. 433–434, 2006.

[43] V. Karapanos, S. de Haan, and K. Zwetsloot, "Real time simulation of a power system with vsg hardware in the loop," in *IECON 37th Annual Conference of the IEEE Industrial Electronics Society*. IEEE, 2011, pp. 3748–3754.

[44] S. A. Bukhari, W. Cao, T. A. Soomro, and D. Guanhao, "Future of microgrids with distributed generation and electric vehicles," *Development and integration of microgrids*, vol. 55, 2017.

[45] C. Ahn, C. Li, and H. Peng, "Optimal decentralized charging control algorithm for electrified vehicles connected to smart grid," *Journal of Power Sources*, vol. 196, no. 23, pp. 10 369–10 379, 2011.

[46] M. Honarmand, A. Zakariazadeh, and S. Jadid, "Optimal scheduling of electric vehicles in an intelligent parking lot considering vehicle-to-grid concept and battery condition," *Energy*, vol. 65, pp. 572–579, 2014.

[47] Q.-C. Zhong and G. Weiss, "Synchronverters: Inverters that mimic synchronous generators," *IEEE Transactions on Industrial Electronics*, vol. 58, no. 4, pp. 1259–1267, 2011.

[48] M. Guan, W. Pan, J. Zhang, Q. Hao, J. Cheng, and X. Zheng, "Synchronous generator emulation control strategy for voltage source converter (VSC) stations," *IEEE Transactions on Power Systems*, vol. 30, no. 6, pp. 3093–3101, 2015.

[49] P. R. Almeida, F. J. Soares, and J. P. Lopes, "Electric vehicles contribution for frequency control with inertial emulation," *Electric Power Systems Research*, vol. 127, pp. 141–150, 2015.

[50] J. A. Suul, S. D'Arco, and G. Guidi, "Virtual synchronous machine-based control of a single-phase bi-directional battery charger for providing vehicle-to-grid services," *IEEE Transactions on Industry Applications*, vol. 52, no. 4, pp. 3234–3244, 2016.

[51] K. Dhingra and M. Singh, "Frequency support in a micro-grid using virtual synchronous generator based charging station," *IET Renewable Power Generation*, vol. 12, no. 9, pp. 1034–1044, 2018.

[52] J. Fang, P. Lin, H. Li, Y. Yang, and Y. Tang, "An improved virtual inertia control for three-phase voltage source converters connected to a weak grid," *IEEE Transactions on Power Electronics*, 2018.

[53] C. Jin, X. Sheng, and P. Ghosh, "Optimized electric vehicle charging with intermittent renewable energy sources," *IEEE Journal of Selected Topics in Signal Processing*, vol. 8, no. 6, pp. 1063–1072, 2014.

[54] J. Van Roy, N. Leemput, F. Geth, J. Büscher, R. Salenbien, and J. Driesen, "Electric vehicle charging in an office building microgrid with distributed energy resources," *IEEE Transactions on sustainable energy*, vol. 5, no. 4, pp. 1389–1396, 2014.

[55] J. G. Matos, F. S. Silva, and L. Ribeiro, "Power control in AC isolated microgrids with renewable energy sources and energy storage systems," *IEEE Transactions on Industrial Electronics*, vol. 62, no. 6, pp. 3490–3498, 2014.

[56] J. Kumar, B. Das, and P. Agarwal, "Optimized switching scheme of a cascade multi-level inverter," *Electric Power Components and Systems*, vol. 38, no. 4, pp. 445–464, 2010.

[57] J. Liu, Y. Miura, H. Bevrani, and T. Ise, "Enhanced virtual synchronous generator control for parallel inverters in microgrids," *IEEE Transactions on Smart Grid*, vol. 8, no. 5, pp. 2268–2277, 2016.

[58] M. Rezkalla, A. Zecchino, M. Pertl, and M. Marinelli, "Grid frequency support by single-phase electric vehicles employing an innovative virtual inertia controller," in *51st International Universities Power Engineering Conference (UPEC)*. IEEE, 2016, pp. 1–6.

[59] K. Sakimoto, Y. Miura, and T. Ise, "Stabilization of a power system with a distributed generator by a virtual synchronous generator function," in *8th International Conference on Power Electronics-ECCE Asia*. IEEE, 2011, pp. 1498–1505.

[60] D. Wang and H. Wu, "Application of virtual synchronous generator technology in microgrid," in *IEEE 8th International Power Electronics and Motion Control Conference (IPEMC-ECCE Asia)*. IEEE, 2016, pp. 3142–3148.

[61] X. Yan, S. Y. Mohamed, D. Li, and A. S. Gadalla, "Parallel operation of virtual synchronous generators and synchronous generators in a microgrid," *The Journal of Engineering*, vol. 2019, no. 16, pp. 2635–2642, 2019.

[62] K. Shi, H. Ye, W. Song, and G. Zhou, "Virtual inertia control strategy in microgrid based on virtual synchronous generator technology," *IEEE Access*, vol. 6, pp. 27 949–27 957, 2018.

[63] J. Liu, Y. Miura, and T. Ise, "Comparison of dynamic characteristics between virtual synchronous generator and droop control in inverter-based distributed generators," *IEEE Transactions on Power Electronics*, vol. 31, no. 5, pp. 3600–3611, 2015.

[64] S. Han, S. Han, and K. Sezaki, "Development of an optimal vehicle-to-grid aggregator for frequency regulation," *IEEE Transactions on smart grid*, vol. 1, no. 1, pp. 65–72, 2010.

[65] A. Aldik, A. T. Al-Awami, E. Sortomme, A. M. Muqbel, and M. Shahidehpour, "A planning model for electric vehicle aggregators providing ancillary services," *IEEE Access*, vol. 6, pp. 70 685–70 697, 2018.

[66] A. Perez-Diaz, E. Gerding, and F. McGroarty, "Coordination of electric vehicle Aggregators: A Coalitional Approach," in *Proceedings of the 17th International Conference on Autonomous Agents and MultiAgent Systems*. International Foundation for Autonomous Agents and Multiagent Systems, 2018, pp. 676–684.

[67] M. A. Ortega, F. Bouffard, and V. Silva, "Electric vehicle aggregator/system operator coordination for charging scheduling and services procurement," *IEEE Transactions on Power Systems*, vol. 28, no. 2, pp. 1806–1815, 2013.

[68] A. Haque, V. S. B. Kurukuru, and M. A. Khan, "Stochastic methods for prediction of charging and discharging power of electric vehicles in vehicle-to-grid environment," *IET Power Electronics*, vol. 12, no. 13, pp. 3510–3520, 2019.

[69] D. Said and H. Mouftah, "A novel electric vehicles charging/discharging management protocol based on queuing model," *IEEE Transactions on Intelligent Vehicles*, 2019.

[70] G. S. Aujla and N. Kumar, "SDN-based energy management scheme for sustainability of data centers: An analysis on renewable energy sources and electric

vehicles participation," *Journal of Parallel and Distributed Computing*, vol. 117, pp. 228–245, 2018.

[71] M. Ghofrani, A. Arabali, M. Etezadi, and M. S. Fadali, "Smart scheduling and cost-benefit analysis of grid-enabled electric vehicles for wind power integration," *IEEE Transactions on Smart grid*, vol. 5, no. 5, pp. 2306–2313, 2014.

[72] M. Honarmand, A. Zakariazadeh, and S. Jadid, "Self-scheduling of electric vehicles in an intelligent parking lot using stochastic optimization," *Journal of the Franklin Institute*, vol. 352, no. 2, pp. 449–467, 2015.

[73] R. Rana, M. Singh, and S. Mishra, "Design of modified droop controller for frequency support in microgrid using fleet of electric vehicles," *IEEE Transactions on Power Systems*, vol. 32, no. 5, pp. 3627–3636, 2017.

[74] H. Bevrani and S. Shokoohi, "An intelligent droop control for simultaneous voltage and frequency regulation in islanded microgrids," *IEEE transactions on smart grid*, vol. 4, no. 3, pp. 1505–1513, 2013.

[75] I. Serban and C. Marinescu, "Battery energy storage system for frequency support in microgrids and with enhanced control features for uninterruptible supply of local loads," *International Journal of Electrical Power and Energy Systems*, vol. 54, pp. 432–441, 2014.

[76] F. Katiraei and M. R. Iravani, "Power management strategies for a microgrid with multiple distributed generation units," *IEEE transactions on power systems*, vol. 21, no. 4, pp. 1821–1831, 2006.

[77] R. Majumder, G. Ledwich, A. Ghosh, S. Chakrabarti, and F. Zare, "Droop control of converter-interfaced micro sources in rural distributed generation," *IEEE Transactions on Power Delivery*, vol. 25, no. 4, pp. 2768–2778, 2010.

[78] I. Usunariz, M. Santamaria, K. Mentesidi, and M. Aguado, "A modified control scheme of droop-based converters for power stability analysis in microgrids," *Journal of Solar Energy*, vol. 2015, 2015.

[79] E. Reihani, A. Eshraghi, M. Motalleb, and S. Jafarzadeh, "Frquency regulation of microgrid with battery droop control," in *2018 IEEE/PES Transmission and Distribution Conference and Exposition (T&D)*. IEEE, 2018, pp. 1–5.

[80] L. Yao, W. H. Lim, and T. S. Tsai, "A real-time charging scheme for demand response in electric vehicle parking station," *IEEE Transactions on Smart Grid*, vol. 8, no. 1, pp. 52–62, 2016.

[81] C. Gouveia, C. L. Moreira, J. A. P. Lopes, D. Varajao, and R. E. Araujo, "Microgrid service restoration: The role of plugged-in electric vehicles," *IEEE Industrial Electronics Magazine*, vol. 7, no. 4, pp. 26–41, 2013.

[82] E. Mortaz and J. Valenzuela, "Microgrid energy scheduling using storage from electric vehicles," *Electric Power Systems Research*, vol. 143, pp. 554–562, 2017.

[83] M. Fanti, A. Mangini, M. Roccotelli, and W. Ukovich, "District microgrid management integrated with renewable energy sources, energy storage systems and electric vehicles," *IFAC-Papers On Line*, vol. 50, no. 1, pp. 10 015–10 020, 2017.

[84] L. K. Panwar, S. R. Konda, A. Verma, B. K. Panigrahi, and R. Kumar, "Operation window constrained strategic energy management of microgrid with electric vehicle and distributed resources," *IET Generation, Transmission and Distribution*, vol. 11, no. 3, pp. 615–626, 2017.

[85] M. Farrokhabadi, C. A. Cañizares, and K. Bhattacharya, "Frequency control in isolated/islanded microgrids through voltage regulation," *IEEE Transactions on Smart Grid*, vol. 8, no. 3, pp. 1185–1194, 2017.

[86] C. Jin, X. Sheng, and P. Ghosh, "Optimized electric vehicle charging with intermittent renewable energy sources," *IEEE Journal of Selected Topics in Signal Processing*, vol. 8, no. 6, pp. 1063–1072, 2014.

[87] A. H. Hajimiragha, M. R. D. Zadeh, and S. Moazeni, "Microgrids frequency control considerations within the framework of the optimal generation scheduling problem," *IEEE Transactions on Smart Grid*, vol. 6, no. 2, pp. 534–547, 2014.

[88] R. Yadav, A. K. Pradhan, and I. Kamwa, "A spectrum similarity approach for identifying coherency change patterns in power system due to variability in renewable generation," *IEEE Transactions on Power Systems*, vol. 34, no. 5, pp. 3769–3779, 2019.

[89] H. Yang, H. Pan, F. Luo, J. Qiu, Y. Deng, M. Lai, and Z. Y. Dong, "Operational planning of electric vehicles for balancing wind power and load fluctuations in a microgrid," *IEEE Transactions on Sustainable Energy*, vol. 8, no. 2, pp. 592–604, April 2017.

[90] L. D. Watson and J. W. Kimball, "Frequency regulation of a microgrid using solar power," in *Twenty-Sixth Annual IEEE Applied Power Electronics Conference and Exposition (APEC)*. IEEE, 2011, pp. 321–326.

[91] A. Khalil and K. Ateea, "Modelling and control of photovoltaic-based microgrid," *International Journal of Renewable Energy Research (IJRER)*, vol. 5, no. 3, pp. 826–835, 2015.

[92] C. Krismadinata, J. Selvaraj, and N. Rahim, "A novel topology and PWM single-phase three-level rectifier," in *International Conference for Technical Postgraduates (TECHPOS)*. IEEE, 2009, pp. 1–6.

[93] J. Selvaraj, N. Rahim, and C. Krismadinata, "Digital PI current control for grid connected pv inverter," in *3rd IEEE Conference on Industrial Electronics and Applications*. IEEE, 2008, pp. 742–746.

[94] S. Bacha, D. Picault, B. Burger, I. Etxeberria-Otadui, and J. Martins, "Photovoltaics in microgrids: An overview of grid integration and energy management aspects," *IEEE Industrial Electronics Magazine*, vol. 9, no. 1, pp. 33–46, 2015.

[95] M. Chamana and B. H. Chowdhury, "Droop-based control in a photovoltaic-centric microgrid with battery energy storage," in *North American Power Symposium (NAPS)*. IEEE, 2013, pp. 1–6.

[96] V. J. Ramaiah, M. K. K. Reddy, and V. Sarkar, "Variable rate LPPT based droop controlled operation of photovoltaic system for microgrid frequency regulation," in *IEEE International Conference on Power Electronics, Drives and Energy Systems (PEDES)*. IEEE, 2016, pp. 1–5.

[97] K. J. Bunker and W. W. Weaver, "Microgrid frequency regulation using wind turbine controls," in *Power and Energy Conference at Illinois (PECI)*. IEEE, 2014, pp. 1–6.

[98] S. Mohandas and A. K. Chandel, "Transient stability enhancement of the power system with wind generation," *TELKOMNIKA (Telecommunication Computing Electronics and Control)*, vol. 9, no. 2, pp. 267–278, 2013.

[99] Y. Han, P. M. Young, A. Jain, and D. Zimmerle, "Robust control for microgrid frequency deviation reduction with attached storage system," *IEEE Transactions on Smart Grid*, vol. 6, no. 2, pp. 557–565, 2014.

[100] X. Li, Y. Song, and S. Han, "Frequency control in micro-grid power system combined with electrolyzer system and fuzzy PI controller," *Journal of Power Sources*, vol. 180, no. 1, pp. 468–475, 2008.

[101] S. D'Arco, J. A. Suul, and O. B. Fosso, "A virtual synchronous machine implementation for distributed control of power converters in smart grids," *Electric Power Systems Research*, vol. 122, pp. 180–197, 2015.

[102] P. Tripathy, S. C. Srivastava, and S. N. Singh, "A divide-by-difference-filter based algorithm for estimation of generator rotor angle utilizing synchrophasor measurements," *IEEE Transactions on Instrumentation and Measurement*, vol. 59, no. 6, pp. 1562–1570, 2009.

[103] S. Mishra, D. Pullaguram, S. A. Buragappu, and D. Ramasubramanian, "Single-phase synchronverter for a grid-connected roof top photovoltaic system," *IET Renewable Power Generation*, vol. 10, no. 8, pp. 1187–1194, 2016.

[104] A. R. Bhatti, Z. Salam, and R. H. Ashique, "Electric vehicle charging using photovoltaic based microgrid for remote islands," *Energy Procedia*, vol. 103, no. 1, pp. 213–218, 2016.

[105] E. Mortaz and J. Valenzuela, "Microgrid energy scheduling using storage from electric vehicles," *Electric Power Systems Research*, vol. 143, pp. 554–562, 2017.

[106] K. Shimizu, T. Masuta, Y. Ota, and A. Yokoyama, "Load frequency control in power system using vehicle-to-grid system considering the customer convenience of electric vehicles," in *International Conference on Power System Technology*. IEEE, 2010, pp. 1–8.

[107] J. P. Lopes, S. A. Polenz, C. Moreira, and R. Cherkaoui, "Identification of control and management strategies for LV unbalanced microgrids with plugged-in electric vehicles," *Electric Power Systems Research*, vol. 80, no. 8, pp. 898–906, 2010.

[108] M. F. Arani and Y. I. Mohamed, "Cooperative control of wind power generator and electric vehicles for microgrid primary frequency regulation," *IEEE Transactions on Smart Grid*, vol. 9, no. 6, pp. 5677–5686, 2017.

[109] A. Amir, A. Amir, H. S. Che, A. Elkhateb, and N. A. Rahim, "Comparative analysis of high voltage gain DC-DC converter topologies for photovoltaic systems," *Renewable energy*, vol. 136, pp. 1147–1163, 2019.

[110] W. Polivka, P. Chetty, and R. Middlebrook, "State-space average modelling of converters with parasitics and storage-time modulation," in *IEEE Power Electronics Specialists Conference*. IEEE, 1980, pp. 119–143.

[111] K. H. Bhalodi and P. Agarwal, "Space vector modulation with DC-link voltage balancing control for three-level inverters," in *International Conference on Power Electronic, Drives and Energy Systems*. IEEE, 2006, pp. 1–6.

[112] J. V. Missula, R. Adda, and P. Tripathy, "Pulse width modulation and SRF based closed-loop control of stand-alone single-phase 5L-ANPC inverter," in *IEEE International Conference on Power Electronics, Drives and Energy Systems (PEDES)*. IEEE, 2018, pp. 1–6.

[113] A. Cuculić, J. Ćelić, and R. Prenc, "Marine diesel-generator model for voltage and frequency variation analysis during fault scenarios," *Pomorski zbornik*, vol. 51, no. 1, pp. 11–24, 2016.

[114] S. Tselepis, "12 years operation of the gaidouromantra microgrid in kythnos island, COI-3869," Dec 2012.

[115] H. Liu, Z. Hu, Y. Song, J. Wang, and X. Xie, "Vehicle-to-grid control for supplementary frequency regulation considering charging demands," *IEEE Transactions on Power Systems*, vol. 30, no. 6, pp. 3110–3119, 2015.

[116] J. Van Roy, N. Leemput, F. Geth, J. Büscher, R. Salenbien, and J. Driesen, "Electric vehicle charging in an office building microgrid with distributed energy resources," *IEEE Transactions on sustainable energy*, vol. 5, no. 4, pp. 1389–1396, 2014.

[117] Y. Wi, J. Lee, and S. Joo, "Electric vehicle charging method for smart homes/buildings with a photovoltaic system," *IEEE Transactions on Consumer Electronics*, vol. 59, no. 2, pp. 323–328, 2013.

[118] J. Traube, F. Lu, D. Maksimovic, J. Mossoba, M. Kromer, P. Faill, S. Katz, B. Borowy, S. Nichols, and L. Casey, "Mitigation of solar irradiance intermittency in photovoltaic power systems with integrated electric-vehicle charging functionality," *IEEE Transactions on Power Electronics*, vol. 28, no. 6, pp. 3058–3067, 2013.

[119] S. Singh, M. Singh, and S. C. Kaushik, "Optimal power scheduling of renewable energy systems in microgrids using distributed energy storage system," *IET Renewable Power Generation*, vol. 10, no. 9, pp. 1328–1339, 2016.

[120] C. Li, C. Ahn, H. Peng, and J. Sun, "Integration of plug-in electric vehicle charging and wind energy scheduling on electricity grid," in *Innovative Smart Grid Technologies (ISGT), 2012 IEEE PES*. IEEE, 2012, pp. 1–7.

[121] P. Goli and W. Shireen, "PV integrated smart charging of PHEVs based on DC link voltage sensing," *IEEE Transactions on Smart Grid*, vol. 5, no. 3, pp. 1421–1428, 2014.

[122] A. Zakariazadeh, S. Jadid, and P. Siano, "Integrated operation of electric vehicles and renewable generation in a smart distribution system," *Energy Conversion and Management*, vol. 89, pp. 99–110, 2015.

[123] H. Liu, Z. Hu, Y. Song, and J. Lin, "Decentralized vehicle-to-grid control for primary frequency regulation considering charging demands," *IEEE Transactions on Power Systems*, vol. 28, no. 3, pp. 3480–3489, 2013.

[124] Z. Moghaddam, I. Ahmad, D. Habibi, and Q. V. Phung, "Smart charging strategy for electric vehicle charging stations," *IEEE Transactions on Transportation Electrification*, vol. 4, no. 1, pp. 76–88, 2018.

[125] R. Rana, M. Singh, and S. Mishra, "Design of modified droop controller for frequency support in microgrid using fleet of electric vehicles," *IEEE Transactions on Power Systems*, vol. 32, no. 5, pp. 3627–3636, 2017.

[126] P. Kundur, N. J. Balu, and M. G. Lauby, *Power system stability and control*. McGraw-hill New York, 1994, vol. 7.

[127] W. Wu, Y. Chen, A. Luo, L. Zhou, X. Zhou, L. Yang, Y. Dong, and J. M. Guerrero, "A virtual inertia control strategy for DC microgrids analogized with virtual synchronous machines," *IEEE Transactions on Industrial Electronics*, vol. 64, no. 7, pp. 6005–6016, July 2017.

[128] P. Sonkar, A. Chandel, and O. Rahi, "Integrated tuning of PID-derivative load frequency controller for two area interconnected system," *International Journal of Engineering, Science and Technology*, vol. 7, no. 3, pp. 42–51, 2015.

[129] C. Pang, P. Dutta, and M. Kezunovic, "BEVs/PHEVs as dispersed energy storage for V2B uses in the smart grid," *IEEE Transactions on Smart Grid*, vol. 3, no. 1, pp. 473–482, 2012.

[130] F. Berthold, A. Ravey, B. Blunier, D. Bouquain, S. Williamson, and A. Miraoui, "Design and development of a smart control strategy for plug-in hybrid vehicles including vehicle-to-home functionality," *IEEE Transactions on Transportation Electrification*, vol. 1, no. 2, pp. 168–177, 2015.

[131] L. K. Panwar, S. Reddy, A. Verma, B. Panigrahi, and R. Kumar, "Optimal schedule of plug in electric vehicles in smart grid with constrained parking lots," in *IEEE 6th International Conference on Power Systems (ICPS)*. IEEE, 2016, pp. 1–6.

[132] J. Traube, F. Lu, D. Maksimovic, J. Mossoba, M. Kromer, P. Faill, S. Katz, B. Borowy, S. Nichols, and L. Casey, "Mitigation of solar irradiance intermittency in photovoltaic power systems with integrated electric-vehicle charging

functionality," *IEEE Transactions on Power Electronics*, vol. 28, no. 6, pp. 3058–3067, 2012.

[133] N. Sujitha and S. Krithiga, "RES based EV battery charging system: A review," *Renewable and Sustainable Energy Reviews*, vol. 75, pp. 978–988, 2017.

[134] S. Gao, K. Chau, C. Liu, D. Wu, and C. C. Chan, "Integrated energy management of plug-in electric vehicles in power grid with renewables," *IEEE Transactions on Vehicular Technology*, vol. 63, no. 7, pp. 3019–3027, 2014.

[135] X. Zhu, M. Xia, and H. Chiang, "Coordinated sectional droop charging control for EV aggregator enhancing frequency stability of microgrid with high penetration of renewable energy sources," *Applied energy*, vol. 210, pp. 936–943, 2018.

[136] K. Kaur, R. Rana, N. Kumar, M. Singh, and S. Mishra, "A colored petri net based frequency support scheme using fleet of electric vehicles in smart grid environment," *IEEE Transactions on Power Systems*, vol. 31, no. 6, pp. 4638–4649, 2016.

[137] G. Xiao, C. Li, Z. Yu, Y. Cao, and B. Fang, "Review of the impact of electric vehicles participating in frequency regulation on power grid," in *Chinese automation congress*. IEEE, 2013, pp. 75–80.

[138] Q. Chen, N. Liu, C. Wang, and J. Zhang, "Optimal power utilizing strategy for PV-based EV charging stations considering real-time price," in *IEEE Conference and Expo Transportation Electrification Asia-Pacific (ITEC Asia-Pacific)*. IEEE, 2014, pp. 1–6.

[139] Q. Chen, N. Liu, X. Lu, and J. Zhang, "A heuristic charging strategy for real-time operation of PV-based charging station for electric vehicles," in *IEEE Innovative Smart Grid Technologies-Asia (ISGT ASIA)*. IEEE, 2014, pp. 465–469.

[140] U. B. Tayab, M. A. B. Roslan, L. J. Hwai, and M. Kashif, "A review of droop control techniques for microgrid," *Renewable and Sustainable Energy Reviews*, vol. 76, pp. 717–727, 2017.

[141] X. Hou, Y. Sun, X. Zhang, J. Lu, P. Wang, and J. M. Guerrero, "Improvement of frequency regulation in VSG-based AC microgrid via adaptive virtual inertia," *IEEE Transactions on Power Electronics*, 2019.